



Platform technology towards the chemical fingerprinting methamphetamine from ephedrine pathways.

AUTHOR(S)

Andrea Pucci

PUBLICATION DATE

01-06-2016

HANDLE

[10536/DRO/DU:30089150](#)

Downloaded from Deakin University's Figshare repository

Deakin University CRICOS Provider Code: 00113B

**PLATFORM TECHNOLOGY TOWARDS THE CHEMICAL
FINGERPRINTING OF METHAMPHETAMINE FROM
EPHEDRINE PATHWAYS**

By

Luke Matthew Andrighetto

Bachelor of Forensic Science (Honours)

Submitted in fulfilment of the requirements for the degree of
Doctor of Philosophy (Forensic Chemistry)

Deakin University

June, 2016



DEAKIN UNIVERSITY

ACCESS TO THESIS - A

I am the author of the thesis entitled:

**PLATFORM TECHNOLOGY TOWARDS THE CHEMICAL FINGERPRINTING OF METHAMPHETAMINE
FROM EPHEDRINE PATHWAYS**

Submitted for the degree of Doctor of Philosophy (Forensic Chemistry)

This thesis may be made available for consultation, loan and limited copying in
accordance with the Copyright Act 1968.

*'I certify that I am the student named below and that the information provided in the
form is correct'*

Full Name: Luke Matthew Andrighetto

Signed:

Signature Redacted by Library

Date: 29th June 2016



DEAKIN UNIVERSITY

CANDIDATE DECLARATION

I certify the following about the thesis entitled:

**PLATFORM TECHNOLOGY TOWARDS THE CHEMICAL FINGERPRINTING OF METHAMPHETAMINE
FROM EPHEDRINE PATHWAYS**

Submitted for the degree of Doctor of Philosophy (Forensic Chemistry)

- a. I am the creator of all or part of the whole work(s) (including content and layout) and that where reference is made to the work of others, due acknowledgment is given.
- b. The work(s) are not in any way a violation or infringement of any copyright, trademark, patent, or other rights whatsoever of any person.
- c. That if the work(s) have been commissioned, sponsored or supported by any organisation, I have fulfilled all of the obligations required by such contract or agreement.

I also certify that any material in the thesis which has been accepted for a degree or diploma by any university or institution is identified in the text.

'I certify that I am the student named below and that the information provided in the form is correct'

Full Name: Luke Matthew Andrighetto

Signed:

Signature Redacted by Library

Date: 29th June 2016

*“If we knew what it was we were doing, it would not be called research,
would it?”*

Albert Einstein

TABLE OF CONTENTS

TABLE OF CONTENTS	V
ACKNOWLEDGEMENTS	VIII
PUBLICATIONS	X
ABBREVIATIONS AND ACRONYMS	XI
ABSTRACT	XIV
CHAPTER 1:	1
INTRODUCTION TO METHAMPHETAMINE	1
1.1 History of Methamphetamine	2
1.2 The Australian Methamphetamine Problem	4
1.2.1 Ice Taskforce	6
1.3 The appeal of Methamphetamine	7
1.4 Local Synthesis	9
1.5 Precursors to methamphetamine	9
1.5.1 Pseudoephedrine/ephedrine	10
1.5.2 Phenyl-2-propanone (P2P)	13
1.6 Detection methods of methamphetamine	14
1.6.1 Police road-side testing	14
1.7 Analytical Separation and Detection Methods for Methamphetamine	15
1.8 Two-dimensional HPLC	17
1.9 In-Silico Optimisation Chromatography (computational modelling)	19
CHAPTER 2:	22
SYNTHESIS OF PSEUDOEPHEDRINE/EPHEDRINE FROM NITROETHANE AND BENZALDEHYDE	22
CHAPTER OVERVIEW	23
2.1 INTRODUCTION	24
2.1.1 Reductive Amination of phenyl-2-propanone (P2P)	25
2.1.2 Pseudoephedrine Reduction	26
2.1.3 Birch Reduction of pseudoephedrine to methamphetamine	27
2.2 EXPERIMENTAL	29
Synthesis of 2-nitro-1-phenyl-1-propanol (mixture of Syn and Anti diastereomers) (8)	29
Synthesis of Phenyl-2-nitropropene (9)	31
2.3 RESULTS AND DISCUSSION	33
2.3.1 Synthesis of 2-Nitro-1-phenylpropanol (8)	33

2.3.1 Synthesis of phenyl-2-nitropropene (9).....	37
2.3.3 Synthesis of norephedrine (10) from 2-nitro-1-phenyl-1-propanol	41
2.3.4 Synthesis of ephedrine/pseudoephedrine (1) from norephedrine (10).....	42
2.3.4 Synthesis of methamphetamine (1) from norephedrine (10)	50
2.4 CONCLUSION.....	52
CHAPTER 3	53
SYNTHESIS OF PSEUDOEPHEDRINE/EPHEDRINE FROM L-ALANINE	53
CHAPTER OVERVIEW.....	54
3.1 INTRODUCTION.....	55
3.2 EXPERIMENTAL	57
Synthesis of Methyl-L-alaninate (16)	58
Synthesis of Methyl <i>N</i> -(toluene-4-sulfonyl) L-alaninate (17)	58
Synthesis of Methyl <i>N</i> -methyl- <i>N</i> -(toluene-4-sulfonyl)-L-alaninate (18).....	59
Synthesis of Methyl (tert-butoxycarbonyl)-L-alaninate (20)	59
Synthesis of 2-(<i>N</i> -(tert-butoxycarbonyl)amino)propanoic acid (22)	60
Synthesis of 2-(<i>N</i> -(tert-butoxycarbonyl)methylamino)propanoic acid (23)	60
Synthesis of 2-(methylamino)propanoic acid (<i>N</i> -methylalanine) trifluoroacetate salt (19)	61
3.3 RESULTS AND DISCUSSION	62
3.4 CONCLUSION.....	74
CHAPTER 4:	75
<i>IN-SILICO</i> OPTIMISATION OF 1D-HPLC AND 2D-HPLC USING DRYLAB® <i>SIMULATION SOFTWARE</i>	75
CHAPTER OVERVIEW.....	76
4.1 Introduction	77
4.2 Experimental.....	82
Standards and Samples - Experiment 1	82
High Performance Liquid Chromatography - Experiment 1	82
DryLab® Optimization - Experiment 1	83
Model Seizure Samples - Experiment 1	83
Chemicals - Experiment 2	83
Standards and Samples - Experiment 2	84
Chromatography Columns - Experiment 2	84
2D-HPLC - Experiment 2.....	84
LC-MS - Experiment 2	85
4.3 Results and Discussion.....	86
4.3.1 1D-HPLC using DryLab®.....	86

4.3.2 2D-HPLC using DryLab®	91
4.3.3 2D-HPLC of a real methamphetamine seizure sample	93
4.3.4 2D-HPLC of a synthesised intermediate sample to methamphetamine	95
4.4 Conclusion.....	99
CHAPTER 5:	100
COLUMN SELECTIVITY STUDY AND CHEMICAL MAPPING	100
CHAPTER OVERVIEW.....	101
5.1 Introduction	102
5.2 Experimental	106
Chemicals and samples.....	106
Liquid Chromatography Mass Spectrometry (LC-MS)	107
Liquid Chromatography Mass Spectrometry (LC-MS) for chemical mapping of synthetic pathway.....	108
Two-dimensional high performance liquid chromatography.....	108
Data Processing.....	109
Principal Component Analysis (PCA).....	109
5.3 Results and Discussion	110
5.3.1 Column Selectivity Study using OpenMS®	110
5.3.2 Chemical mapping of impurities for a pathway to methamphetamine	122
5.3.3 Preliminary PCA Study	135
5.4 Conclusion.....	143
CHAPTER 6:	145
CONCLUDING REMARKS AND FUTURE WORK.....	145
6.1 Concluding Remarks	146
6.2 Future Work.....	147
REFERENCES.....	149

ACKNOWLEDGEMENTS

I would like to extend my gratitude to a number of people for their help, support and advice throughout my PhD.

Firstly, to my primary supervisor and friend Dr Xavier Conlan. Thank you for all your encouragement, support, understanding and advice. Without you I would not be here today and words cannot describe how grateful I am for everything you have done for me over this long journey. We have had a lot of laughs and great memories together that I will forever treasure.

To my co-supervisor and friend Dr Paul Stevenson. Thank you so much for all your hard work, help, support and advice. It is greatly appreciated and never forgotten. Without you I would not have finished my PhD this decade. Your brilliant mind and programming skills have contributed a great deal to my research and I can't thank you enough for all your patience.

To my co-supervisor Dr Luke Henderson. Thank you for all your help, support and advice. We have been on a long journey together from Honours to here and I could not have got here without you. Your synthetic knowledge is second to none and I really appreciate all your help and guidance. I will miss the constant bantering between us.

To my external co-supervisor Dr Jim Pearson. Thank you for all your help and advice, it is greatly appreciated. Your guidance and internal information has contributed significantly to my research and I am very grateful.

To Alfred Deakin Professor Neil Barnett and Dr Fred Pfeffer. Thank you for all your advice and support over the past 4 years. We have had many laughs together and I hope for many more.

To my dear friends Niki and Natalie. Thank you for our daily lunches and laughs together. It has been the only thing keeping me sane some days. I will miss our little lunch dates.

To all my friends that I have had the privilege of working with or beside (soon to be Dr Niki Burns, Dr Zoe Smith, Dr Gregory Barbante, Dr Brendan Holland, Dr Danielle Bassanese, Dr Jarrad Altimari, Dr Shane Hickey, Ashton Theakstone, Hannah Brozinski, Ryan Robson) thank you for making the work-place an enjoyable place to be.

To my dearest partner Lillian. Where do I start? Words don't do justice to how much you mean to me and I definitely could not have finished this journey without you. Your love, support, encouragement and belief in me over the past 7 years has been overwhelming and I cannot thank you enough.

To my parents. I did it. Dr Luke Andrighetto. Thank you for all your unconditional love, support, encouragement and guidance over the past 25 years. I literally would not have been here if it weren't for you both. Thank you.

PUBLICATIONS

1. **L.M. Andrighetto**, N.K Burns, L.C. Henderson, C.J Bowen, J.R. Pearson, P.G. Stevenson and X.A. Conlan, *In-silico* optimisation of two-dimensional HPLC for the determination of Australian methamphetamine seizure samples, *Forensic Science International*, 266, 511-516 (2016).
 - The work from this paper is included in **Chapter 4**

2. N.K Burns †, **L.M Andrighetto** †, S.D Purcell, N.W Barnett, J. Denning, P.S Francis, X.A Conlan and P.G. Stevenson, Blind column selection protocol for two-dimensional high performance chromatography, *Talanta*, 154, 85-91 (2016) DOI: 10.1016/j.talanta.2016.03.056. † **(Co-first author)**
 - The work from this paper is included in **Chapter 5**

3. **L.M. Andrighetto**, L.C. Henderson, J.R. Pearson, P.G. Stevenson and X.A. Conlan, Influence of base on nitro-aldol reaction products for alternative clandestine pathways, *Australian Journal of Forensic Sciences*, (2016) DOI: 10.1080/00450618.2015.1112429.
 - The work from this paper is included in **Chapter 2**

4. **L.M. Andrighetto**, F.M. Pfeffer, P.G. Stevenson, S.M. Hickey, G.J. Barbante, L.C Henderson, J.R Pearson and X.A. Conlan, Three step synthesis of N-methylalanine – A precursor to ephedrine, pseudoephedrine, and methamphetamine, *Journal of the Clandestine Laboratory Investigating Chemists Association*, 24, 33-37 (2014).
 - The work from this paper is included in **Chapter 3**

5. **L.M. Andrighetto**, P.G. Stevenson, J.R. Pearson, L.C. Henderson, X.A. Conlan, DryLab® optimised two-dimensional high performance liquid chromatography for differentiation of ephedrine and pseudoephedrine based methamphetamine samples, *Forensic Science International*, 244, 302-305 (2014)
 - The work from this paper is included in **Chapter 4**

ABBREVIATIONS AND ACRONYMS

μm	Micrometre
^{13}C NMR	Carbon Nuclear Magnetic Resonance
1D-HPLC	One-Dimensional High Performance Liquid Chromatography
^1H NMR	Proton Nuclear Magnetic Resonance
2D-HPLC	Two-Dimensional High Performance Liquid Chromatography
ACN	Acetonitrile
amu	Atomic Mass Unit
ATS	Amphetamine Type Substance
Boc	Tert-butyloxycarbonyl
Boc ₂ O	Di-tert-butyl dicarbonate
CDCl ₃	Deuterated Chloroform
d ₆ -DMSO	Deuterated Dimethylsulfoxide
DCM	Dichloromethane
DIAD	Diisopropyl Azodicarboxylate
DIOS-MSI	Desorption Ionisation on Silicon - Mass Spectrometry Imaging
DMSO	Dimethylsulfoxide
EC	Endcapped
ECL	Electrochemiluminescence
EIC	Extracted Ion Chromatogram
EM-SPME	Electromembrane Surrounded-Solid Phase Microextraction
eq.	Equivalents
ESI-MS	Electrospray Ionisation – Mass Spectrometry
Et ₃ N	Triethylamine
EtOH	Ethanol
FDA	Food and Drug Administration
g	Grams
GC/FT-IR	Gas Chromatography/ Fourier Transform - Infrared Spectroscopy
GC-MS	Gas Chromatography – Mass Spectrometry
h	Hours

HILIC	Hydrophilic Interaction Liquid Chromatography
HIV	Human Immunodeficiency Virus
HPLC	High Performance Liquid chromatography
HRMS	High Resolution Mass Spectrometry
IRMS	Isotope Ratio Mass Spectrometry
JOEL	Japan Electron Optics Laboratory
kV	Kilovolt
LC-MS	Liquid Chromatography – Mass Spectrometry
LC-UV	Liquid Chromatography with Ultraviolet- Visible Detection
LOD	Limit of Detection
L-PAC	L-phenylacetylcarbinol
M	Molar
<i>m/z</i>	Mass to Charge ratio
MA	Methamphetamine
MALDI-MS	Matrix-assisted laser desorption/ionization – Mass Spectrometry
MDMA	Methylenedioxymethamphetamine
MeOH	Methanol
mg	Milligrams
mm	Millimetre
mmol	Millimole
mol	Mole
Mp	Melting Point
MS	Mass Spectrometry
P2P	Phenyl-2-propanone
PCA	Principal Component Analysis
Pd/C	Palladium on Carbon
PDC	Pyruvate Decarboxylase
PE	Pseudoephedrine
PFP	Pentafluorophenyl
ppm	Parts per Million
psi	Pounds per Square Inch

r.t	Room Temperature
RP	Reverse Phase
SPR	Surface Plasmon Resonance
TFA	Trifluoroacetic acid
THC	Tetrahydrocannabinol
THF	Tetrahydrofuran
TIC	Total Ion Chromatogram
TMS	Trimethylsilyl
UPLC	Ultra-Performance Liquid Chromatography
V	Volts
v/v	Volume per Volume
VPFSD	Victoria Police Forensic Services Department
w/w	Mass per Mass (Weight per Weight)

ABSTRACT

Australian clandestine drug laboratories are constantly seeking and utilising alternative methods to produce methamphetamine. These methods are in response to restrictions placed by government on chemicals such as phenyl-2-propanone (P2P) in the early 1980s, or pseudoephedrine from the mid-2000s. Law enforcement agencies have taken great interest in the nitro-aldol reaction occurring between nitroethane and benzaldehyde that can be used in a number of synthetic pathways to methamphetamine. As such, an investigation is warranted into what products can be formed from this reaction and exactly how these compounds fit into the manufacture of methamphetamine. The resulting products, namely phenyl-2-nitropropene (from the P2P pathway) and 2-nitro-1-phenyl-1-propanol (from the ephedrine pathway) are directly dependant on which chemical base is used; the base may therefore be used to provide an indication of a possible methamphetamine manufacture pathway at a clandestine laboratory.

Restrictions on pharmaceutical drugs containing pseudoephedrine were introduced by the Australian government in 2006. Here, an investigation is carried out in conjunction with Victoria Police Forensic Services Department (VPFSD) after a large quantity of L-alanine (an amino acid) was seized from a clandestine laboratory. As this amino acid can be bought in large quantities very cheaply from any supplement store, its potential as a precursor of a synthetic pathway to methamphetamine was examined. This pathway focused on the formation of pseudoephedrine *via* a three step synthesis of *N*-methylalanine.

As new methods are being developed for the manufacture of methamphetamine, a detection system that can handle complex samples containing methamphetamine and its associated precursors and cutting agents is needed to detect new compounds. *In-silico* optimised one dimensional and two-dimensional high performance liquid chromatographic (2D-HPLC) separations of a model methamphetamine seizure sample provided an excellent match between simulated and real separations and are described for the first time. Targeted

separation of model compounds was completed with significantly reduced method development time. This separation was completed in the heart-cutting mode of 2D-HPLC where a selected portion of a peak is transferred from one dimension into another dimension of different retention mechanisms. C18 columns were used in both dimensions taking advantage of the selectivity difference of methanol and acetonitrile as the mobile phases. This method development protocol is most significant when optimising the separation of chemically similar compounds, as it eliminates hours of trial-and-error injections commonly required to identify the optimised experimental conditions. After only four screening injections the gradient profile for both 2D-HPLC dimensions was optimised *via* simulations. Importantly this process ensured the baseline resolution of diastereomers (ephedrine and pseudoephedrine) in 9.7 min which has been a great challenge for analysts.

The selection of two orthogonal columns for 2D-HPLC separation of complex drug samples can be a labour intensive and time consuming process as conventional methods utilise a trial-and-error approach. A novel column selectivity protocol was established that was capable of identifying the most appropriate orthogonal columns, for the separation of interested compounds. A data processing pipeline, created in the open source application OpenMS[®], was developed to map the components of equal mass across a library of HPLC columns whilst having limits of detection comparable to literature values across both dimensions. The two-dimensional separation space was compared by measuring the fractional surface coverage, $f_{coverage}$. A model methamphetamine sample was made and tested with this system and identified two sets of suited column combinations (Kinetex PFP/Synergi Hydro and Bonus RP/Pursuit XRs Diphenyl) that predicted an $f_{coverage}$ of 0.44. OpenMS[®], in conjunction with algorithms designed in house, have allowed for a significantly quicker selection of two orthogonal columns, which have been optimised for a 2D-HPLC separation of methamphetamine-type samples.

The Kinetex PFP and the Onyx Monolithic C18 columns were selected after further analysis of the stationary phases and were used in the chemical mapping of a

methamphetamine pathway, using 2D-HPLC and LC-MS. The impurities and by-products were mapped from start to finish to create a tabular chemical fingerprint that helped in the identification of synthetic route and precursors used. An alternative method for the identification of synthetic route was trialled using LC-MS and principal component analysis on 22 real methamphetamine seizure samples. The preliminary study was able to differentiate pseudoephedrine based on concentration (intensity count), thus demonstrating the importance of this platform technology.

This thesis presents a platform technology protocol for the comprehensive chemical fingerprinting of methamphetamine seizure samples of interest to the Victoria Police Forensic Services Department. Further key aspects of methamphetamine synthesis have been developed including the investigation of the simple amino acid L-alanine as a viable alternative precursor.

Highlights of this research include:

- The successful synthesis of novel pathways to methamphetamine from easily accessible materials.
- The optimisation of one-dimensional and two dimensional HPLC separations using simulation software of forensically important samples.
- The development of platform technology that allows for chemical mapping of clandestine pathways for illicit drugs.
- The use of principal component analysis to efficiently identify synthetic route in random methamphetamine seizure samples.

CHAPTER 1:

INTRODUCTION TO METHAMPHETAMINE

Author's Note: As this thesis deals with both analytical chemistry and some general synthetic chemistry a broad introduction of methamphetamine will be offered in Chapter 1 with a *niche* introduction presented at the start of each results chapter.

1.1 History of Methamphetamine

Methamphetamine and amphetamine are highly addictive psychostimulant drugs that affect the neurotransmitter systems of the brain, providing the user with increased alertness, energy and euphoria [1]. Ephedrine (Figure 1, Compound 1) was first used as a precursor for the synthesis of methamphetamine (Figure 1, Compound 2) by Akira Ogata, in 1919 [2]. The active alkaloid ephedrine was discovered within the Ephedra plant (*Ephedra sinica*) in 1885. The use of the Ephedra plant has been thoroughly studied [3] and its use dates back well over five thousand years in Chinese medicine [4]. Upon the discovery of the active alkaloid of ephedrine, other species of the *Ephedra* plant have been analysed in order to identify the compound. It is now known that only 25 of the 45 species of *Ephedra* contain ephedrine, which is found within the leaves and in low concentrations of 1-2% [5]. Medically, ephedrine is known to offer a variety of therapeutic benefits for nasal decongestion, appetite suppression, stimulation, and the relief of asthma and bronchitis [2].

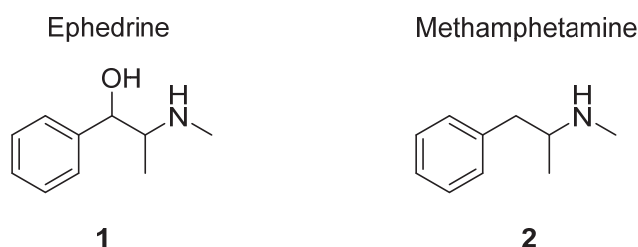


Figure 1: Ephedrine **1** and methamphetamine **2** structures.

Methamphetamine, similar to amphetamine but more potent, is water soluble, making it suitable for intravenous delivery into the body [6]. Because of this methamphetamine was widely used by the British, Japanese and the Americans during World War II as an aid to keep allied troops awake. Also, Japanese suicide pilots were given particularly large doses before their missions, enabling them to stay alert and fly for long hours [2]. The end of the war meant that military stores of the drug in Japan were readily available to the public on top of the already abundant over the counter pharmacy supply [4], inducing the first

methamphetamine epidemic in Japan. Methamphetamine abuse grew and reached its peak in 1954, where the number of methamphetamine abusers was estimated at 550,000, with 55,000 people suffering methamphetamine-induced psychosis [7]. In 1940, the Burroughs Wellcome Company in Britain, commercially introduced methamphetamine tablets by the name of Methedrine [8], along with intravenous amphetamines of the same name used for bringing patients out of anaesthesia [9]. During the 1940's and 1950's this methamphetamine tablet was marketed as a diet aid and, asthma, attention deficit disorder, narcolepsy and depression treatment [9]. In America, the product was deemed safe by the Food and Drug Administration (FDA) [9] and without risk of addiction, and as such was prescribed for many different ailments without caution or monitoring. Due to its accessibility it was abused by athletes, students and truck drivers as a non-medical stimulant [9].

Amphetamine inhalers have been available since the early 1930s in the United States with the S. Pfeiffer Company introducing 'Valo inhalers'. However, in the late 1950's the inhalers contained 150-200 mg of methamphetamine [10], resulting in drug abusers breaking open the inhalers to ingest the contents [10]. Widespread acts of violence and crime were linked to inhaler use and abuse, resulting in an FDA ruling in 1959 which found the inhalers available by prescription only. The 1960s saw an increase in injectable methamphetamine being prescribed to treat heroin addiction and increased abuse of this type of the drug [10]. This decade also marked the emergence of methamphetamine related health and societal issues in Australia [11]. The 1970s brought about a legislative change due to the increase of abuse, seeing all amphetamine products receiving a schedule II classification. This meant that although two types of amphetamine tablets were still available upon prescription; methylphenidate (Ritalin) and the diet drug phenmetrazine (Preludin) a new prescription had to be filled every time these drugs were prescribed [12]. Following increasing abuse, most of the nasal inhalers were also removed from the market completely by 1971 [13].

By the 1980s prescriptions were down 90% from those generated for methamphetamines in the 1960s, with this figure dropping again by a third around

1990 [14]. As restrictions were established and enforced on prescription methamphetamine, clandestine production of the drug was on the rise, using precursors which were legal and easily obtained during this time [4, 15]. By the mid-1980s nearly all street methamphetamine was produced in clandestine laboratories, rather than being sourced from legally produced pharmaceuticals (such as cold and flu medication) [4].

1.2 The Australian Methamphetamine Problem

The crystalline form of methamphetamine, also known by the street names; ice, crystal meth, meth, glass, crystal, shard, puff, shabba, rock, yaba and tweak first became a drug of concern in Australia in the early 1990s and since 2010 there has been an increase in both supply and demand for it [16]. While this escalation was observed throughout the world, the increase in Australia was substantially more than was seen internationally. Globally the weight of methamphetamines seized between 2009 and 2014 nearly tripled (see Figure 1.1), whilst the latest Australian statistics show the weight of border seizures has increased 60 fold between 2010 and 2014.

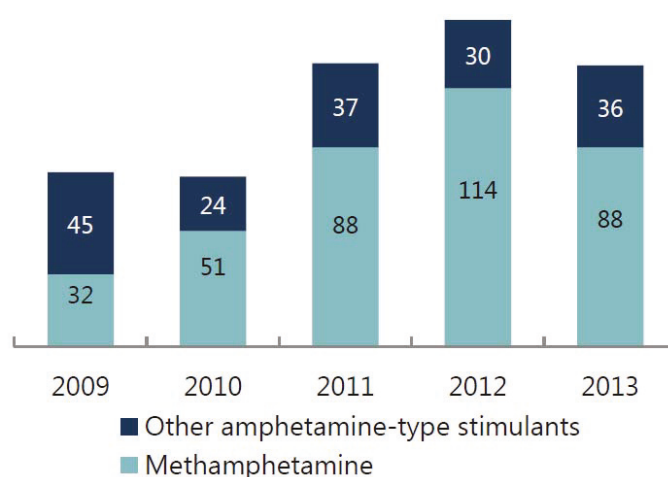


Figure 1.1: Weight of global seizures of methamphetamine and amphetamine-type stimulants, in tonnes [16].

Methamphetamine is now the second most commonly used illicit drug in Australia, second only to cannabis [17]. Ice demand and supply has also outstripped that of other amphetamines, contributing 79% of all amphetamine based border seizures in 2013-2014 up from 61% in 2010-2011 [17]. A significant issue with the policing of methamphetamine supply in Australia is that it is one of the only drugs which is both produced locally in large quantities, and imported from overseas [17]. The main precursor for ice manufacture; pseudoephedrine, was listed as a controlled substance under the Victorian Drugs, Poisons and Controlled Substances Act 1981. This made it harder to obtain the precursor for manufacturing purposes and has contributed to an increase of methamphetamine product being introduced from other countries [17].

There were in excess of 268,000 regular users of methamphetamine in Australia between the years 2014 and 2015, which is almost triple that identified in 2010 [18]. There were significant increases in amphetamine related ambulance call-outs between 2013 and 2014, including a 23% increase in metropolitan Melbourne and 27.2% increase in regional Victoria [18]. This increase has been attributed to the increase in methamphetamine use. It is now the fourth most common drug involved in ambulance call-outs [19]. The median purity of methamphetamine (Figure 1.2) is also increasing significantly going from 7% in 2009-2010 to 62% in 2013-2014 [17] this may be a contributing factor to the ambulance callouts involving methamphetamine as the drug available now is much more concentrated than it was less than ten years ago.

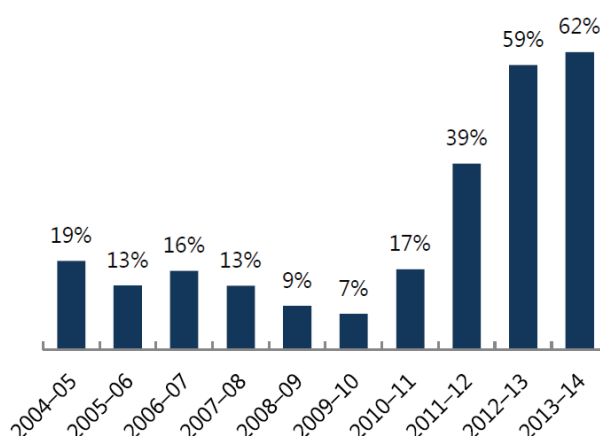


Figure 1.2 Median purity of methamphetamine between years 2004-2014 [17].

1.2.1 Ice Taskforce

It is for these reasons the Australian Government, as part of the national ice action strategy created the 'National Ice Taskforce' on the 8th April 2015. The taskforce spoke to over 100 experts on research, prevention, education, treatment and law enforcement and released a report detailing the methamphetamine related statistics and a list of recommendations to help with the 'ice epidemic'.

The executive summary of the ice taskforce report highlights many areas which need attention to combat the use of ice within Australia. Including;

- The need to support families and communities to enable them to better handle people affected by ice.
- Strengthen efforts to reduce the demand for ice.
- Treatment and support services for users.
- Prevention of first time use.
- Co-ordinated and targeted efforts to disrupt supply.
- Better data, more research and reporting to keep responses on track.

In particular there are two recommendations listed below that highlight the need for better analytical chemistry platforms for illicit drug profiling (see Figure 1.3):

Recommendation 36
The Commonwealth Government should establish and fund a new research programme to support law enforcement responses to illicit drugs, including ice.
The scope of the research programme should be confined to illicit drug and precursor markets, focusing on key gaps and priorities identified in the first instance by the National Ice Taskforce, and subsequently by the Intergovernmental Committee on Drugs.
Recommendation 36
The Commonwealth Government should establish and fund a new research programme to support law enforcement responses to illicit drugs, including ice.
The scope of the research programme should be confined to illicit drug and precursor markets, focusing on key gaps and priorities identified in the first instance by the National Ice Taskforce, and subsequently by the Intergovernmental Committee on Drugs.

Figure 1.3: Extracts from the 2016 national ice taskforce report [17].

1.3 The appeal of Methamphetamine

As methamphetamine is an extremely powerful stimulant, it is in very high demand despite its extreme addictive properties [17]. People using ice are said to experience confidence, for example, the case of use in local football which has recently come to light, with players as young as 14 taking the drug “to feel like superman” when running onto the football field [20]. Other sought after effects of ice include: euphoria, which is diminished after taking the drug regularly, much higher doses are needed to achieve this feeling [6], and enhanced sexual pleasure [21]. The popularity and word-of-mouth among society has led to more people wanting to try and experience the effects of the drug [17].

From a production perspective methamphetamine is an ideal drug presenting a high profit margin particularly in Australia where methamphetamine sells for \$675/g AUD compared to Europe at \$49/g AUD (Figure 1.4) [17]. It is therefore, feasible for dealers to carry small amounts which can be easily concealed and transported while still making a sufficient profit. Unlike many other illicit drugs methamphetamine does not depend on plant based material availability and is also very flexible; it can be produced on a small scale or large. There is not one single precursor or methodology for synthesis, but rather many materials and pathways which can lead to its production. This flexibility of production makes it harder for law enforcement to apprehend producers, it also means that if restrictions are placed on one precursor an alternative method can be used or developed, switching to a readily available precursor, always staying one step ahead of the law. Australia is also the most attractive import destination due to relative high wealth of the population and high demand of the product [17], the price per gram for methamphetamine in Australia substantially exceeds that of other countries, even after taking into account external monetary forces (Figure 1.4).

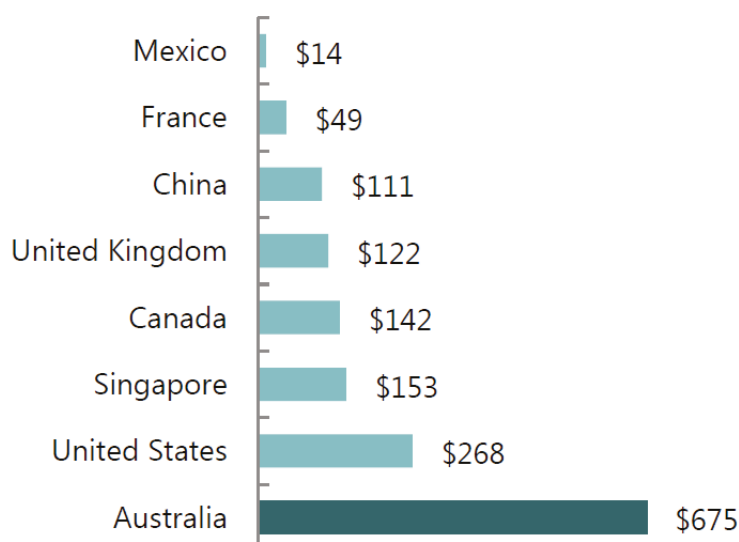


Figure 1.4: Median street price of a gram of ice in Australian dollars (AUD) [17].

Border seizure figures in Australia in recent times have reflected this increase in importation of methamphetamine. Almost 3 tonnes of the drug has been seized at the border between 2010 and 2015 (Figure 1.5) [17]. These seizures have varied from small to large scales, over a variety of smuggling methods, including; within aeroplanes, ships and mail, hidden in food, toys, on people, in machinery and as parts shipments [17].

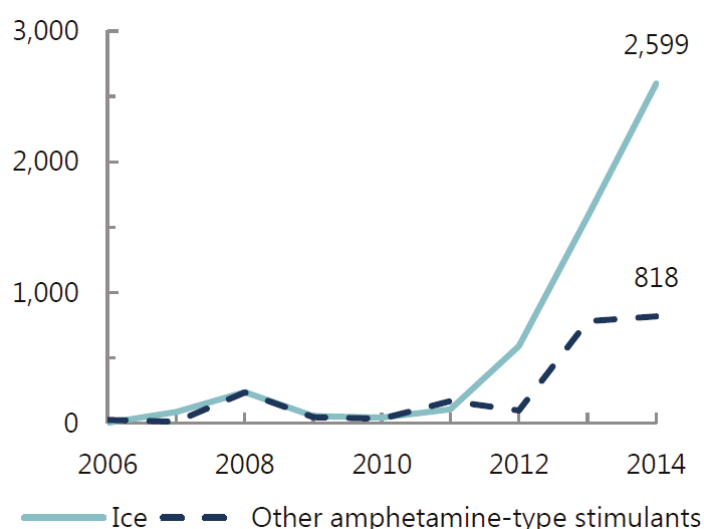


Figure 1.5: Weight of Australian border seizures of ice and other amphetamine-type stimulants in kilograms [17].

1.4 Local Synthesis

In addition to the drug being imported, large amounts of precursors have been intercepted on their way into Australia, in an attempt to combat the restrictions on chemical precursors and to continue drug synthesis within Australia [17]. Domestic seizures of the drug have also been rapidly increasing, which could indicate a rise in local synthesis. The weight of seizures between 2010 and 2014 has increased over five fold. Organised crime groups are at the centre of the importation, manufacture and distribution of ice, in fact, accounting for approximately two thirds of the groups on the 'Australian Crime Commission's National Criminal Target List' and three quarters of the crime groups judged as high risk to the community. The organised crime groups have evolved over the years from working within their own niche base to working co-operatively with other crime groups. This collaboration is based on financial and criminal benefit, rather than loyalty [17].

Methamphetamine produced in Australia is synthesised from precursors such as pseudoephedrine (or less commonly ephedrine) and phenyl-2-propanone [17]. These precursors also have legitimate pharmaceutical or pesticide uses, and as such were readily available until their illicit use was identified [5]. Often either the methamphetamine is imported from another country, or a precursor material is imported for the synthesis of the drug [17].

1.5 Precursors to methamphetamine

The methods of methamphetamine manufacture carried out in clandestine laboratories have changed over time as precursors have become controlled [22]. As a precursor that was readily available becomes harder to obtain, other methods to reach the final product evolved to ensure the production of the drug could continue [23]. As methamphetamine synthesis advances with control changes in precursors, forensic chemists need to be able to identify new methods/pathways in the clandestine laboratory scene [22]. Clandestine

synthesis of drugs begin with a precursor either distant (a compound which is converted to an immediate precursor, followed by conversion to the drug) or from immediate precursors. Immediate precursors are ideal for the manufacturer however the more they are used, the more chance they have of being restricted by law enforcement authorities [22]. Anyone can access step-by-step instructions on the manufacture of methamphetamine from a range of precursors on websites such as 'Erowid' [24]. The challenge therefore becomes obtaining these precursors, and not so much the conversion of them to methamphetamine.

1.5.1 Pseudoephedrine/ephedrine

In 2014, the Australian crime commission reported that from the 448 major clandestine laboratories detected, 91% of seized methamphetamine had been synthesised using pseudoephedrine [25]; it is safe to assume that it is the largest precursor source for methamphetamine manufacture in Australia. In Victoria, there have been cases where pseudoephedrine was synthesised rather than extracted from over the counter medication [personal correspondence with Dr Jim Pearson at Victoria Police Forensic Services Department]. The selective synthesis of the correct pseudoephedrine enantiomer for methamphetamine becomes a difficult task as two stereocentres (highlighted by red circles in Figure 1.6) are formed in the synthesis.

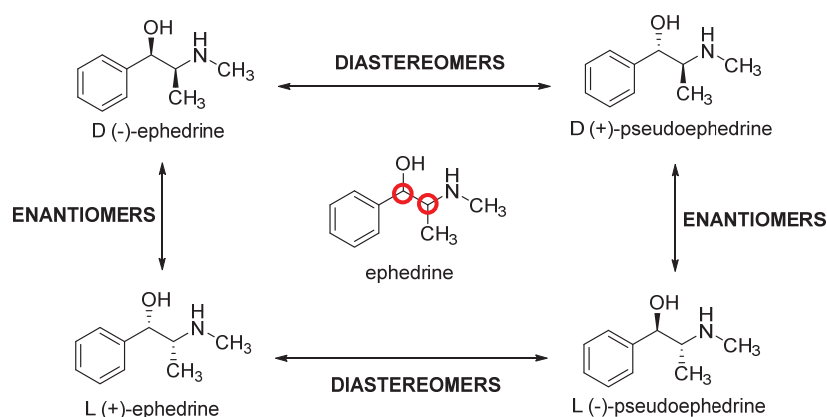


Figure 1.6: The 2 enantiomers and 2 diastereomers formed in the synthesis of pseudoephedrine.

One set of diastereomers form D-methamphetamine, a psychoactive drug; The other set of diastereomers (see Figure 1.7) form the significantly less active L-methamphetamine, which is similar to the properties of pseudoephedrine and is likewise known to be used for the relief of nasal decongestion and is in products such as 'Vicks Vapour Inhalers'.

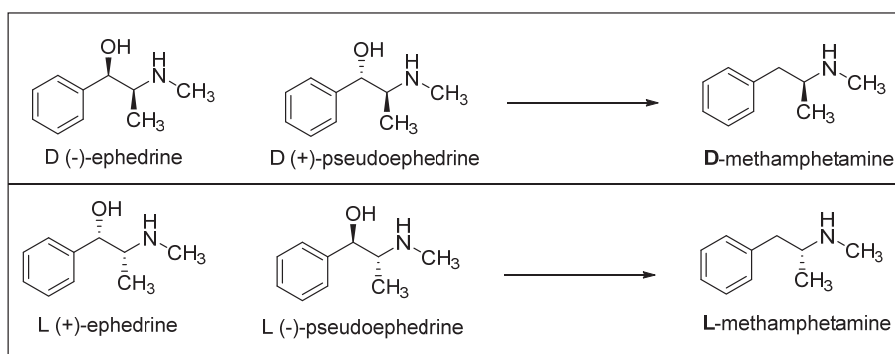


Figure 1.7: The formation of D-methamphetamine and L-methamphetamine from different diastereomers.

Clandestine synthesis of pseudoephedrine/ephedrine is relatively uncommon due to the complex and sometimes lengthy procedures, resulting in racemic mixtures which require enantiomeric purification; an extremely challenging task for synthetic organic chemists [26].

The extraction process of pseudoephedrine from cold and flu medication is quite simple that requires only a glass vessel, caustic soda, ethanol /methylated spirits, and a filter [27]. This process has been investigated by Pigou *et al.* [26] and it was found to extract other active ingredients that in turn react in the conversion process to methamphetamine producing by products. Additionally it was found that the use of ethanol or methanol as extraction solvents lead to the formation of *N*-ethyl-ephedrine and *N*-methyl-ephedrine, especially when using the hypophosphorous acid method to make methamphetamine [26].

However, in Victoria all medication containing pseudoephedrine is controlled and access to substantial amounts can become problematic. Every time a person purchases medication with pseudoephedrine, they are required by law to present their drivers licence and have their details recorded on a national database. This

alone can be a deterrent as their identity is now on record for the purchase of this precursor.

Recently, an alternative fermentation method which uses cheap and easy to source ingredients has been used for the biosynthesis of the ephedrine precursor, L-phenylacetylcarbinol (L-PAC) [28]. The fermentation process converts benzaldehyde into L-phenylacetylcarbinol (L-PAC) which is a precursor for the production of L-ephedrine [28, 29]. Enzymes from certain yeast strains are able to catalyse a reductive amination reaction. The same yeast (baker's yeast - *Saccharomyces cerevisiae*) is used in this process as for most alcohol fermentations, as it is robust. The enzyme responsible for the conversion of the benzaldehyde is pyruvate decarboxylase (PDC) [30]. Fermentation of glucose with yeast results in the formation of pyruvic acid (pyruvate) which then undergoes decarboxylation (*via* PDC catalysis) to form acetaldehyde, shown in Figure 1.8. When acetaldehyde is in the presence of benzaldehyde it condenses to form L-PAC [26]. However, while this enzyme is able to synthesise L-PAC it is also associated with the production of benzyl alcohol, an unwanted by-product of the synthesis which when coupled with the oxidation of the benzaldehyde to benzoic acid results in a diminished yield of useable product [30].

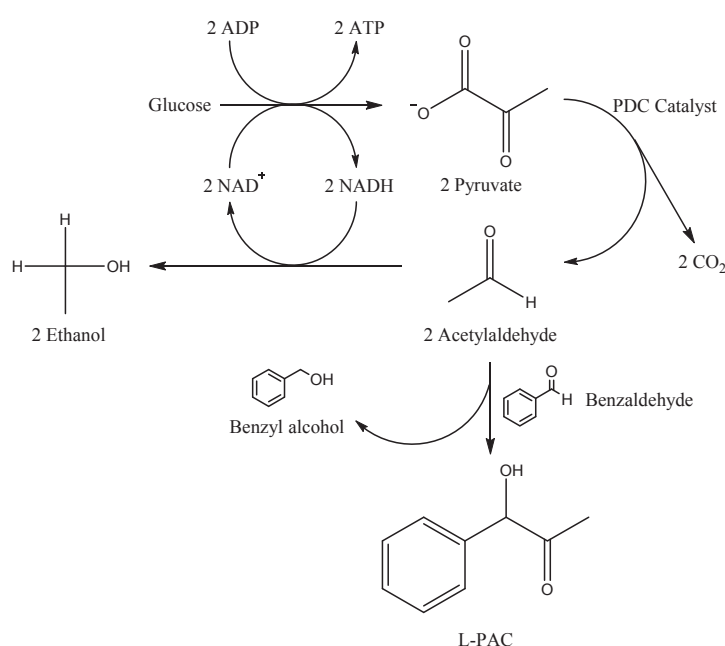


Figure 1.8: Fermentation of precursor L-PAC.

1.5.2 Phenyl-2-propanone (P2P)

Phenyl-2-propanone (P2P) is the second most common precursor used in clandestine manufacture of methamphetamine [17]. It is usually prepared from phenylacetic acid which is then treated with lead (II) acetate at high temperatures or stirring a mixture of acetic anhydride and sodium acetate/pyridine at reflux [26, 31]. The production of methamphetamine using P2P frequently involves a large amount of precursor, converting 10-20 kilograms of P2P to make a single kilogram of methamphetamine [17]. The reaction between phenylacetic acid and acetic anhydride is complex but is well described by Allen *et al.* [31] who proposed mechanism illustrated in Figure 1.9.

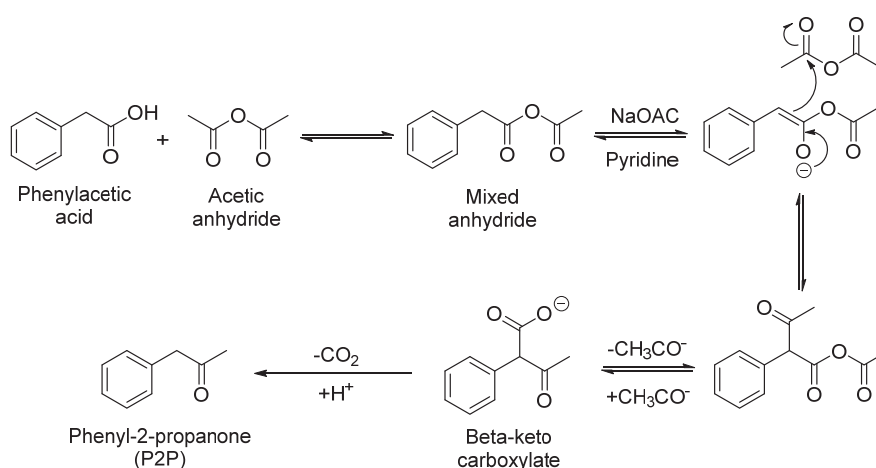


Figure 1.9: Reaction between phenylacetic acid and acetic anhydride [31].

Phenyl-2-propanone can also be prepared from benzaldehyde, which is reacted with nitroethane to produce β -methyl- β -nitrostyrene and will be discussed in more detail in Chapter 2. The nitrostyrene product can then be directly reduced to P2P using iron and hydrochloric acid [32].

Both complex pathways (phenylacetic acid and benzaldehyde) to P2P, have numerous side reactions resulting in characteristic impurities. Allen *et al.* [31] indicated that route-specific by-products could be detected in crude reaction mixtures. Specifically, with the phenylacetic acid method a by-product detected that has significant relevance is the production of dibenzyl ketone. This ketone is

difficult to separate from P2P, as such non-commercial P2P will probably contain dibenzyl ketone, important information for police to know when trying to trace the source of the precursor.

1.6 Detection methods of methamphetamine

1.6.1 Police road-side testing

Since 1976, legislative framework in Victoria has been in place to screen drivers for alcohol [33]. Since this type of testing came into effect the number of drivers tested and found to be driving with excessive alcohol in their system has reduced significantly [33]. However, the decrease of alcohol involvement in road trauma incidents also saw an increase in the involvement of other types of drugs such as methamphetamine, amphetamine type substances (ATS) and cannabis [33].

In 2000, legislation was introduced by the Victorian Government to prosecute drivers who were impaired by other drugs, however this was based on the recognition of impairment in drivers and enforcement was not high. In 2004 legislation was introduced which mimicked that of the random alcohol screening for drivers using oral fluid testing at the roadside to detect the presence of methamphetamine, methylenedioxymethamphetamine (MDMA), and cannabis (THC) [33]. In fact, out of the 4,497 oral fluid samples collected under the road safety act of Victoria in 2015, the Victorian Institute of Forensic Medicine found methamphetamine in 73.5% of cases, amphetamine in 71% of cases and cannabis in 53.9% of cases [34].

The roadside screening is a three part process, initially involving an alcohol screen by the roadside then a preliminary roadside oral fluid test using an absorbent collector which takes approximately 3 to 5 minutes. If the results are negative the driver is free to continue on, however if a target drug is detected the driver accompanies police into the roadside vehicle to provide a second oral fluid sample which is tested on an oral fluid screening device by a trained and authorised police officer. If the result is positive the driver is informed of the results and details are collected for charges to be laid in the event of laboratory confirmation. The third

stage in the process, where one or more of the target drugs are confirmed by laboratory analysis results in the driver being charged with an offence [33].

1.7 Analytical Separation and Detection Methods for Methamphetamine

Methamphetamine has received a great deal of attention from research groups all over the world as the ice epidemic continues to grow and make headlines [35]. Identifying methamphetamine in different mediums such as urine [36], saliva [34], blood [37], plasma [38], hair [39], finger nails [40], fingerprints [41], sweat [42] and semen [43] have been areas of interest for forensic analysts. Because of the range of sample types and their complex nature, a variety of instrumentation has been used for the analysis of samples containing methamphetamine, details of which are summarised in Table 1.1 below.

Table 1.1: Literature work that has been carried out in the detection of methamphetamine.

Detection Method	Medium type	Literature Reference
GC-MS	Plasma and urine	[38]
GC-MS	Blood	[37]
GC-MS	Hair	[39]
GC-MS	Insects	[44]
GC-MS	Nails	[45]
HPLC	Commercial tablets	[46]
2D-HPLC	Street sample	[47]
LC-MS	Urine	[48]
LC-MS	Fingerprint	[49]
LC-MS/MS	Urine	[50]
MALDI-MS	Fingerprint	[41]
Chemiluminescence	Urine	[51]
Electrochemiluminescence (ECL)	Street samples	[52]
Electrospray ionisation (ESI-MS)	Human urine	[53]
HPLC Fluorescence	Human urine	[36]
Fluorescence Polarisation Immunoassay	Purchased standards	[54]
GC/FT-IR	Purchased standards	[55]
Head-space solid phase microextraction/GC-MS	Purchased Standards	[56]
Ion mobility spectrometry	Hair	[57]
Isotope ratio MS	Street samples	[58]
Laser microscopy	Hair	[59]
Desorption ionisation on silicon mass spectrometry imaging (DIOS-MSI)	Fingerprint Sweat	[60]
NMR	Purchased standards	[61]
² H NMR	Synthetic pathway products	[62]
Capillary electrophoresis	Urine	[63]
Electromembrane surrounded-solid phase microextraction (EM-SPME)	Urine and blood	[64]
Surface plasmon resonance (SPR)	Purchased standards	[65]
Field Assymetric Ion Mobility Spectrometry	Air	[66]
Colourimetric test	Mobile telephone	[67]

Interestingly, the development of analytical technology for forensic applications is often limited by the uptake of new methods, due to the implications in the court room. New analytical methodologies need to be thoroughly tested and come under strict scrutiny in cross examination of expert witnesses. Regarding methamphetamine determination, GC-MS is the most commonly used analysis method due to it being one of the first utilised in this space and tested under law.

Typically GC-MS systems are coupled with quadrupole mass spectral detectors affording only low resolution data, whereas LC-MS is commonly coupled with high resolution detectors (such as time of flight) which has improved the determination of methamphetamine. Bespoke techniques such as the others listed in Table 1.1 are typically used in the research domain. While these are not commonly used for prosecution purposes they play a strong role informing the forensic analysts towards reliable methamphetamine detection.

1.8 Two-dimensional HPLC

Liquid chromatography is a method used by analytical and synthetic chemists to separate components within a mixture, based on the retention properties of the mobile phase (eluent) and the stationary phase (column) [68]. The most common form of liquid chromatography is known as 'reverse phase' which utilises a non-polar adsorbent stationary phase with a more polar mobile phase to ensure differential migration [68]. The use of liquid chromatography was first reported in 1903 by Mikhail Tswett with his work on plant cells and chloroplasts [68]. Tswett successfully separated plant pigments for the first time with a column, packed with various adsorbents [68]. In 1967, Horváth and co-workers established the very first pressurised chromatography system, known today as high performance liquid chromatography (HPLC) [69].

The separation power of conventional HPLC is limited when it comes to analysing complex samples [70]. A significant amount of effort has been dedicated to overcoming the limits of separation and resolving power of single dimension systems [70, 71]. This has resulted in the rapid development and evolution of two-dimensional high performance liquid chromatography (2D-HPLC)

The advantage of 2D-HPLC over conventional one-dimensional HPLC is its superior resolving power, taking full advantage of increased separation space [70, 72, 73]. Traditionally, two-dimensional separations are a very time consuming process [74], as numerous parameters such as stationary phase selection, mobile phase

selection, sampling frequency and analysis time must be optimised to realise the full potential of the system [75].

Two-dimensional HPLC has been recently used in fields that require the analysis and separation of complex samples such as pharmaceuticals [76], food analysis [77], wine [78], metabolomics [71, 72], proteomics [79] and environmental analysis [80]. It is significant for a technique to be used in such a broad range of scientific fields and 2D-HPLC has helped analysts understand and visualise the complexity of some samples.

There are two different types of 2D-HPLC: offline and online - both having their own advantages and disadvantages [81]. Offline operates by collecting and storing fractions as they elute from the first dimension column [81], followed by individual injection of those fractions into the second dimension. The advantage of this is its extremely large separation power based on the peak capacity generated by the uniqueness of the retention mechanisms [81], and the downfall being it is a labour intensive process (hours to weeks) with extraordinarily long analysis times, depending on the complexity of the analysed sample [82].

Online 2D-HPLC works by transferring eluting fractions from the first dimension to a second dimension which is running simultaneously using a switching valve and sample loops shown in Figure 1.10. This transfer can be done for the entire first dimension, known as 'comprehensive' or for selected peaks of interest, known as 'heart-cutting' [74]. The advantage of online is the fact it is fully automated by the system and can be done rapidly. However, when using online 2D-HPLC the second dimension needs to be configured to elute a compound before the next fraction is transferred in order to minimise the chance of any peak overlap from different fractions, placing a serious time constraint on second dimension analysis time [74]. This emphasises the need for 2D-HPLC systems that can operate at high speeds, particularly in the second dimension [74].

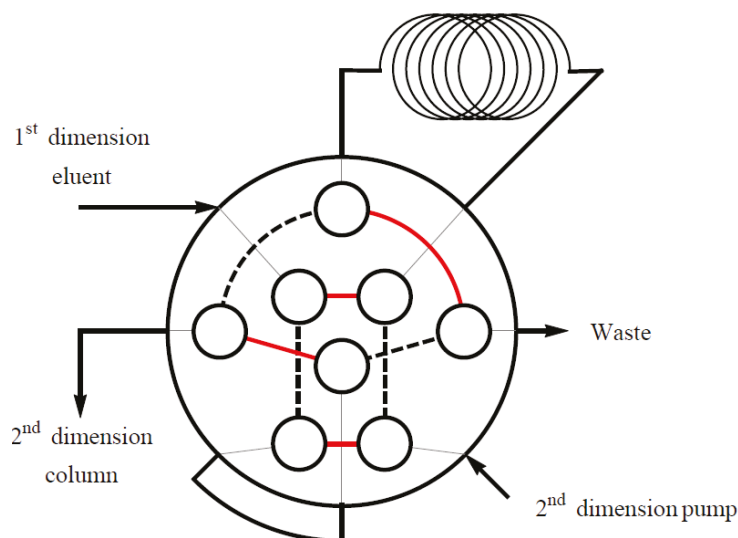


Figure 1.10: Online 2D-HPLC switching valve.

1.9 In-Silico Optimisation Chromatography (computational modelling)

Computer supported, chromatography method development started in the mid-1980s as IBM released the first PC (personal computer) [83]. Tju-lik *et al.* used computer simulations to study the abnormal peak shapes caused by chromatographic solvents, highlighting that peak splitting and distortion can be modelled by the effect of the solvent on the column [84]. Following this, the first simulation software (DryLab®) for HPLC was released in 1988 after significant fundamental development by Horváth and co-workers into the solvophobic interactions [85], ionogenic substance interactions [86], and ion-pair formation of nonpolar stationary phases [87]. Snyder, Dolan and co-workers used Drylab® software in order to interrogate isocratic [88] and gradient [89] high performance liquid chromatography, highlighting the importance of a simulation approach such as for significant industrial problems. This type of modelling was further developed by Lewis *et al.* [90] who incorporated the pH of the mobile phase into

the prediction of the separation. Challenges in applying simulation predictions to large molecules were identified by Ghrist *et al.* [91] who went on to show that with precautionary adjustments of the simulated separation gradient these issues can be overcome. Temperature has been highlighted as a key parameter for the optimisation of simulations that was initially developed by Hancock *et al.* [92] and further reviewed by Dolan [93]. The testing of temperatures was applied to peptides and proteins [94], highlighting that optimisation of both temperature and gradient steepness [95] is advantageous through the application on herbicides [96] and protein digests [96].

Also, octanol water partition has been used as a separation tool for scientists and Giaginis *et al.* [97] showed the importance of n-octanol as a mobile phase additive for polar compounds. The effect on n-octanol was shown to decrease as the lipophilicity increased, highlighting the importance of hydrogen bonding in the simulation mechanism for carboxylic acids. Monks *et al.* [98] emphasises the robust nature of this process and incorporates a two variable optimisation system; one for the column and one for the eluent bringing them together. This concept is important as the ability to combine the design space and opens up the opportunity to explore the use of this approach to a second stationary phase, which is required for the *in-silico* optimisation of two-dimensional HPLC.

Simulation software has been of interest to a range of areas of chemistry and has been successfully applied to drugs and pharmaceuticals [96, 99], phenolic pollutants [96], protein digests [96], enantiomers [100], protein-protein interactions [101], marine pigment samples [102] and fatty acid methyl esters [96]. Additionally, there are a range of chromatography modelling software packages available such as 'PESOS' made by Perkin-Elmer [103] and 'Simplex' made by Berridge [104].

This thesis will incorporate two different parts, as illustrated in Figure 1.11. The first part, described in chapters 2 and 3 will investigate the viability of some contemporary clandestine methamphetamine synthetic pathways in order to assess the risk of their potential appearance in future clandestine seizures. The second part outlined in chapters 4 and 5 will explore the optimisation for

advanced separations of complex seizure samples, followed by the development of platform technology for the chemical mapping and identification of precursors and synthetic route. This technology will be fully assessed in order to test its suitability to generate more advanced chemical fingerprinting analytical capacity for seizure sample analysis.

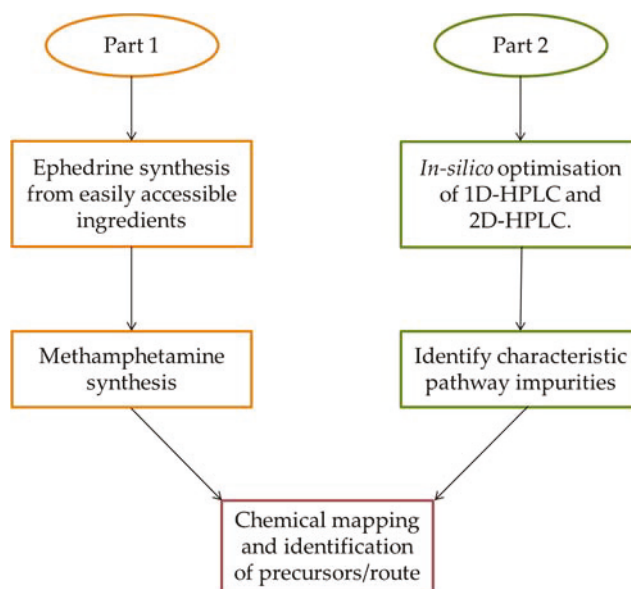


Figure 1.11: Generalised overview of the multidisciplinary approach taken in this thesis.

CHAPTER 2:

SYNTHESIS OF
PSEUDOEPHEDRINE/EPHEDRINE FROM
NITROETHANE AND BENZALDEHYDE

Author's Note: There are two synthetic chapters (2 & 3) included in this thesis which were undertaken in an alternative style to the more traditional synthetic chemistry format. As this thesis examines the chemical mapping of potential clandestine laboratory pathways, isolation and purification of compounds were deliberately not carried out, to effectively map all potential impurities from each step. The synthetic pathways investigated were performed to determine if it is a viable pathway to methamphetamine manufacture.

CHAPTER OVERVIEW

This chapter provides a brief introduction to the Henry Reaction (nitroaldol) and will discuss its history, mechanism, and literature reported uses in a range of different fields. It will also discuss the two main synthetic pathways used in the manufacture of methamphetamine, linking the Henry reaction (using benzaldehyde and nitroethane) to both routes.

A synthetic investigation will be carried out on the reaction between benzaldehyde **6** and nitroethane **7**. The products 2-nitro-1-phenyl-1-propanol **8** and phenyl-2-nitropropene **9** formed from this reaction was solely dependent on the bases used, illustrated in Figure 2.1. Coincidentally, both products are precursors to different clandestine pathways (ephedrine and P2P) which is of great interest to Victoria Police Forensic Services Department.

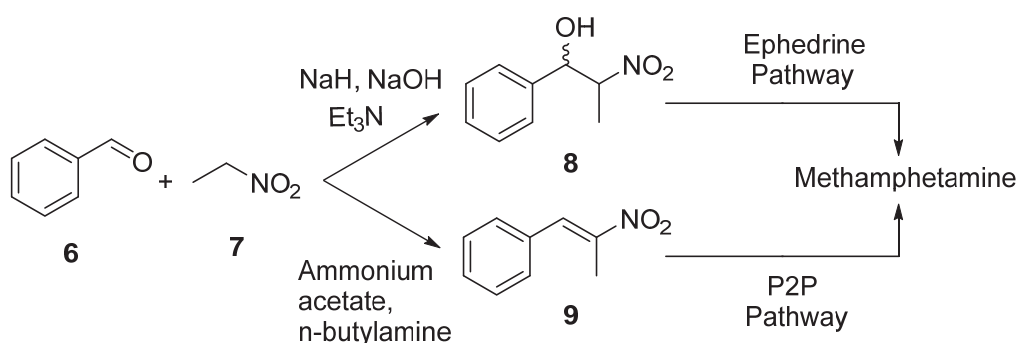


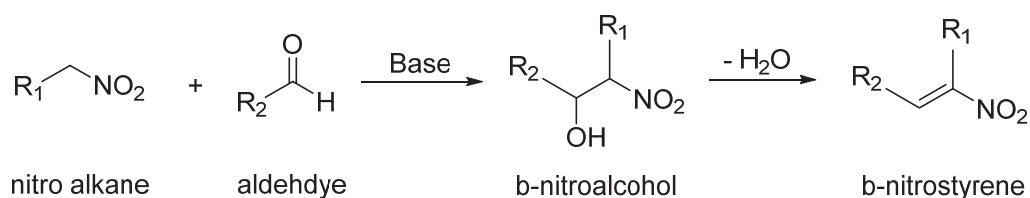
Figure 2.1: Resulting clandestine pathways when using different bases in the reaction between benzaldehyde and nitroethane.

Likewise, a full pathway to methamphetamine was explored from the 2-nitro-1-phenyl-1-propanol **8** product. Chemical mapping of each synthetic step and associated impurities will be carried out in Chapter 5, to identify by-products characteristic of the synthetic route used to generate the clandestine products.

2.1 INTRODUCTION

The Henry reaction, also known as the 'Nitro-aldol' reaction, was first reported in 1895 and is a base catalysed carbon-carbon bond forming reaction between nitroalkanes and aldehydes or ketones [105]. The reaction involves generating a highly reactive nitronate species *in situ* followed by nucleophilic addition to the carbonyl group of an aldehyde or ketone [106]. The Henry reaction is frequently used due to its highly functional scaffold and universal synthetic capabilities by easy manipulation of both the nitro and hydroxyl functional groups to make β -nitro alcohols (conventional product of the Henry reaction) [105]. Nitro alcohols can be easily converted to intermediates such as nitroalkenes (dehydration), α -nitro ketones (oxidation) and β -amino alcohols (reduction) [105]. These intermediates have found use in synthesis of pharmaceuticals (β -blockers, HIV protease inhibitor, antibiotics) [107], asymmetric synthesis and biocatalytic applications [107, 108]. As a consequence, there has been much effort to improve the Henry reaction with research into the use of catalysts, including catalyst controlled asymmetric reactions [106], catalyst controlled direct asymmetric reactions [109], rare earth catalysis [110], Zinc(II) based catalysis [111], copper based catalysis [112], cobalt based catalysis [113], organocatalysis [114], and anti-selective catalysis [115].

Benzaldehyde and nitroethane can be used in a nitroaldol reaction to form either of two products, a β -nitroalcohol or a β -nitrostyrene (Scheme 2.1). Interestingly, each of these two products can be used in synthetic pathways for two common, but alternative, precursors to the synthesis of methamphetamine, namely phenyl-2-propanone (P2P) and ephedrine/pseudoephedrine [58].

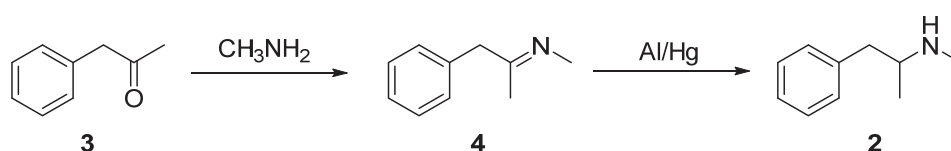


Scheme 2.1: Alternative products from the Henry reaction.

According to the Australian Crime Commission Illicit drug data report 2013-2014, benzaldehyde is classed as a 'significant precursor' to the manufacture of methamphetamine and approximately 10 tonnes of benzaldehyde was seized in Australia within the year of the report [25]. As such, the investigation of any synthetic reactions towards the synthesis of illicit drugs involving benzaldehyde is of utmost importance to clandestine laboratory investigators. The implications of this chemistry on the formation of methamphetamine needs to be considered as it relates to the two major pathways, the reductive amination of P2P and the conversion from ephedrine.

2.1.1 Reductive Amination of phenyl-2-propanone (P2P)

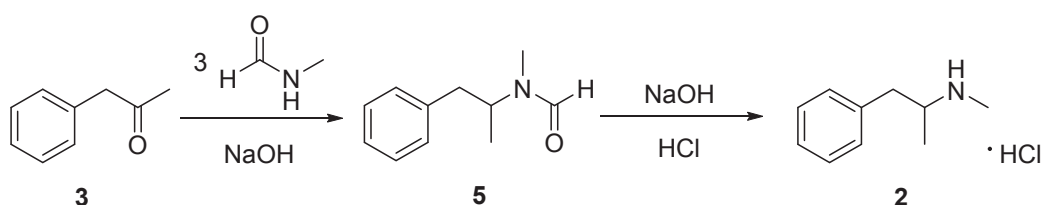
Phenyl-2-propanone (**3**) is an example of an immediate precursor and its conversion to methamphetamine (**2**) is the more complex of the two common methods. It initially requires the formation of an imine (**4**) with methylamine, followed by a metal reduction [22], as shown in Scheme 2.2.



Scheme 2.2: The reductive amination of P2P to Methamphetamine.

Alternatively, the Leuckart reaction can be used as shown in Scheme 2.3. This reaction produces the *N*-dialkylformamide (**5**) after the nucleophilic nitrogen

attacks the carbonyl carbon and subsequent reduction, using formic acid [15]. The intermediate product can then undergo a hydrolysis to form methamphetamine. In 1981, P2P (also known as phenylacetone) was listed as a controlled substance under the Drugs Poisons and Controlled Substances Act (Victoria), as well as in other Australian legislation, in an attempt to cut off the supply of precursors to clandestine laboratories. The act had the desired effect; with the number of seizures of clandestine labs decreasing for a few years [22]. However, a new age in methamphetamine production arose with the use of pseudoephedrine or ephedrine as a precursor [22].



Scheme 2.3: The Leuckart reaction of methamphetamine synthesis.

2.1.2 Pseudoephedrine Reduction

Pseudoephedrine (and to a lesser extent ephedrine) is a common ingredient in cold and allergy medications, with many having only pseudoephedrine as the active ingredient [116] (Figure 2.2).

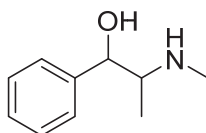


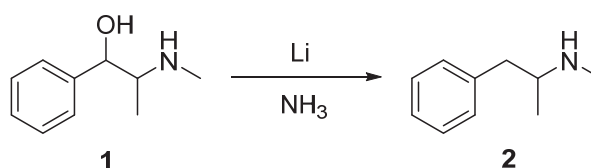
Figure 2.2: Structure of pseudoephedrine.

As P2P became more difficult to obtain in the 1980s, the development of alternative synthetic routes led to an increase of these medications being stolen, diverted or purchased in bulk for use in clandestine laboratories. In response, the

sales of products containing pseudoephedrine or ephedrine were reined in under strict regulations with the introduction of new laws [22]. While these compounds are now regulated, they are still available over the counter and do still provide methamphetamine cooks with a precursor for easy conversions on a small scale. There are two main processes for the conversion of pseudoephedrine to methamphetamine; the Birch reduction (also referred to as the 'Nazi method') and red-phosphorus/hydriodic acid methods [117].

2.1.3 Birch Reduction of pseudoephedrine to methamphetamine

The pseudoephedrine pathway shown in Scheme 2.4 involves pseudoephedrine (**1**) being added to a mixture of lithium metal (usually obtained from batteries) in anhydrous ammonia. The ammonia can be obtained from purchased gas cylinders or alternatively generated *in situ* from fertilizer products. When lithium is added to ammonia the solution turns blue; this is short lived, with the solution changing to grey as the reaction progresses [118]. Similar to all methods of methamphetamine production the Birch method has both advantages and disadvantages. Some advantages of this method are that the residual lithium is easily decomposed by water or alcohol and that excess ammonia is boiled off in the process [118]. The main disadvantage is that anhydrous ammonia is needed which is a difficult substance to handle as it is corrosive, hazardous, and potentially explosive.

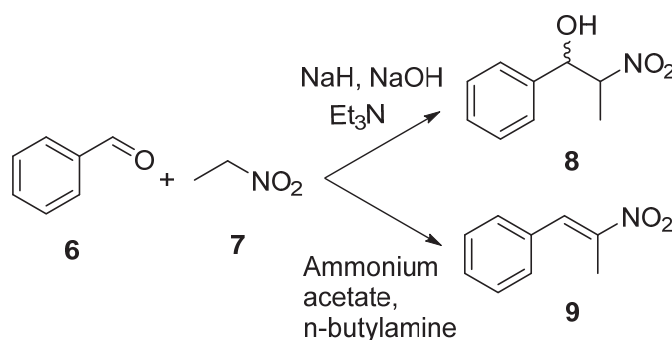


Scheme 2.4 Birch reduction of pseudoephedrine to methamphetamine.

The second common pseudoephedrine based method used is the red-phosphorus/hydriodic acid method, this is an appealing method due to the fact that it is quick, can produce relatively high yields and can be carried out in a 'one pot' process [119]. This method is functions by reducing the alcohol group to a

hydrogen [119]. There are several variations of this method, including one in which the reactant is cold or mildly heated (<60 °C) and others which involve heating the reaction to reflux [119]. The reaction variations involves both red phosphorus, which a clandestine laboratory may obtain from matches or flares, and hydriodic acid, either purchased or produced *in situ* [119]. Another variation of the same reaction process uses hypophosphorous acid and iodine to generate the hydriodic acid *in situ* [120].

The implications of base in the common Henry reaction when carried out using benzaldehyde (**6**) and nitroethane (**7**) was investigated, particularly as described in clandestine online drug forums such as the website 'Erowid' [24]. For the first time a comprehensive study of the Henry reaction using alternative bases is presented in this chapter (Scheme 2.5).



Scheme 2.5: Resulting products when using different bases in the reaction between benzaldehyde and nitroethane.

The range of synthetic routes for the generation of methamphetamine offer both a significant challenge for the forensic analysts while also affording a significant opportunity. The fact that there is a vast array of synthetic routes means that analysts must have a broader understanding of the chemistry, however with a range of routes the capacity to individualise samples is increased. Generally, methamphetamine seizure samples in Victoria are very pure and as such it is difficult to identify the route of manufacture. This opens up the opportunity to use intermediate samples in order to profile the provenance of the

methamphetamine. The nature of this task requires a multidisciplinary approach and requires analytical methodologies to inform the synthetic route investigation.

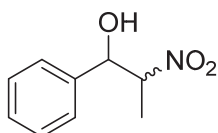
2.2 EXPERIMENTAL

All chemicals were sourced from Sigma Aldrich. All ^1H spectra were recorded on a JEOL JNM-EX 270 MHz. Samples were dissolved in deuterated chloroform (CDCl_3) with the residual solvent peak used as an internal reference ($\text{CDCl}_3 - \delta$ 7.26 ppm). Proton spectra are reported as follows: chemical shift δ (ppm), (integral, multiplicity (s = singlet, br. s = broad singlet, d = doublet, dd = doublet of doublets, t = triplet, q = quartet, m = multiplet), coupling constant J (Hz), assignment).

High resolution mass spectrometry (HRMS) was performed using an Agilent 6210 MSD TOF mass spectrometer with the following settings: gas temperature (350°C), vaporizer (28°C), capillary voltage (3.0 kV), cone voltage (40 V), nitrogen flow rate (0.5 mL min^{-1}), nebuliser (15 psi). Samples were dissolved in MeOH (0.5 mg mL^{-1}) prior to injection.

Synthesis of 2-nitro-1-phenyl-1-propanol (mixture of Syn and Anti diastereomers) (8)

The synthesis of the title compound was carried out using three different bases; triethylamine, sodium hydroxide and sodium hydride (optimised conditions described). The ^1H NMR of the products from the 3 different bases were identical, all producing a 61:39 ratio of Syn and Anti diastereomers and the spectra is shown in Figure 2.2.



Triethylamine Base (Et_3N)

To a stirring solution of nitroethane (6.8 mL, 94.2 mmol, 4.0 eq.) and triethylamine (6.6 mL, 47.1 mmol, 2.0 eq.) in dichloromethane (5 mL), benzaldehyde (2.5 mL, 23.5 mmol, 1.0 eq.) was added slowly over 2 minutes. The mixture was left to stir for 16 hours where the solution then turned a bright yellow colour. The mixture was transferred to a separating funnel where it was washed with sodium bisulfite (3 × 20 mL) to remove any excess benzaldehyde and then washed with brine (3 × 20 mL). The organic layer was dried over MgSO_4 , filtered and the solvent removed *in vacuo* to afford the title compound as a yellow oil (3.63 g, 85 %). **Syn diastereomer**; ^1H NMR (270 MHz, CDCl_3): δ 7.45-7.29 (m, 5H, Ar), 5.03 (d, 1H, $J_{\text{HH}} = 8.90$ Hz, CH), 4.83-4.65 (m, 1H, CH), 2.48 (br-s, 1H, OH), 1.32 (d, 3H, $^3J_{\text{HH}} = 6.80$ Hz, CH_3). **Anti diastereomer**; ^1H NMR (270 MHz, CDCl_3): δ 7.45-7.29 (m, 5H, Ar), 5.40 (d, 1H, $J_{\text{HH}} = 3.60$ Hz, CH), 4.83-4.65 (m, 1H, CH), 2.48 (br-s, 2H, OH), 1.51 (d, 3H, $J_{\text{HH}} = 6.80$ Hz, CH_3). MS (ESI, m/z) calculated $[\text{C}_9\text{H}_{11}\text{NO}_3 + \text{Na}]^+$ 204.06311 found m/z 204.06493.

^1H NMR spectral properties matched that of the literature [121].

Sodium Hydroxide Base (NaOH)

To a stirring solution of nitroethane (13.5 mL, 188.5 mmol, 4.0 eq.), sodium hydroxide solution (20 mL, 94.2 mmol, 2.0 eq.) was added in a single portion. Then benzaldehyde (5.0 mL, 47.1 mmol, 1.0 eq.) was added slowly over 2 minutes. The mixture was left to stir for 16 hours where the solution then turned a bright yellow colour. The mixture was transferred to a separating funnel where CH_2Cl_2 (20 mL) was added. The organic layer was washed with sodium bisulfite (3 × 20 mL) to remove any excess benzaldehyde and then washed with brine (3 × 20 mL). The organic layer was dried over MgSO_4 , filtered and the solvent removed *in vacuo* to afford the title compound as a yellow oil (7.94 g, 93 %). **Syn diastereomer**; ^1H NMR (270 MHz, CDCl_3): δ 7.45-7.29 (m, 5H, Ar), 5.03 (d, 1H, $J_{\text{HH}} = 8.90$ Hz, CH), 4.83-4.65 (m, 1H, CH), 2.48 (br-s, 1H, OH), 1.32 (d, 3H, $J_{\text{HH}} = 6.80$ Hz, CH_3). **Anti diastereomer**; ^1H NMR (270 MHz, CDCl_3): δ 7.45-7.29 (m, 5H, Ar), 5.40 (d, 1H, $J_{\text{HH}} = 3.60$ Hz, CH), 4.83-4.65 (m, 1H, CH), 2.48 (br-s, 2H, OH), 1.51 (d, 3H, $^3J_{\text{HH}} = 6.80$ Hz, CH_3). MS (ESI, m/z) calculated $[\text{C}_9\text{H}_{11}\text{NO}_3 + \text{Na}]^+$ 204.06311 found m/z 204.06500.

^1H NMR spectral properties matched that of the literature [121].

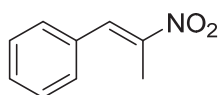
Sodium Hydride Base (NaH)

To a stirring solution of nitroethane (8.08 mL, 113.08 mmol, 4.0 eq.) and dry THF (15 mL), sodium hydride 60% dispersion mineral oil (2.26 g, 56.54 mmol, 2.0 eq.) was cautiously added and left to stir until gas evolution had completed. Benzaldehyde (2.88 mL, 28.27 mmol, 1.0 eq.) was then added under inert conditions ($\text{N}_2(\text{g})$) with a dropping funnel over 5 minutes. The mixture was left to stir for 16 hours where the solution was then quenched with water cautiously (10 mL). The mixture was transferred to a separating funnel with CH_2Cl_2 (20 mL), where it was washed with sodium bisulfite (3×20 mL) to remove any excess benzaldehyde and then washed with brine (3×20 mL). The organic layer was dried over MgSO_4 , filtered and the solvent removed *in vacuo*. The compound was then dissolved up in hexane and poured through a silica plug to remove the mineral oil. Then ethyl acetate was used to flush out the target product from the silica. The organic layer was dried over MgSO_4 , filtered and the solvent removed *in vacuo* to afford the title compound as a yellow oil (3.89 g, 76%). **Syn diastereomer**; ^1H NMR (270 MHz, CDCl_3): δ 7.45-7.29 (m, 5H, Ar), 5.03 (d, 1H, $J_{\text{HH}} = 8.90$ Hz, CH), 4.83-4.65 (m, 1H, CH), 2.48 (br-s, 1H, OH), 1.32 (d, 3H, $J_{\text{HH}} = 6.80$ Hz, CH_3). **Anti diastereomer**; ^1H NMR (270 MHz, CDCl_3): δ 7.45-7.29 (m, 5H, Ar), 5.40 (d, 1H, $J_{\text{HH}} = 3.60$ Hz, CH), 4.83-4.65 (m, 1H, CH), 2.48 (br-s, 2H, OH), 1.51 (d, 3H, $J_{\text{HH}} = 6.80$ Hz, CH_3). MS (ESI, m/z) calculated $[\text{C}_9\text{H}_{11}\text{NO}_3 + \text{Na}]^+$ 204.06311 found m/z 204.06493.

^1H NMR spectral properties matched that of the literature [121].

Synthesis of Phenyl-2-nitropropene (9)

The synthesis of the titled compound was carried out using two different bases; *n*-butylamine and ammonium acetate. The ^1H NMR of the products from the 2 different bases, were identical and the spectra is shown in Figure 2.3.



2.2.1 *n*-Butylamine Base (*n*-BuNH₂)

To a stirring solution of nitroethane (2.02 mL, 28.27 mmol, 1.0 eq.) and ethanol (5 mL), *n*-butylamine (0.3 mL, 2.82 mmol, 0.1 eq.) was added in a single portion and left to stir for 5 minutes. Benzaldehyde (2.88 mL, 28.27 mmol, 1.0 eq.) was then added slowly over 2 minutes. The mixture was left to stir at reflux for 8 hours, when the solution turned a bright yellow colour. The solvent was removed *in vacuo* and allowed to cool. As the yellow oil cooled, yellow crystals formed to afford the title compound. (3.26 g, 71 %). ¹H NMR (270 MHz, CDCl₃): δ 8.10 (s, 1H, CH), 7.50-7.40 (m, 5H, Ar), 2.46 (s, 3H, CH₃). MS (ESI, *m/z*) calculated [C₉H₉NO₂+H]⁺ 164.07060 found *m/z* 164.0636.

¹H NMR spectral properties matched that of the literature [122].

Ammonium acetate base (NH₄OAc)

To a stirring solution of nitroethane (2.02 mL, 28.27 mmol, 1.0 eq.), ammonium acetate (0.22 g, 2.82 mmol, 0.1 eq.) and glacial acetic acid (5 mL) was added in a single portion and left to stir for 5 minutes. Benzaldehyde (2.88 mL, 28.27 mmol, 1.0 eq.) was then added slowly over 2 minutes. The mixture was left to stir at reflux for 4 hours, when the solution turned a bright yellow colour. The solvent was removed *in vacuo* and allowed to cool. As the yellow oil cooled, yellow crystals formed to afford the title compound. (2.72 g, 59%). ¹H NMR (270 MHz, CDCl₃): δ 8.10 (s, 1H, CH), 7.50-7.40 (m, 5H, Ar), 2.46 (s, 3H, CH₃). MS (ESI, *m/z*) calculated [C₉H₉NO₂+H]⁺ 164.07060 found *m/z* 164.0589.

¹H NMR spectral properties matched that of the literature [122].

2.3 RESULTS AND DISCUSSION

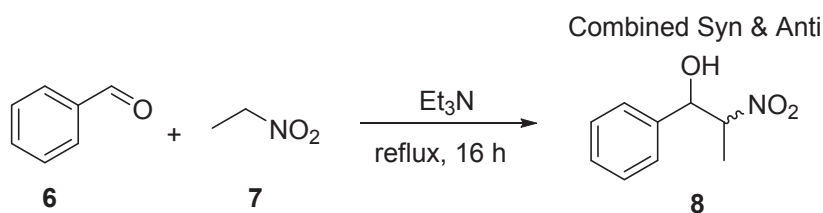
2.3.1 Synthesis of 2-Nitro-1-phenylpropanol (**8**)

In order to understand the influence of a base on the Henry reaction, benzaldehyde and nitroethane were reacted in the presence of 5 different bases; triethylamine, sodium hydroxide, sodium hydride, *n*-butylamine, and ammonium acetate.

Initially, the triethylamine base (1 equivalent) was trialled where it was reacted with one equivalent of benzaldehyde and one equivalent of nitroethane (Entry 1, Table 2.1). The ¹H NMR spectrum of the crude reaction product showed the product 2-nitro-1-phenylpropanol **8**, with some benzaldehyde (starting material) present. This reaction was then optimised to minimise the amount of unreacted benzaldehyde that was present in the crude extract. The conditions trialled are presented below (Table 2.1) and the best yield attained was 85% (1.0 g – 3.0 g scale) (Entry 7, Table 2.1). For an extensive comparison of bases, 0.2 equivalents of triethylamine was also used to ensure a range of base concentrations were trialled (Entry 9, Table 2.1).

In the case of low yielding reactions (Entries 1, 2 & 9, Table 2.1) no other products were identified, just substantial amounts of recovered benzaldehyde. Significantly, no nitrostyrene (dehydrated product) was observed in these reactions despite the reaction of benzaldehyde and nitroethane to form nitrostyrenes being mentioned throughout the literature [123].

Table 2.1: Triethylamine conditions of nitroaldol reaction.



Entry	Benzaldehyde (Eq.)	Nitroethane (Eq.)	Triethylamine (Eq.)	Solvent	Yield (%)
1	1.0	1.0	1.0	Neat	28
2	1.0	1.0	2.0	Neat	33
3	1.0	2.0	1.0	Neat	41
4	1.0	2.0	1.0	DCM	44
5	1.0	3.0	1.3	Neat	56
6	1.0	3.0	1.3	DCM	62
7	1.0	4.0	2.0	DCM	85
8	1.0	5.0	2.0	DCM	84
9	1.0	4.0	0.2	DCM	12

Analysis by ^1H NMR and LC-MS confirmed the formation of the product 2-nitro-1-phenyl-1-propanol as diastereomers, *syn*- and *anti*-. ^1H NMR spectroscopy (Figure 2.3) was used to determine a 61:39 ratio of *syn/anti* diastereomers for 2-nitro-1-phenylpropanol **8** by integration and the chemical shifts reported by Blay *et al.* [121].

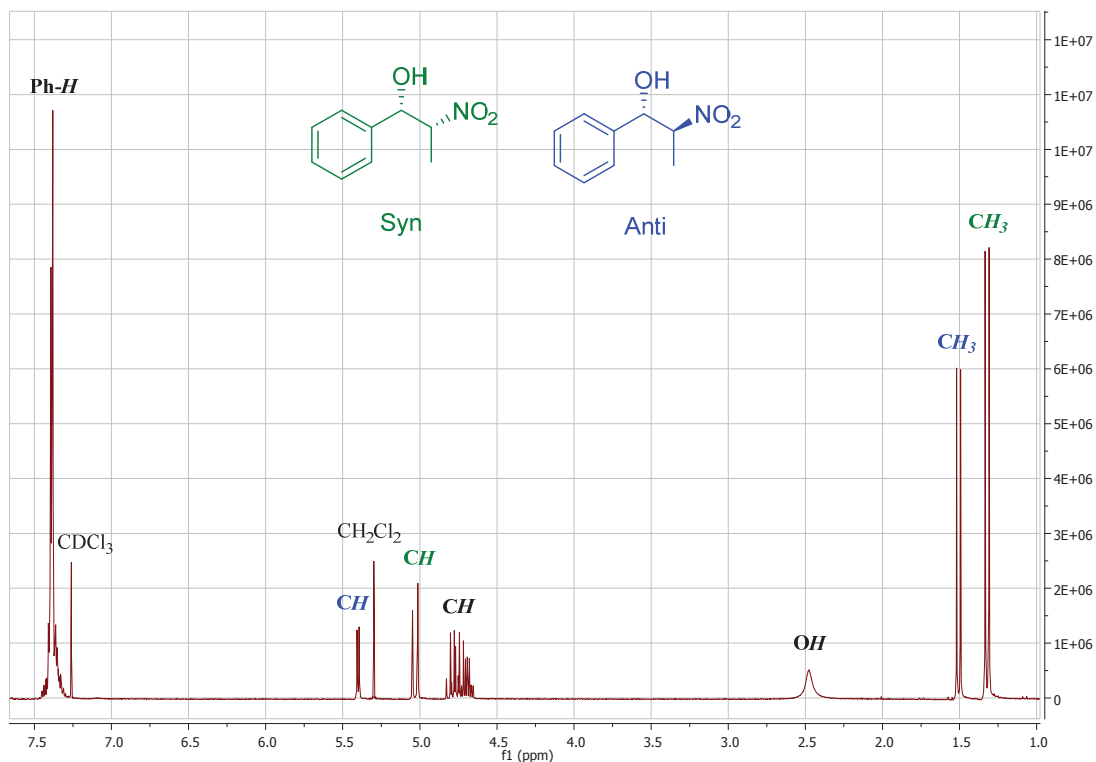
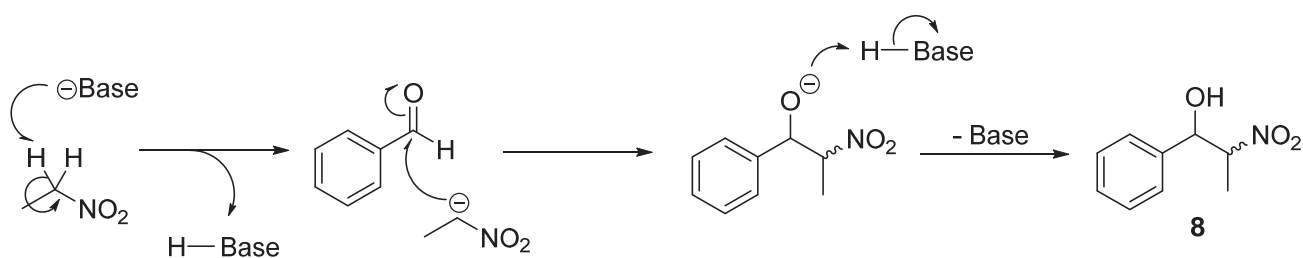


Figure 2.3: ^1H NMR spectrum of mixed product 2-nitro-1-phenyl-1-propanol **8**, where green represents Syn, blue represents Anti and black represents both.

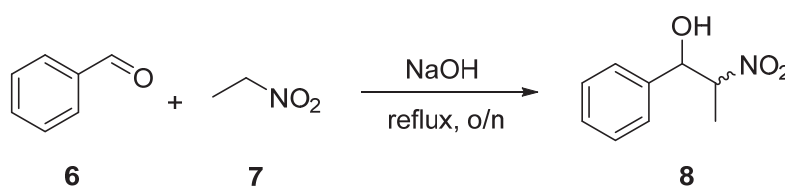
The general mechanism for the formation of the 2-nitro-1-phenyl-1-propanol product **8** is shown below in Scheme 2.6, whereby the Re and Si face attack of the aldehyde is responsible for the generation of the diastereomers.



Scheme 2.6: General mechanism for 2-nitro-1-phenyl-1-propanol **8**.

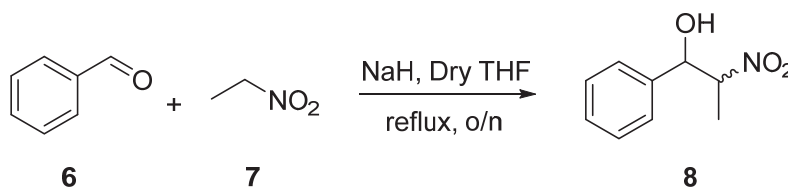
As more than one equivalent of triethylamine was required to obtain a good yield, attention then turned to a stronger base in order to increase the reaction yield. Sodium hydroxide (an inorganic base) was used making the reaction biphasic. Initially, the reaction was trialled with one equivalent each of benzaldehyde, nitroethane and sodium hydroxide and as expected, the same product was formed (2-nitro-1-phenyl-1-propanol) with a large excess of benzaldehyde still present. Thus, optimisation was carried out as shown in Table 2.2, where the best yield achieved was 93% (**Entry 4** (1.0 g – 3.0 g scale)).

Table 2.2: Sodium hydroxide conditions of the nitroaldol reaction.



Entry	Benzaldehyde (Eq.)	Nitroethane (Eq.)	Sodium Hydroxide (Eq.)	Solvent	Yield (%)
1	1.0	1.0	1.0	H ₂ O	32
2	1.0	1.0	2.0	H ₂ O	46
3	1.0	2.0	1.3	H ₂ O	78
4	1.0	4.0	2.0	H₂O	93
5	1.0	4.0	0.2	H ₂ O	14

A large excess (4 equivalents) of nitroethane and 2 equivalents of the base was required to obtain high yields from this reaction, indicating the hydroxide species still may not be basic enough, due to poor solubility in nitroethane, to drive an efficient reaction. Thus a stronger base, sodium hydride, was employed as outlined in Scheme 2.7 below.



Scheme 2.7: Nitroaldol reaction using sodium hydride.

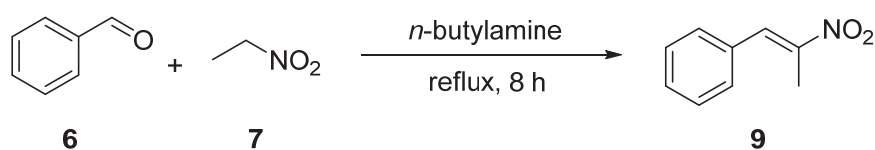
Benzaldehyde and nitroethane (1.0 equivalent each) were reacted with 2.0 equivalents of base (sodium hydride) under an inert atmosphere (N₂) using anhydrous THF as the solvent. On completion of the reaction the same product as described in Table 2.1 and Table 2.2 (2-nitro-1-phenyl-1-propanol **8**) was formed in high yield (72%). Of note the presence of some unreacted benzaldehyde was detected in the ¹H NMR spectrum and the LC-MS chromatogram, highlighting that the strength of the base had no influence on the equivalents ratio of the benzaldehyde and nitroethane. From this it seemed, simply an excess of nitroethane is required for efficient conversion. In light of this observation, the reaction was repeated using 4.0 equivalents of nitroethane with 1.0 equivalent of benzaldehyde and 2.0 equivalents of sodium hydride to produce a yield of 76%. As the nitroethane used throughout the experiments was not anhydrous, it is possible some adventitious moisture from the nitroethane could have quenched some of the sodium hydride, reducing the potential yield.

According to the literature, typically the yield of the nitro-aldol is best optimised by having a substantial excess of the nitroalkane (> 3.0 eq.) [124], which follows the same trend as the optimisation conditions (Table 2.2).

2.3.1 Synthesis of phenyl-2-nitropropene (**9**)

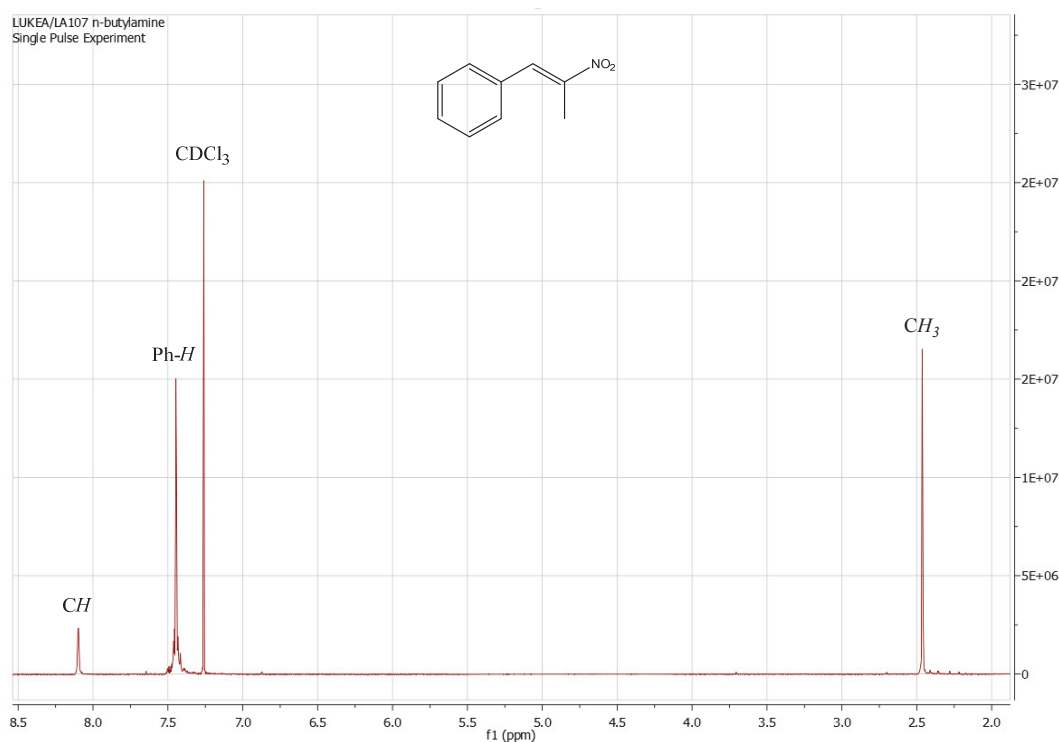
Two alternative bases commonly found in clandestine literature were also evaluated; *n*-butylamine and ammonium acetate. According to the online drug forums [24], both of the bases are used in catalytic amounts (10 mol% and 20 mol%, respectively) to produce phenyl-2-nitropropene (**9**).

Initially, 1.0 equivalent of benzaldehyde and nitroethane was reacted (neat) with 0.1 equivalents of *N*-butylamine to form phenyl-2-nitropropene **9** in 71% yield, as shown in Table 2.3. The ¹H NMR spectrum showed in Figure 2.4 matched that of previously reported literature [122].

Table 2.3: Nitroaldol reaction with *n*-butylamine.

Entry	Benzaldehyde (Eq.)	Nitroethane (Eq.)	<i>N</i> -butylamine (Eq.)	Solvent	Yield (%)
1	1.0	1.0	0.1	Neat	71
2	1.0	2.0	0.1	EtOH	70
3	1.0	2.0	2.0	EtOH	nil**

**Product unidentified/complex mixture of products

Figure 2.4: ^1H NMR spectrum of phenyl-2-nitropropene **9**.

The same reaction was then repeated using ethanol as a solvent and 2.0 equivalents of nitroethane, to see if the amount of nitroethane would improve the yield at all. This produced a yield of 70%, therefore the slight increase in nitroethane did not seem to impact the yield when using *n*-butylamine as the base

(Table 2.3). Finally, 2.0 equivalents of *n*-butylamine was trialled as a comparison with previous bases. Interestingly, upon analysis neither 2-nitro-1-phenyl-1-propanol nor phenyl-2-nitropropene were observed in ^1H NMR spectrum, instead it appeared that a complete degradation had occurred in the ^1H NMR spectra, with a poor mass recovery.

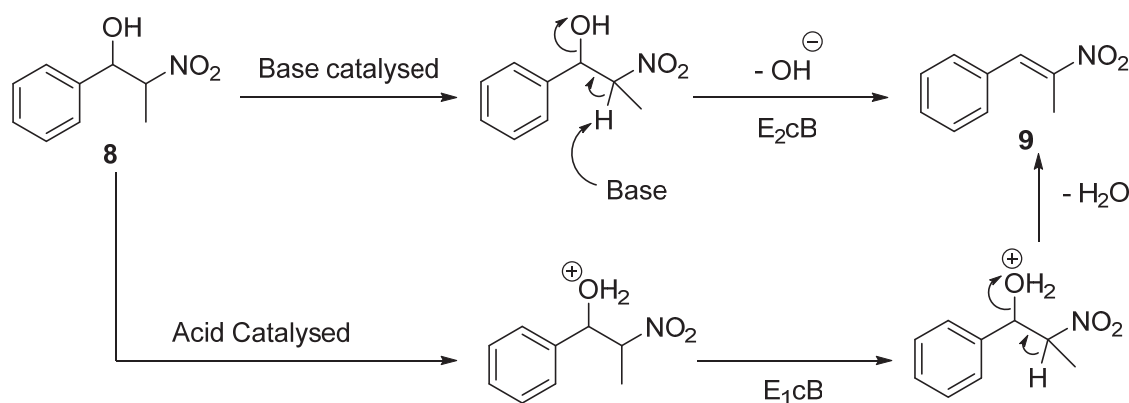
The final base studied was ammonium acetate, using 0.2 equivalents with 1.0 equivalent of both benzaldehyde and nitroethane in the presence of glacial acetic acid (Table 2.4), producing a yield of 59% of the nitrostyrene. Likewise, nitroethane was increased to 2.0 equivalents, again having no influence producing a yield of 57%. The reaction was trialled again using 2.0 equivalents of ammonium acetate to produce a yield of 58 %, with trace amounts of 2-nitro-1-phenyl-1-propanol **9** present confirmed *via* ^1H NMR.

Table 2.4: Nitroaldol reaction with ammonium acetate.

c1ccccc1C=O (6) + CC[N+](=O)[O-] (7) $\xrightarrow[\text{reflux, 4 h}]{\text{ammonium acetate}}$ c1ccccc1C=C[N+](=O)[O-] (9)

Entry	Benzaldehyde (Eq.)	Nitroethane (Eq.)	Ammonium acetate (Eq.)	Solvent	Yield (%)
1	1.0	1.0	0.2	Neat	59
2	1.0	2.0	0.2	Neat	57
3	1.0	2.0	2.0	Neat	58

The formation of phenyl-2-nitropropene **9** can occur *via* two alternate mechanisms from the initial nitro alcohol (**8**), either acid or base catalysed, both of which are outlined in Scheme 2.8.



Scheme 2.8: General mechanism for phenyl-2-nitropropene **9**.

It is interesting to note that despite being vastly different bases, phenyl-2-nitropropene **9** was only the major product when *n*-butylamine and sodium acetate were employed, and the nitro-aldol product was not isolated. Though counterintuitive, when examining the nature of the other bases on an individual basis this becomes clearer, keeping the base catalysed mechanism outlined in Scheme 2.8 in mind.

Triethylamine could be too sterically hindered to facilitate deprotonation of **8**, thus preventing this dehydration pathway from proceeding despite the excess base being present in the reaction mixture. Sodium hydride, while exceptionally basic, generally exists for only a short amount of time before being consumed by adventitious moisture, this is especially the case when all reagents (in this case nitroethane and benzaldehyde) have not been meticulously dried. In the case of sodium hydroxide the biphasic nature of this reaction is thought to be the major reason for the lack of **9** being present in the reaction mixture, as the effective concentration of the base in the organic phase would be very low in addition to the competing deprotonation of unreacted nitroethane.

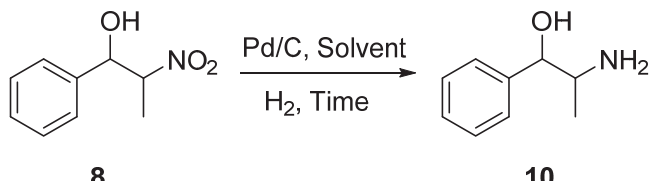
Conversely, *n*-butylamine is a primary amine which is soluble in organic solvents, thus the requirements of minimal steric hindrance around the amine moiety and high concentration of this reagent in the organic phase are easily met. We have attributed the formation of **9**, in this instance, to *n*-butylamine facilitating the base catalysed pathway outlined in Scheme 2.8. This is consistent with the use of

cyclohexylamine reported by McAnda and co-workers [125] and it is important to note that cyclohexylamine and n-butylamine are both small molecule primary amines that have very similar pKa values of 10.64 and 10.59, respectively. Sodium acetate, on the other hand, is only a mild base with poor organic solubility but still capable of facilitating this reaction at high temperatures, as evinced by the formation of **9** in good yield. The critical factor in this reaction is the presence of excess acetic acid promoting the protonation of **8**, this high energy intermediate, then undergoes a simple dehydration to give **9**, *via* the acid catalysed pathway, again, outlined in Scheme 2.8. Importantly this study used pure starting materials and from a clandestine laboratory perspective one must also consider the implications of impure starting materials. This may have some implications on the types of intermediates that may be present in real world clandestine samples and as such detailed chemical profiling will be investigated in Chapter 5.

2.3.3 Synthesis of norephedrine (**10**) from 2-nitro-1-phenyl-1-propanol

Having identified a high yielding method for the synthesis of 2-nitro-1-phenyl-1-propanol, focus then turned to converting this product to ephedrine. The first step was to convert the nitro functional group into a primary amine as shown in Table 2.5.

Table 2.5: Conversion of phenyl-2-nitropropene **8** to the norephedrine **10**.

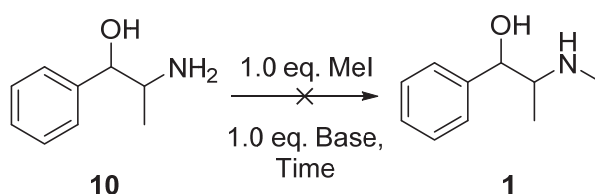
				
Entry	Pd/C Equivalent	Solvent	Time	Yield
1	0.1	MeOH	6 h	-
2	0.1	MeOH	18 h	-
3	0.1	EtOH	6 h	59 %
4	0.1	EtOH	12 h	86 %
5	0.1	EtOH	18 h	94 %

A common reductive hydrogenation method reported in the literature was trialled (Entry 1) as it has been widely used on similar compounds [126]. 2-Nitro-1-phenyl-1-propanol (**8**) was stirred in methanol with 10% w/w of palladium on activated carbon, in a hydrogen environment. The ^1H NMR spectrum showed this to be unsuccessful at 6 hour and 18 hour reaction times (Entries 1 & 2). Although methanol is the more common solvent for this type of reaction it was not suitable with phenyl-2-nitropropene **8**. Ethanol, another common literature hydrogenation solvent [127] was then trialled (entry 3). ^1H NMR spectroscopy and mass spectrometry matched the spectral properties reported in the literature [128] for norephedrine **10**. Using ethanol, the product was formed in a 94% yield after stirring for 18 hours.

2.3.4 Synthesis of ephedrine/pseudoephedrine (**1**) from norephedrine (**10**)

Focus then turned to the synthesis of ephedrine/pseudoephedrine. As the only difference between norephedrine **10** and pseudoephedrine is the methyl group on the amine, methylations using methyl iodide were trialled first (Table 2.6).

Table 2.6: Methylation of norephedrine **10**.



Entry	Base	Solvent	Time	Yield
1	NaH	Dry THF	8 h	n/a
2	NaH	Dry THF	18 h	n/a
3	Et_3N	CH_2Cl_2	6 h	n/a
4	Et_3N	CH_2Cl_2	18 h	n/a
5	K_2CO_3	CHCl_3	6 h	n/a
6	K_2CO_3	CHCl_3	18 h	n/a

Initially, methylation using a strong base (Entry 1 & 2) was tried as per the literature [129]. This appeared to have deprotonated both the amine and hydroxyl groups encouraging additional methylation and side products. A weaker base

(triethylamine) was then tried (Entry 3 & 4) as successful methylation generates hydriodic acid, which will in turn protonate the amine, while triethylamine ‘mops up’ any excess acid present. This made very little difference and the use of triethylamine produced similar ^1H NMR spectra. The next step was to try an alternative weak base like potassium carbonate (Entry 5 & 6); to avoid stripping the protons from the hydroxyl group. After mass spectrometry and ^1H NMR, it was clear ephedrine or pseudoephedrine was not formed in any of the 6 entries, which can be expected when using methyl iodide. The second methylation (dimethylation) can occur faster due to the ability of the mono-methylated intermediate to act as a nucleophile, reacting with methyl iodide faster than the free primary amine [130]. However, the formation of two possible side products are suggested here, based on high resolution mass spectrometry, as shown in Figure 2.4. Two major products were identified *via* LC-MS with m/z ratios of 194.15399 and 180.13824, which agree with the exact masses presented in Figure 2.5.

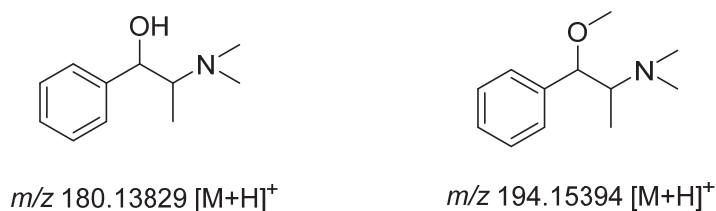
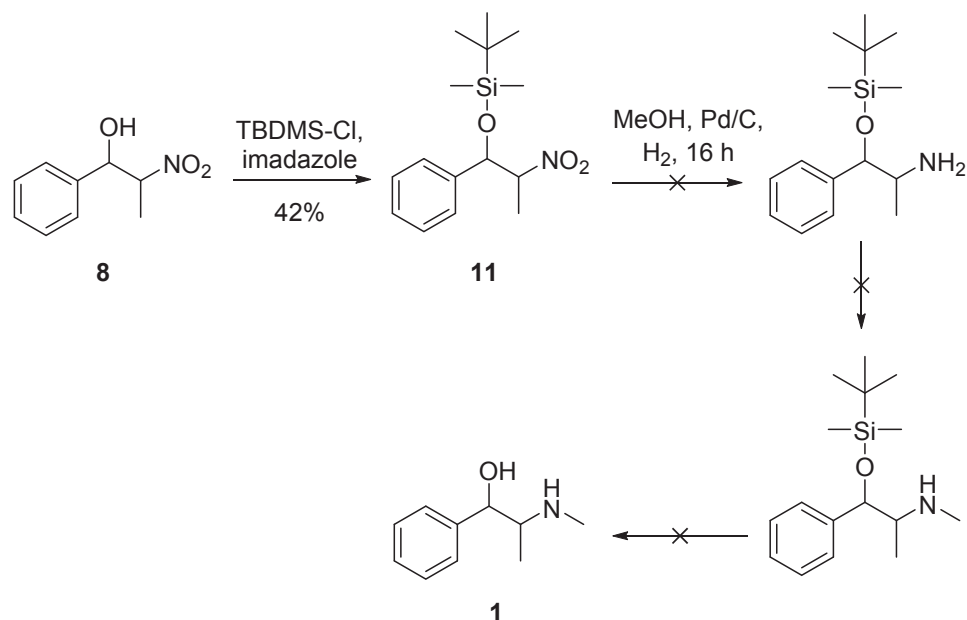


Figure 2.5: Potential impurities and associated exact masses formed in the methylation of norephedrine **10**.

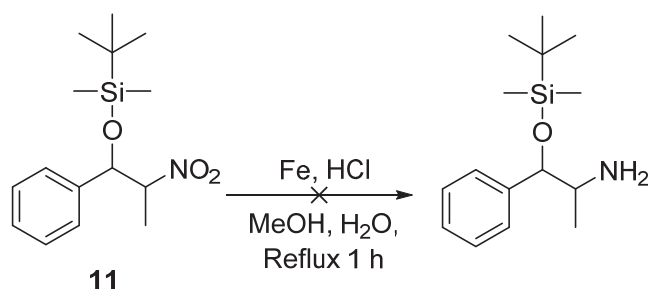
Given that methylation occurred at both the amine and hydroxyl functional groups, a new synthetic pathway was designed to a) first protect the alcohol group, b) hydrogenate the nitro functional group to an amine, c) methylate the amine, and finally d) deprotect the alcohol group (Scheme 2.9). This pathway was designed around a reported method by Denis *et al.* on a selective *n*-demethylation procedure [131]. Therefore, if the hydroxyl functional group was protected and

dimethylation occurred again, the literature method [131] could be applied to reach the target product ephedrine/pseudoephedrine **1**.



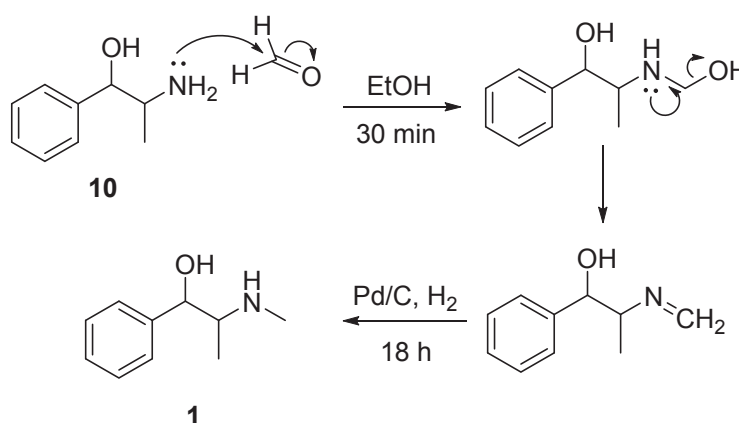
Scheme 2.9: New pathway to avoid over methylation.

The first step (alcohol protection - **11**) successfully produced a yield of 42% which was enough to take on to the next step of the reaction. However, reducing the nitro group to an amine proved problematic as only starting material could be seen on the ¹H NMR spectra. The hydrogenation was repeated using an alternative catalyst (palladium acetate) and alternative solvent (ethanol) under the same conditions, unsuccessfully. A different method reported by Desai *et al.* [132] was tried as outlined in Scheme 2.10, however this also was unsuccessful. Only starting material was detected in the ¹H NMR spectrum.



Scheme 2.10: Reduction with iron and hydrochloric acid.

Attention then turned to using a less aggressive methylating agent which could potentially limit the number of possible alkylation sites on compound **10**. Thus, a new synthetic pathway was designed (Scheme 2.11) for a two-step, one pot reaction to ephedrine/pseudoephedrine.



Scheme 2.11: Two-step one pot synthesis to ephedrine/pseudoephedrine.

Mass Spectrometry and ^1H NMR spectroscopy confirmed that no ephedrine/pseudoephedrine was present, however the formation of two other side products (Figure 2.6) were observed.

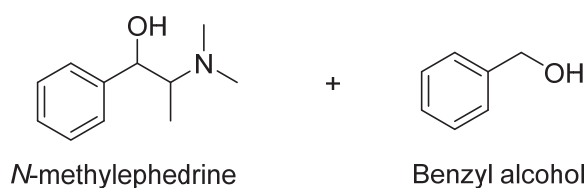
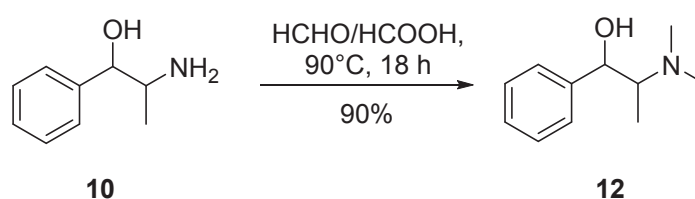


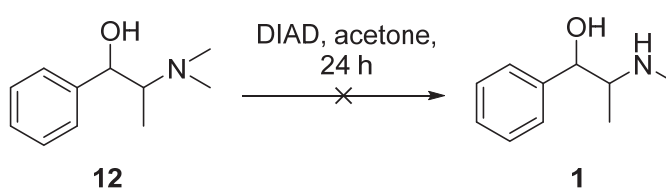
Figure 2.6: Impurities formed from two-step one pot reaction.

As mono-methylation proved problematic, an alternative approach was considered as dimethylation kept occurring. Over methylation of the primary amine was observed with both methyl iodide and formaldehyde reagents, so the literature was consulted for a selective demethylation method [133]. Firstly a published method [134] was used to synthesise *N*-methylephedrine **12** as per the scheme below (Scheme 2.12).



Scheme 2.12: Synthesis of N-methylephedrine.

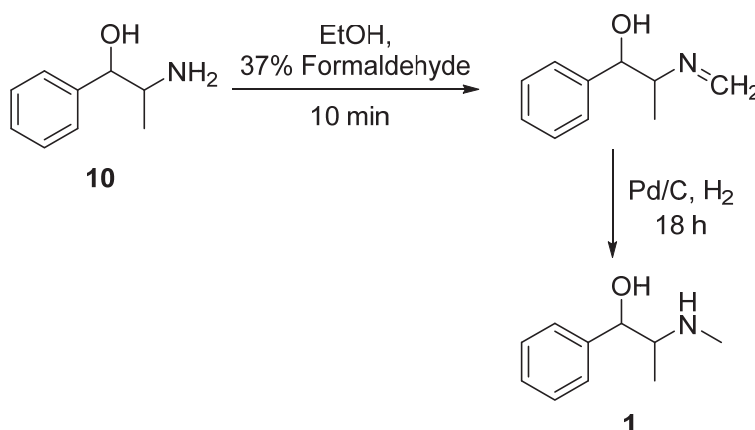
With the product (*N*-methylephedrine **12**) in hand, the next step was to try and selectively remove one methyl group from the nitrogen in Compound **12** as per Denis *et al.* [131, 133].



Scheme 2.13: Demethylation of N-methylephedrine [131].

For this reaction, 1.1 equivalents of Diisopropyl azodicarboxylate (DIAD) were added to a stirring solution of *N*-methylephedrine **12** in acetone and left for 24 hours (Scheme 2.13). The ^1H NMR spectrum showed only the presence of starting material, indicating the reaction did not work. The reaction was then repeated with 2.5 equivalents of DIAD, again with no product observed.

Attention turned to optimising the previously described two-step one pot reaction to ephedrine/pseudoephedrine (Scheme 2.14). As dimethylation of the amine occurred, the reaction was repeated, changing the reaction temperature to 0 °C reducing the stirring time to 10 minutes from 30 minutes, before adding the Pd/C. The reasoning behind doing this reaction on ice is to slow down how fast the formaldehyde reacts with the amine functional group, encouraging mono-methylation of the amine providing the desired product.



Scheme 2.14: Two Step, one pot reaction to ephedrine/pseudoephedrine.

The ^1H NMR spectrum of the product showed a mixture of ephedrine/pseudoephedrine and *N*-methylephedrine but due to the complexity, high resolution LC-MS analysis was carried out on the same sample for confirmation. As seen in the chromatogram (Figure 2.7), although not clean there are three main peaks indicating the formation of three major products (**A**, **B**, **C**).

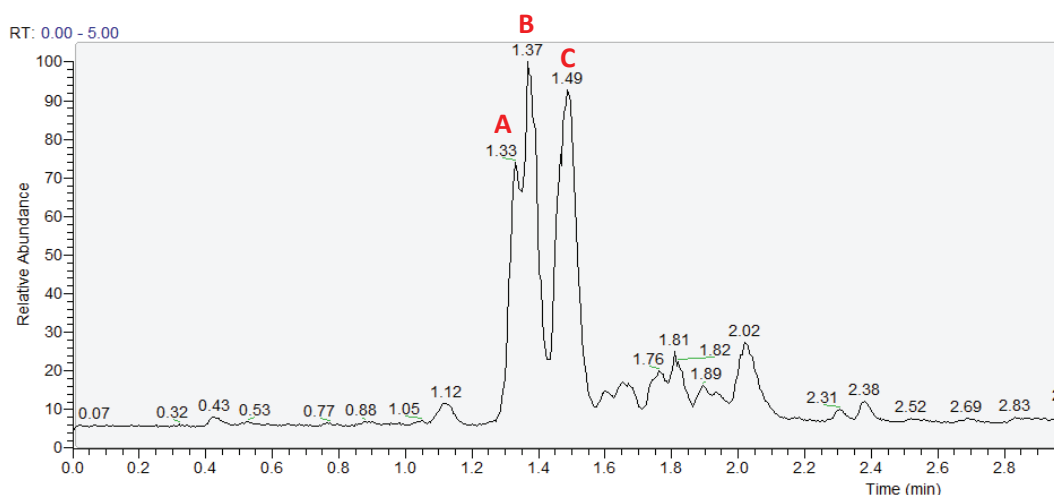


Figure 2.7: Identification of three major peaks (A, B, C) in High Resolution LC-MS chromatogram of two-step, one pot reaction.

As this reaction is not stereo-selective, it is expected that both ephedrine and pseudoephedrine diastereomers will be present, accounting for two of the peaks (A and B). The first co-eluting peak had a retention time of 1.33 minutes and associated pseudo-molecular ion $(M+H)^+$ mass of 166.12265 amu; representative of either ephedrine or pseudoephedrine (Figure 2.8).

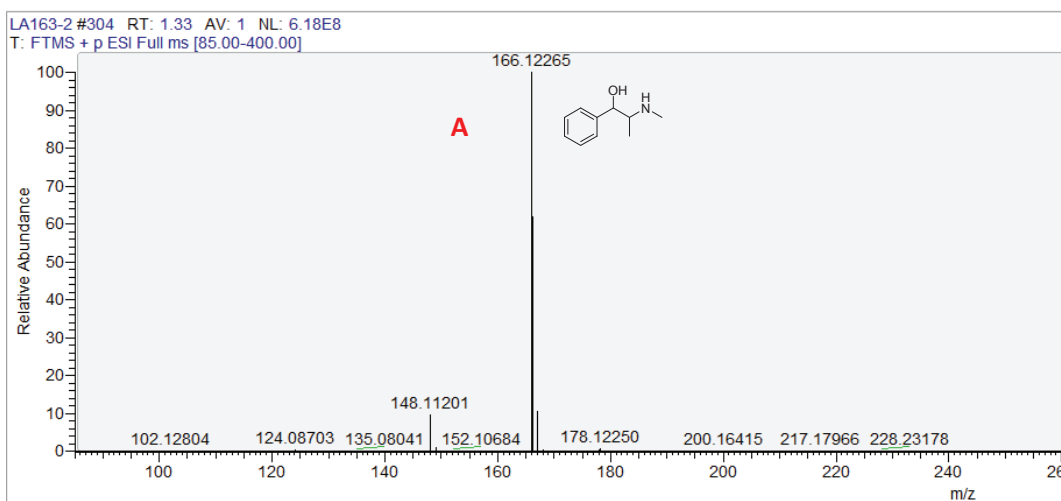


Figure 2.8: LC-MS Analysis, corresponding mass of peak A at Rt 1.33 min (ephedrine or pseudoephedrine – m/z 166.12265 amu).

The second co-eluting peak had a retention time of 1.37 minutes and associated mass of the pseudo-molecular ion $(M+H)^+$ m/z 166.12262 amu, proposed here to be the other diastereomer (Figure 2.9). The third and final peak had a retention time of 1.49 minutes and corresponding mass of the pseudo-molecular ion $(M+H)^+$ m/z 180.13823 amu (Figure 2.10) indicating the formation of the *N*-methylephedrine.

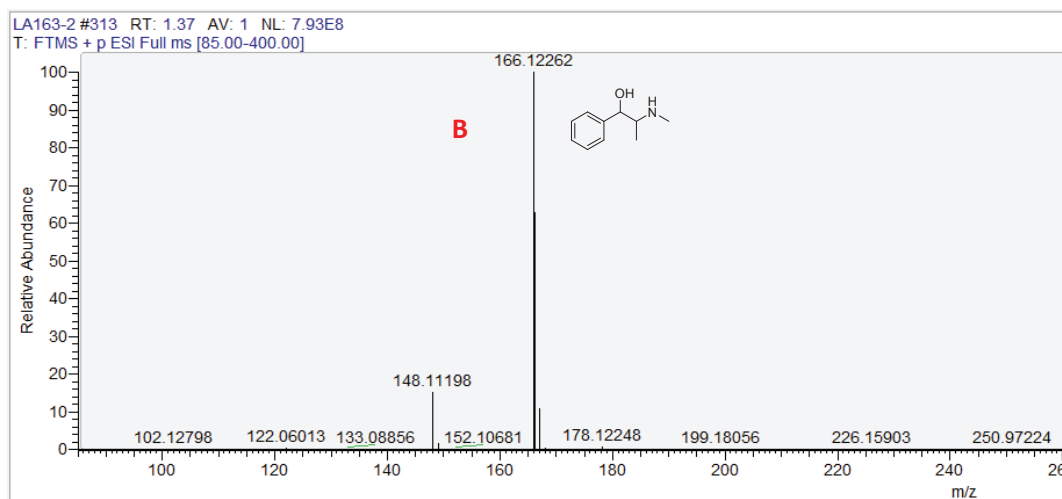


Figure 2.9: LC-MS Analysis, corresponding mass of peak **B** at Rt 1.37 min (ephedrine/pseudoephedrine – m/z 166.12262 amu).

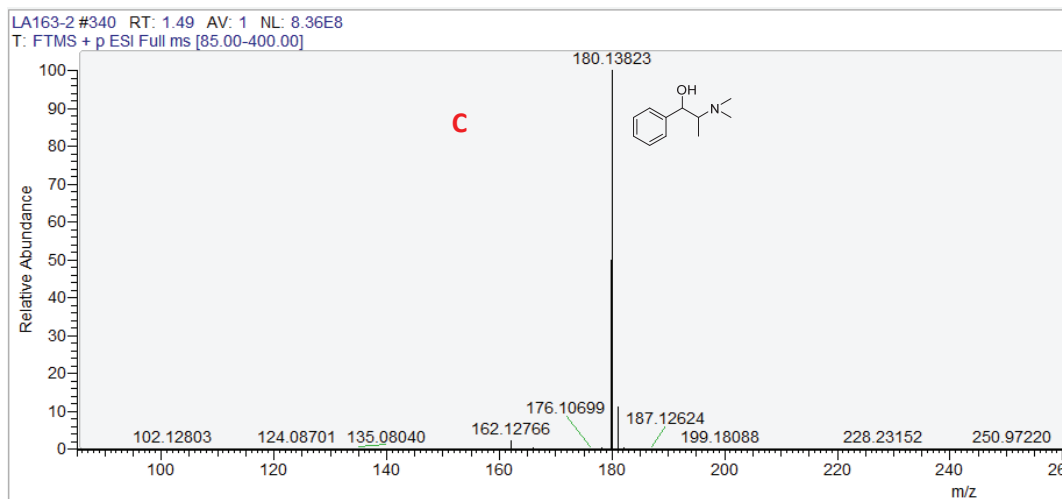


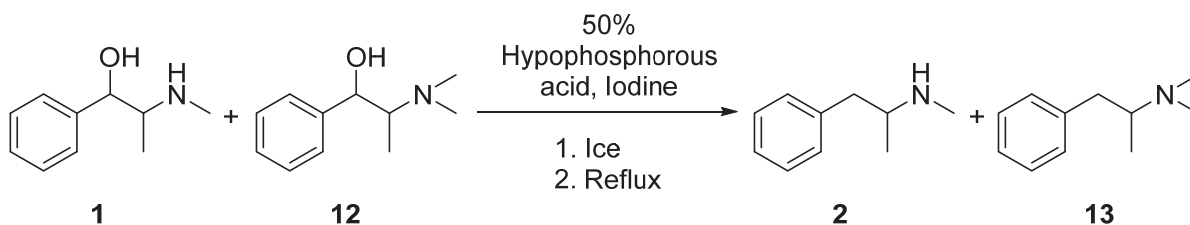
Figure 2.10: LC-MS Analysis, corresponding mass of peak **C** at Rt 1.49 min (*N*-methylephedrine m/z 180.13823 amu).

Further purification and optimisation was not necessary and is outside this scope of work, as a plausible synthetic route to ephedrine/pseudoephedrine has been confirmed. It is quite important in this case that purification is not carried out as a chemical fingerprint cannot be identified for this pathway (further discussed in chapter 5) without the presence of its associated impurities. In this way the samples investigated in the platform technology developed in Chapter 5 are representative of the types of samples that may be present in a clandestine laboratory.

2.3.4 Synthesis of methamphetamine (1) from norephedrine (10)

The next step was to take the same product mixture in another reaction (Scheme 2.15) to confirm if any methamphetamine can be synthesised *via* this pathway, making sure to carry through impurities from each step for the aforementioned chemical mapping.

A commonly encountered reduction method (Scheme 2.15) [135] for the conversion of pseudoephedrine to methamphetamine was acquired, using 0.5 mL of 50% w/w hypophosphorous acid was stirred on ice for 15 minutes before the slow addition of Iodine (0.5 g). The reaction mixture initially turned a deep maroon colour but as the iodine reacted (forming hydriodic acid) it turned colourless. Once the solution mixture turned clear it was taken off the ice bath and allowed to reach room temperature. Then 0.5 g of the mixture of ephedrine, pseudoephedrine and *N*-methylephedrine was added in a single portion and set to reflux for 1 hour. The mixture was then basified to pH 13 with 5M NaOH solution and extracted in toluene.

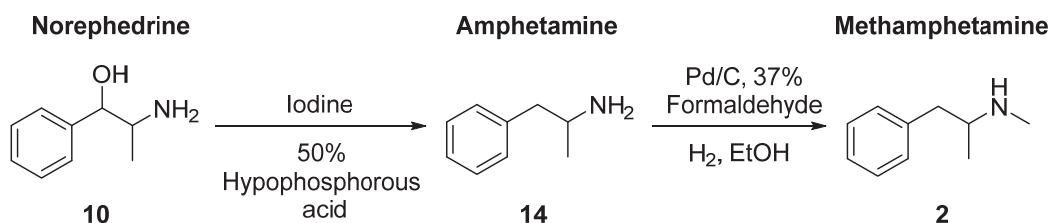


*Scheme 2.15: Reduction of ephedrine/pseudoephedrine and *N*-methylephedrine.*

The ^1H NMR spectrum was very complex, identification of any compound was extremely challenging so high resolution LC-MS was utilised again. This showed the formation of methamphetamine **2** (m/z 150.12755) and *N*-methylmethamphetamine **13** (m/z 164.14320) in small amounts. However, this reaction formed large amounts of unknown by-products, which will be extremely useful for the chemical mapping of this pathway (Chapter 5). A list of identified masses (m/z) in order of intensity (largest to smallest) is outlined here: a) 240.17432, b) 330.22116, c) 256.16931, d) 346.21603, e) 238.15868, f) 226.15874, g) 302.18985, h) 254.18988, i) 270.18491, j) 226.15874, k) 224.14308, l) 194.15372, m) 283.21646, n) 148.11197, o) 162.12749, p) 180.13795, q) 158.96384, r) 297.23206, s) 150.12755, t) 164.14320. It becomes clear that with potentially more than 20 compounds formed, it is the impurities of a seizure sample that may provide the most information about the manufacturing process of methamphetamine.

As a full possible synthetic pathway to methamphetamine has now been confirmed from easily accessible ingredients (benzaldehyde and nitroethane) attention turned to designing another potential pathway. It should be pointed out that the difficulties associated with the above processes make it unlikely this effort would be undertaken in a clandestine laboratory however these samples are of interest for the development of chemical profiling technology.

A pathway that removes the hydroxyl group before methylation would be ideal in order to avoid methylating both the amine and hydroxyl groups. Therefore, a pathway was designed in which methylation can only occur at the primary amine of amphetamine (Scheme 2.16).



Scheme 2.16: Alternative pathway to methamphetamine.

The first step is an exact repeat of the conditions outlined in Scheme 2.15 (reduction method of pseudoephedrine to methamphetamine) except using norephedrine **10** instead of pseudoephedrine. High resolution LC-MS confirmed the formation of amphetamine **14** (m/z 136.11206) as the minor product along with the unknown major product mass of m/z 226.15880. The next step is to methylate using the two step, one pot reaction which again showed a small amount of methamphetamine present with at least 15 other impurities. This is also confirmed as a plausible pathway for the manufacture of methamphetamine **2** and will be later analysed in order to fully realise the potential of the chemical profiling technology in Chapter 5.

2.4 CONCLUSION

The choice of base when reacting benzaldehyde and nitroethane together is significant to clandestine laboratory investigating chemists as it has been demonstrated here to be a determining factor as to which precursor to methamphetamine has been used. Synthesis using triethylamine, sodium hydroxide or sodium hydride produces 2-nitro-1-phenyl-1-propanol **8**; a precursor to ephedrine/pseudoephedrine. In contrast, when using *n*-butylamine and ammonium acetate as the base, phenyl-2-nitropropene **9** is produced; a precursor to P2P. This information will be significant as the identification of the base in use may provide additional support to the determination of the synthetic route to methamphetamine. Likewise a full synthetic route to methamphetamine was carried out and confirmed from the 2-nitro-1-phenyl-1-propanol **8** product.

The work presented in this chapter has been published as: **L.M. Andrighetto**, L.C. Henderson, J.R. Pearson, P.G. Stevenson and X.A. Conlan, Influence of base on nitro-aldol (Henry) reaction products for alternative clandestine pathways, *Australian Journal of Forensic Sciences*, (2016) DOI: 10.1080/00450618.2015.1112429

CHAPTER 3

SYNTHESIS OF
PSEUDOEPHEDRINE/EPHEDRINE FROM
L-ALANINE

CHAPTER OVERVIEW

This chapter provides a brief literature summary of *N*-methyl amino acids and their previous uses in areas such as peptide manipulation. It also highlights the increasing interest by law enforcement agencies in *N*-methylalanine, due to large quantities recently being identified at clandestine laboratories.

A simple pathway was designed for the synthesis of *N*-methylalanine from alanine, as introduced by Painter *et al.* [136] in a restricted journal. Painter's study was limited to identification of ephedrine in trace amounts from *N*-methylalanine and benzaldehyde *via* a simplistic GC-MS method. To further this research, a range of different conditions were trialled to fully establish the synthetic route and assess the robustness of this clandestine method.

3.1 INTRODUCTION

The inclusion of *N*-methyl amino acids within peptides has been shown to improve pharmacokinetic properties such as metabolic stability, membrane permeability and oral bioavailability [137-139]. As such, *N*-methyl amino acids have been of great interest in areas such as peptidomimetics [140]. Despite this interest, the *N*-methylation of amino acids can be a challenging process and to date, there have been numerous methods reported for this procedure in the literature. Methods for the formation of *N*-methyl-amino acids include; nucleophilic substitution of α -bromo acids [141], *N*-methylation of carbamates and amides [142], transition metal catalysed reductions [143], reductive aminations [139] and borohydride reductions [144], illustrated in Figure 3.1.

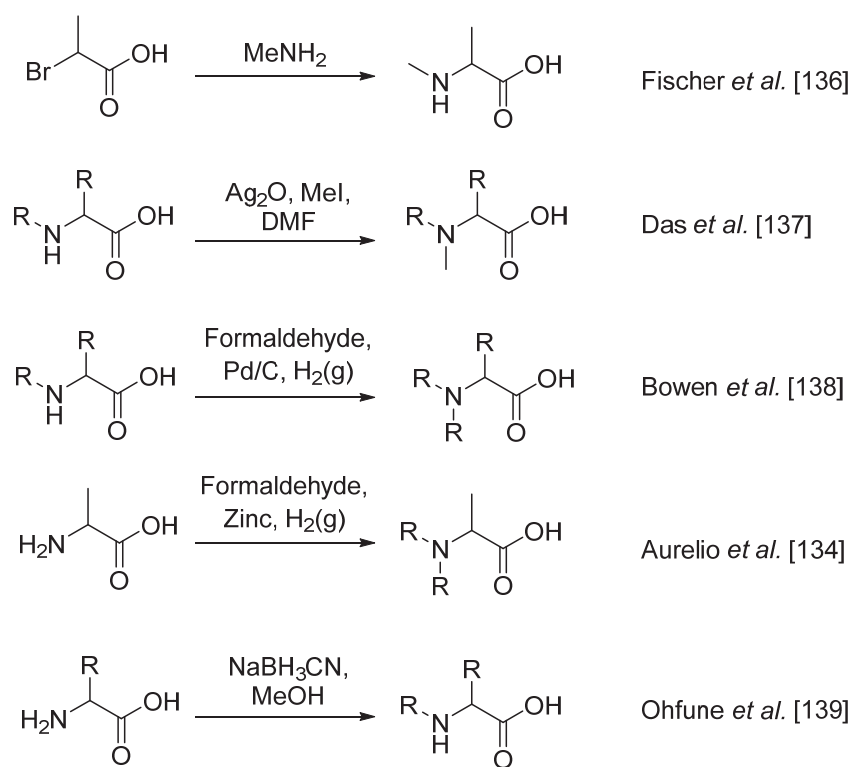


Figure 3.1: Examples of synthetic methods for *N*-methyl amino acids.

Alanine has been identified at several clandestine laboratories in Victoria [personal correspondence with Dr Jim Pearson at the Victoria Police Forensic Services Department] and is a cheap amino acid, which is readily available to the public in many sports supplements or body building shops. Therefore, the synthesis of *N*-methylalanine from alanine is a potential area of interest to clandestine teams. Although there are numerous methodologies in the literature for the synthesis of *N*-methylalanine, there are limited reports for the synthesis of *N*-methylalanine from alanine itself [139]. The later editions of Uncle Fester's (popular 'Meth cookbooks') 'Secrets of Methamphetamine Manufacture' [145] offer one such method using aqueous formaldehyde and zinc [146], but as the author of the text points out this was not an effective or practical procedure for the preparation of *N*-methylalanine. As such, a key aim of this chapter is to develop a simple and efficient method for the conversion of alanine to *N*-methylalanine, a process that has significant potential for the manufacture of illicit drugs [147]. A very recent publication [148] (April 2016) in a restricted clandestine laboratory journal investigated a simple method for the 'clandestine synthesis of *N*-methylalanine from 2-bromopropionic acid', highlighting the recent attention *N*-methylalanine is receiving within the drug manufacturing scene.

Painter *et al.* [136] investigated the Akabori-Momotani reaction (shown in Figure 3.2) on a small scale (0.2 g) with *N*-methylalanine and benzaldehyde as an alternative method of synthesising ephedrine/pseudoephedrine.

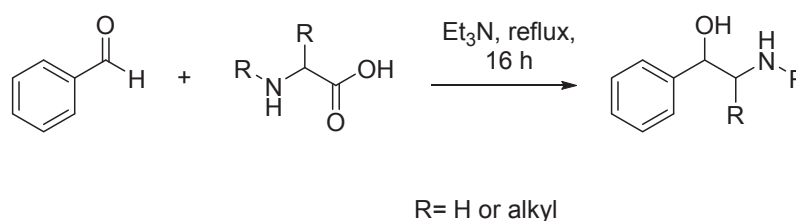


Figure 3.2: Akabori-Momotani reaction [136].

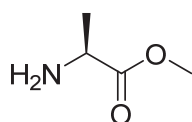
Although Painter *et al.* [136] confirmed the presence ephedrine/pseudoephedrine *via* GC-MS within a mixture of products, the yields, practicality, isolation or purification of generated products from this pathway was not discussed. Nevertheless, the presence of benzaldehyde or *N*-methylalanine in a clandestine laboratory can signify the synthesis of ephedrine/pseudoephedrine and subsequently methamphetamine.

Large quantities of *N*-methylalanine has been recovered in multiple clandestine laboratories, which were imported from other countries as the chemical is very expensive (\$894 AUD for 5 grams – Sigma Aldrich) [149]. As such, a simple clandestine method for the synthesis of *N*-methylalanine will be investigated in this chapter, along with the conversion of *N*-methylalanine to ephedrine/pseudoephedrine under alternative conditions.

3.2 EXPERIMENTAL

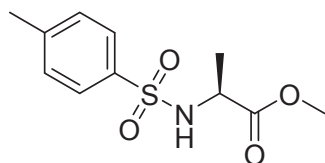
All ^1H and ^{13}C NMR spectra were recorded on a JEOL JNM-EX 270 MHz. Samples were dissolved in deuterated DMSO (d_6 -DMSO) or deuterated chloroform (CDCl_3) with the residual solvent peak used as an internal reference (d_6 -DMSO – δ 2.50 ppm, CDCl_3 – δ 7.26 ppm). Proton spectra are reported as follows: chemical shift δ (ppm), (integral, multiplicity (s = singlet, br. s = broad singlet, d = doublet, dd = doublet of doublets, t = triplet, q = quartet, m = multiplet), coupling constant J (Hz), assignment). High resolution mass spectrometry (HRMS) was performed using an Agilent 6210 MSD TOF mass spectrometer with the following settings: gas temperature (350 °C), vaporizer (28 °C), capillary voltage (3.0 kV), cone voltage (40 V), nitrogen flow rate (0.5 mL min $^{-1}$), nebuliser (15 psi). Samples were dissolved in MeOH (0.5 mg mL $^{-1}$) prior to injection.

Synthesis of Methyl-L-alaninate (16)



A cooled (0 °C) solution of L-alanine (2.00 g, 22.45 mmol, 1.0 eq.) in methanol (15 mL) was stirred for 15 minutes before thionyl chloride (2.2 mL, 15.41 mmol, 0.7 eq.) was added dropwise over 20 minutes. The mixture was refluxed for 3 hours, then brought to room temperature and further stirred for 16 hours. The mixture was basified by adjusting the pH to 12 using 1M NaOH, then transferred to a separating funnel where the crude product was extracted 3 times with toluene (3 × 15 mL). The organic layers were combined and dried over MgSO₄, then the toluene was removed *in vacuo* to afford the title compound as an off-white solid (2.51 g, 81 %). ¹H NMR (270 MHz, CDCl₃): δ 8.76 (br.s, 2H, NH₂), 4.26 (m, 1H, CH), 3.81 (s, 3H, CH₃), 1.73 (d, 3H, *J*_{HH} = 7.2 Hz, CH₃).

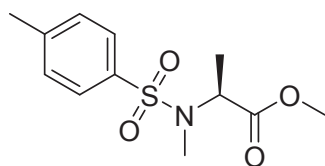
¹H NMR spectral properties matched that of the literature [150].

Synthesis of Methyl *N*-(toluene-4-sulfonyl) L-alaninate (17)

To a cooled (0 °C) solution of methyl-L-alaninate (2.20 g, 21.1 mmol, 1.0 eq.) in CH₂Cl₂ (10 mL), triethylamine (5.89 mL, 42.2 mmol, 2.0 eq.) was added in a single portion. Tosyl chloride (3.62 g, 18.9 mmol, 0.9 eq.) was then added drop-wise over 30 minutes and the reaction left to stir for 6 hours. The pH was adjusted to 11 using 1M NaOH and then transferred to a separating funnel where the organic layer was isolated and washed 3 times with brine (3 × 20 mL). The organic layer was then dried over MgSO₄, filtered and the solvent removed *in vacuo* to afford the title compound as a cream solid (3.37 g, 72%). ¹H NMR (270 MHz, CDCl₃): δ 7.72 (d, 2H, *J*_{HH} = 7.24 Hz, Ph-*H*), 7.29 (d, 2H, *J*_{HH} = 7.23, Ph-*H*), 3.99 (m, 1H, CH), 3.54 (s, 3H, CH₃), 2.42 (s, 3H, CH₃), 1.38 (d, 3H, *J*_{HH} = 7.24, CH₃).

¹H NMR spectral properties matched that of the literature [151].

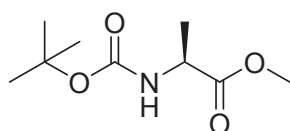
Synthesis of Methyl *N*-methyl-*N*-(toluene-4-sulfonyl)-L-alaninate (18)



A cooled (0 °C) solution of methyl tosyl-L-alaninate (450 mg, 1.75 mmol, 1.0 eq.) and anhydrous THF (5 mL) was stirred for 10 minutes under an inert atmosphere of N₂(g). Sodium hydride (126 mg, 5.25 mmol, 3.0 eq.) was added cautiously and left to stir until gas evolution had finished. Methyl iodide (1.09 mL, 17.50 mmol, 10 eq.) was then added drop-wise over 15 minutes. The mixture was allowed to warm to room temperature and stirred for a further 18 hours. The mixture was quenched cautiously with water (2.0 mL) and then transferred to a separating funnel where CH₂Cl₂ (20 mL) was added. The organic layer was washed with brine (3 × 20 mL) and then dried over MgSO₄, filtered and the solvent removed *in vacuo* to afford the title compound as an off-white solid (374.90 mg, 79%). ¹H NMR (270 MHz, CDCl₃): δ 7.72 (d, 2H, *J*_{HH} = 6.9, Ph-*H*), 7.29 (d, 2H, *J*_{HH} = 6.9, Ph-*H*), 3.99 (m, 1H, CH), 3.54 (s, 3H, CH₃), 2.83 (s, 3H, CH₃), 2.42 (s, 3H, CH₃), 1.38 (d, 3H, *J*_{HH} = 6.8, CH₃).

¹H NMR spectral properties matched that of the literature [152].

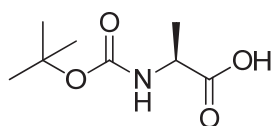
Synthesis of Methyl (tert-butoxycarbonyl)-L-alaninate (20)



To a cooled (0 °C) stirring solution of methyl-L-alaninate (500 mg, 4.8 mmol, 1.0 eq.) in CH₂Cl₂ (5 mL), Boc₂O (1.05 g, 4.8 mmol, 1.0 eq.) was diluted in CH₂Cl₂ (10 mL) and added dropwise over 15 minutes with a dropping funnel. The mixture was left to stir for 16 hours at room temperature and then transferred to a separating funnel where it was washed with brine (3 × 15 mL). The organic layer was dried over MgSO₄, filtered and the solvent removed *in vacuo* to afford the title compound as a cream solid (665.5 mg, 68%). ¹H NMR (270 MHz, CDCl₃): δ 4.32 (m, 1H, CH), 3.74 (s, 3H, CH₃), 1.44 (s, 9H, *t*-Bu), 1.38 (d, 3H, *J*_{HH} = 7.1, CH₃).

¹H NMR spectral properties matched that of the literature [153].

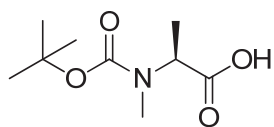
Synthesis of 2-(*N*-(tert-butoxycarbonyl)amino)propanoic acid (22)



To a cooled (0 °C) cloudy solution of L-alanine (1.0 g, 11.2 mmol, 1.0 eq.) in dioxane (22 mL) and water (11 mL), Boc₂O (2.45 g, 11.2 mmol, 1.0 eq.) was added slowly over 5 minutes under N_{2(g)}. The mixture was left to stir for 3 hours at room temperature until the solution turned clear, where upon ethyl acetate (100 mL) was added. The pH was then slowly adjusted to 2.0 with 2M HCl. The mixture was transferred to a separating funnel where the aqueous layer was separated and extracted with ethyl acetate (2 × 15 mL). The combined organic layers were dried over MgSO₄, filtered and the solvent removed *in vacuo* to afford the title compound as a white solid (1.93 g, 91%). Mp = 79 °C (80 °C - 83 °C [154]). ¹H NMR (270 MHz, *d*₆-DMSO): δ 7.11 (d, 1H, ³*J*_{HH} = 5.40 Hz, NH), 3.91 (m, 1H, CH), 1.37 (s, 9H, *t*-Bu), 1.21 (d, 3H, *J*_{HH} = 5.40 Hz, CH₃). HRMS (ESI, *m/z*) calculated [C₈H₁₅NO₄+Na]⁺ 212.08933 found *m/z* 212.08964.

¹H NMR spectral properties and melting point matched that of the literature [154, 155].

Synthesis of 2-(*N*-(tert-butoxycarbonyl)methylamino)propanoic acid (23)

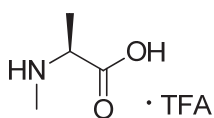


To a cooled (0 °C) stirring solution of Boc-L-alanine (1.43 g, 7.54 mmol, 1.0 eq.) and dry THF (20 mL), sodium hydride 60% dispersion in mineral oil (905 mg, 22.61 mmol, 3.0 eq.) was added cautiously. Then methyl iodide (3.9 mL, 60.3 mmol, 8.0 eq.) was added drop-wise under inert conditions (N₂). The mixture was left to stir for 18 hours at room temperature and was then quenched cautiously with water (3 mL). The mixture was transferred to a separating funnel where diethyl ether (20 mL) was added. The aqueous layer was separated and carefully acidified (5M HCl) to pH 3.0, and then the crude product was extracted using chloroform (2 × 20 mL). The combined organic layers were then dissolved up in hexane and poured through a silica plug to remove the mineral oil. Then ethyl acetate was used to flush the product out of the silica. The organic layer was dried over MgSO₄, filtered

and the solvent was removed *in vacuo* to afford the title compound as a white solid (1.35 g, 89%). Mp = 90 °C (89 °C - 91 °C [154]). ^1H NMR (270 MHz, d_6 -DMSO, 80 °C): δ 4.44 (br. s, 1H, CH), 2.75 (s, 3H, N-CH₃), 1.39 (s, 9H, *t*-Bu), 1.30 (d, 3H, J_{HH} = 5.2 Hz, CH₃). HRMS (ESI, m/z) calculated [C₉H₁₇NO₄+ Na]⁺ 226.10498 found m/z 226.10585.

^1H NMR spectral properties and melting point matched that of the literature [154, 156].

Synthesis of 2-(methylamino)propanoic acid (*N*-methylalanine) trifluoroacetate salt (19)



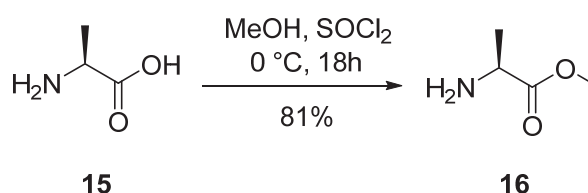
To a stirring mixture of 2-(*N*-(tert-butoxycarbonyl)methylamino)propanoic acid **3** (520 mg, 2.6 mmol, 1.0 eq.) in CH₂Cl₂ (20 mL), 20% trifluoroacetic acid (4 mL) was added dropwise over 5 minutes. The mixture was left to stir for 18 hours at room temperature and the solvent removed *in vacuo*. The product was dissolved in CH₂Cl₂ (25 mL) and the solvent removed again *in vacuo* and was repeated a total of 3 times to afford the title compound as an off-white solid (491 mg, 96%). Mp = 288°C. ^1H NMR (270 MHz, d_6 -DMSO): δ 8.90 (br s, 1H, OH), 3.96 (q, 1H, J_{HH} = 5.38 Hz, CH), 3.57 (br, 1H, NH), 2.57 (s, 3H, N-CH₃), 1.41 (d, 3H, J_{HH} = 5.40 Hz, CH₃). ^{13}C NMR (67.5 MHz, d_6 -DMSO) δ 13.9, 55.3, 99.4, 171.0. ^{19}F NMR (470MHz, d_6 -DMSO) δ -74.99. HRMS (ESI, m/z) calculated [C₄H₉NO₂+Na]⁺ 126.05255 found m/z 126.05399.

^1H NMR and ^{13}C NMR spectral properties matched that of the literature [157].

3.3 RESULTS AND DISCUSSION

The low solubility in organic solvents and zwitterionic nature of amino acids make the synthetic manipulation of the carboxylate and protonated amino regions challenging [158]. Initially, to avoid the over methylation issue presented previously in Chapter 2 (Figure 2.5), the aim was to first protect the carboxylic acid group as the methyl ester. Then perform a mono-methylation followed by the deprotection of the carboxylic acid to form the desired product *N*-methylalanine.

A commonly used literature method [150] involving the ester formation using thionyl chloride and methanol was carried out, shown in Scheme 3.1. This reaction functions by first forming the acid chloride, followed by methanol undergoing a nucleophilic attack on the carbonyl carbon [130], which results in the departure of the chloride ion (leaving group) and the formation of the target methyl ester **16**.

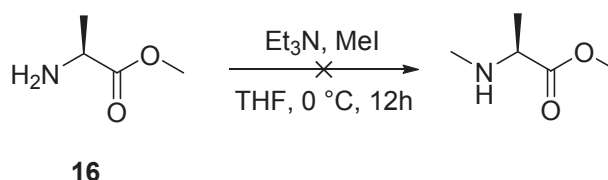


*Scheme 3.1: Synthesis of methyl-L-alaninate **16**.*

Thionyl chloride was added dropwise over 15 minutes to a cooled stirring solution 0 °C of L-alanine **15** (1.0 equivalent) in methanol. After the reaction mixture was refluxed (3 hours) it was left to stir at room temperature for a further 14 hours and then basified, which formed the desired product **16** in 81% yield. The ¹H NMR spectrum matched that of the literature and was quite clean

The next step was the methylation of the amine (Scheme 3.2), however in order to prevent dimethylation, the methyl iodide (1.0 equivalent) was added dropwise over 40 minutes to a cooled solution of methyl-L-alaninate **16** (1.0 equivalent) and

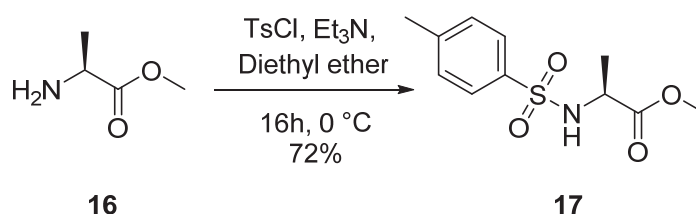
triethylamine (1.1 equivalents) in anhydrous THF (Scheme 3.2). The slow addition of methyl iodide into a cold solution can slow down the reaction, potentially minimising the chance of di-alkylation.



*Scheme 3.2: Methylation of methyl-L-alaninate **16**.*

There were no traces of the desired product observed in the ^1H NMR spectrum of this reaction. Many literature methods [139] report successful *N*-methylation of similar amino acids, by first protecting the primary amine followed by methylation and then deprotection of both the carbonyl and amine.

In this case, the amine group of L-alanine methyl ester **16** was protected using 4-toluenesulfonyl chloride (Tosyl Chloride/TsCl), which is a group that has been used in the literature for the protection of amines [159, 160] (Scheme 3.3).

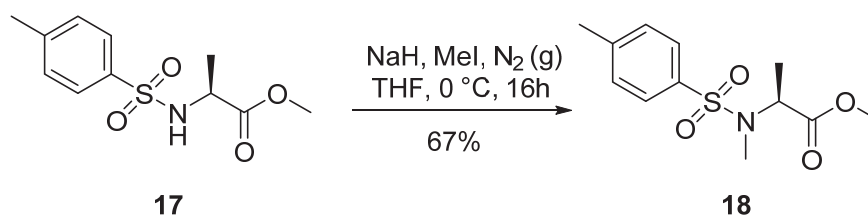


*Scheme 3.3: Synthesis of methyl N-(toluene-4-sulfonyl) L-alaninate **17**.*

The methyl ester **16** (1.0 equivalent) was stirred in diethyl ether and triethylamine (2.0 equivalents) on ice for 20 minutes before tosyl chloride (1.0 equivalent) was added slowly and left to stir for 16 hours. The ^1H NMR spectrum of the crude product showed that the desired tosyl protected methyl ester **17** had formed and

some unreacted tosylic acid also remained. Therefore, the reaction was repeated with a longer reaction time of 24 hours and the amount of tosylic acid present decreased. An aqueous work-up was carried out with bicarbonate to remove any leftover tosylic acid or hydrochloric acid from the crude product.

The next step was to *N*-methylate the protected alanine **17**. Under inert conditions (nitrogen gas), methyl iodide (1.0 equivalents) was slowly added to a cold stirring solution of anhydrous THF, triethylamine (1.1 equivalents) and methyl *N*-(toluene-4-sulfonyl) L-alaninate **17** (1.0 equivalents). There were no traces of the desired product **18** observed in the ^1H NMR spectrum from the reaction. As triethylamine is a weak organic base, the experiment was repeated using sodium hydride to ensure the base would be strong enough to deprotonate the secondary amine (Scheme 3.4).



*Scheme 3.4: Methylation of protected amine of methyl *N*-(toluene-4-sulfonyl) L-alaninate **17**.*

The use of this stronger base successfully formed the desired product in a 67% yield (0.4 g – 0.6 g scale) as confirmed in the ^1H NMR spectrum. The crude product was washed 3 times with brine and appeared quite clean, as illustrated in Figure 3.3.

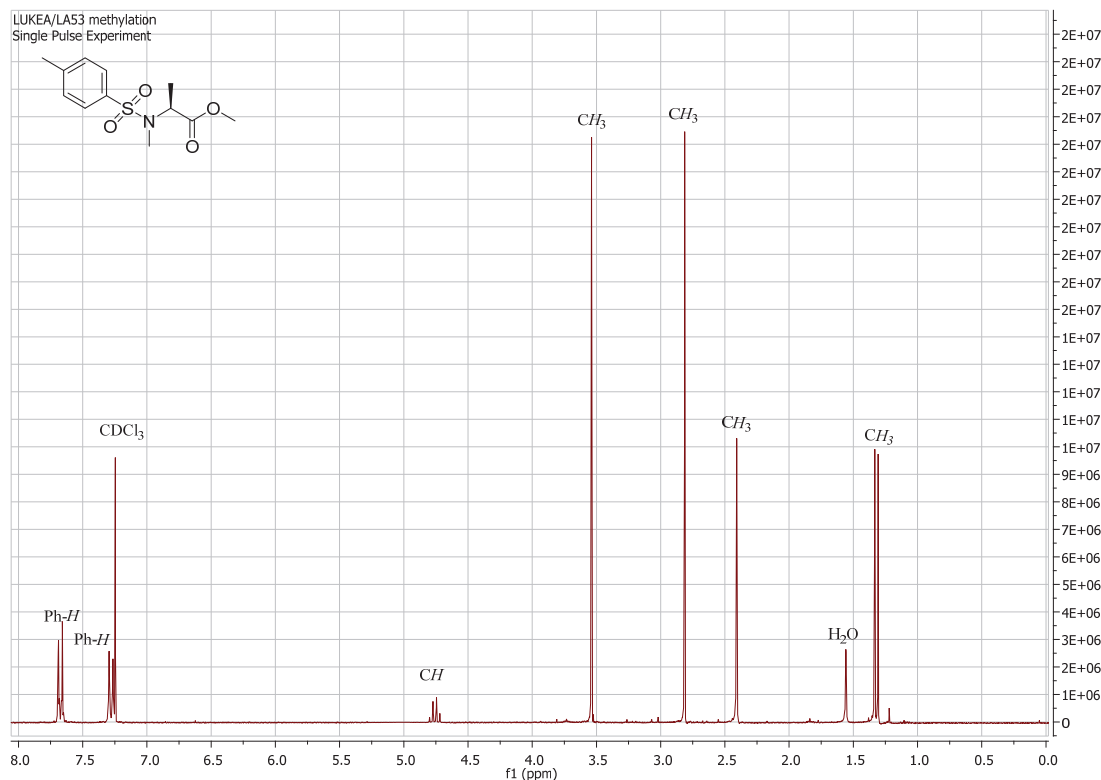
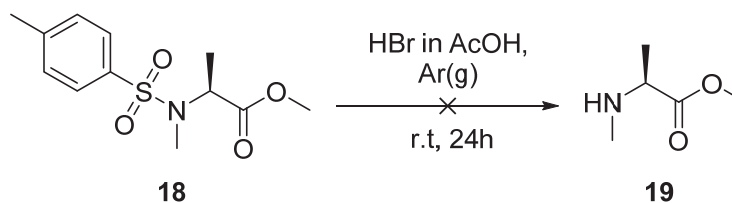


Figure 3.3: ^1H NMR spectrum of methyl N-methyl-N-(toluene-4-sulfonyl)-L-alaninate **18**.

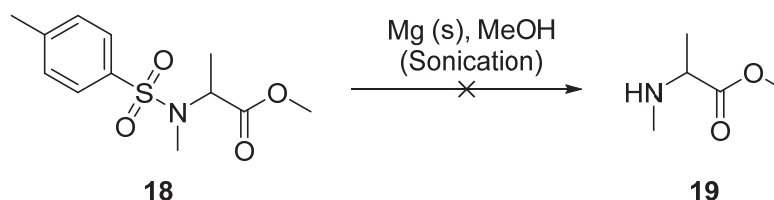
Having successfully methylated methyl N-(toluene-4-sulfonyl) L-alaninate **17**, attention turned to deprotecting the amine by removing the sulfonamide protecting group from the molecule. Hydrogen bromide (HBr) has been used frequently within the literature [161] to cleave sulfonamide groups. A solution of hydrogen bromide in acetic acid at two different concentrations (25 wt. % and 33 wt. %), under argon, at room temperature and a 24 hour stirring time were trialled, shown in Table 3.1.

Table 3.1: Conditions for tosyl deprotection of **18**.

Entry	HBr Concentration	Solvent
1	25 wt. % in acetic acid	Neat
2	25 wt. % in acetic acid	DCM
3	33 wt. % in acetic acid	Neat
4	33 wt. % in acetic acid	DCM

All 4 experiments (Entries 1 – 4) failed and no desired product **19** was observed in the ^1H NMR of the crude reaction product. An alternative method [162] for the removal of the tosyl group was trialled (Table 3.2). This reaction utilises cathodic cleavage due to electron transfer and has been previously used to cleave primary and secondary alkyl phenyl sulfones [162].

Table 3.2: Deprotection using magnesium in absolute methanol.

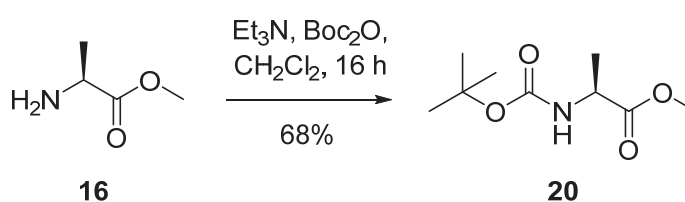


Entry	Magnesium Form	Magnesium Equivalents	Time
1	Turnings	5.0	1 h
2	Turnings	10.0	6 h
3	Powder	10.0	1 h
4	Powder	10.0	8 h

Methyl *N*-methyl-*N*-(toluene-4-sulfonyl)-L-alaninate **18** (1.0 equivalent) was placed into a 10 mL volumetric flask with anhydrous methanol and 5.0 equivalents of magnesium turnings. The resulting suspension was then sonicated for 1 hour. After 1 hour, the mixture was diluted with dichloromethane and poured into 1M

HCl, followed by the organic phase being washed with 1M sodium bicarbonate. No deprotected product **19** was observed in the ^1H NMR spectrum of the reaction, so the reaction was repeated doubling the magnesium equivalents (10.0) and increasing the sonication time to 6 hours, with only starting material present. In order to increase the amount of surface area allowed to react, magnesium powder was substituted for the larger turnings and were trialled for 1 hour and 8 hour sonication times, however these were all unsuccessful.

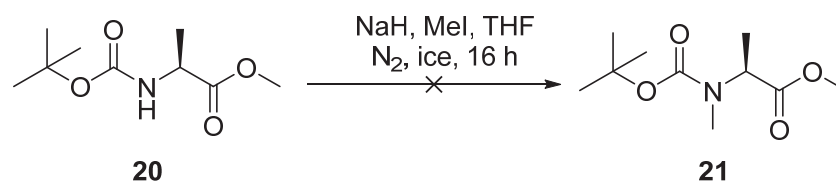
Although there are a range of amine protecting groups within the literature [159, 160], a specific protecting group that can be easily cleaved at later stages of the synthetic pathway would be ideal. Tert-butyloxycarbonyl (Boc) has been used throughout organic chemistry for the protection of amines [163, 164], as removal is as simple as exposing it to an acidic environment. Therefore, 1.0 equivalent of the reagent di-tert-butyl dicarbonate (Boc_2O) was dissolved in CH_2Cl_2 and added dropwise to a cooled stirring solution of methyl-L-alaninate **16** (1.0 equivalent), CH_2Cl_2 and triethylamine (1.5 equivalents). It was left to stir for 16 hours upon which the ^1H NMR spectrum of the crude reaction product confirmed the successful Boc protection, and formation of target product methyl (tert-butoxycarbonyl)-L-alaninate **20** in 68 % yield (Scheme 3.5).



*Scheme 3.5: Boc protection of methyl L-alaninate **16**.*

Now with the target methyl (tert-butoxycarbonyl)-L-alaninate **20** in hand, the next step was to methylate the protected amine [165], shown in Scheme 3.6. To a cooled stirring solution of methyl (tert-butoxycarbonyl)-L-alaninate **20** (1.0 equivalent) and dry THF, sodium hydride (3.0 equivalents) was added cautiously. Then methyl iodide (1.0 equivalent) was added drop-wise under inert

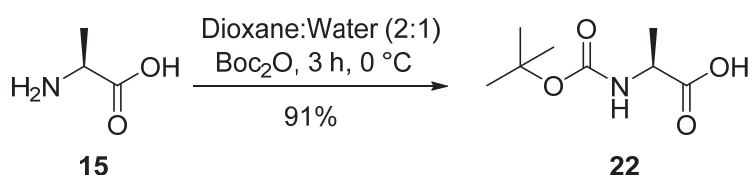
conditions (N_2). The mixture was left to stir for 16 hours at room temperature and was then quenched with water (2 mL) cautiously.



*Scheme 3.6: Methylation of Boc₂O protected L-alanine methyl ester **20**.*

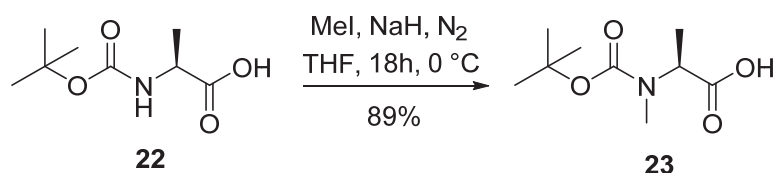
The desired product (Compound **21**) was neither observed in the 1H NMR spectrum or LC-MS chromatogram of the crude reaction product.

Alternative approaches were then considered. As the amine is far more nucleophilic than the hydroxyl functional group, the synthetic pathway was repeated using Boc as the protecting group without first forming the L-alanine methyl ester (protecting the hydroxyl group). That is, Boc₂O was used to protect L-alanine, forming a carbamate [165], a protocol that has been commonly used to methylate the amine in individual amino acids [166]. The procedure described by Jacubec *et al.* [167] was carried out using dioxane : water (2 : 1). Importantly, only one equivalent of Boc₂O was used in this reaction, which is less than usual [167] in order to limit the amount of unreacted Boc₂O in the crude sample mixture; thus obtaining a spectroscopically cleaner product. The reaction time was also increased slightly from 1 hour to 3 hours. Using these conditions, yields ranged from 85% to 91% (0.5 g – 1.0 g scale) of the protected amine compound **22**, shown in Scheme 3.7.



*Scheme 3.7: Synthesis of 2-(N-(tert-butoxycarbonyl)amino)propanoic acid **22**.*

The second step involved the methylation of the target protected amine **22**, achieved with methyl iodide, sodium hydride and dry tetrahydrofuran, a slight variation of known procedures [167, 168]. This mixture was stirred under an inert atmosphere (N_2) in a round bottom flask. Initially the sample was cooled to 0 °C prior to sodium hydride and methyl iodide addition, allowed to warm to room temperature and further stirred for 18 hours. A large excess of sodium hydride (8.0 equivalents) was used, following previous methods regarding the methylation of amino acids [129]. A yield of 89% for the desired product 2-(N-(tert-butoxycarbonyl)methylamino)propanoic acid **23** was achieved (Scheme 3.8). It is unknown as to why the methylation of the ester (compound **20**, Scheme 3.6) was unsuccessful previously.



*Scheme 3.8: Synthesis of 2-(N-(tert-butoxycarbonyl)methylamino)propanoic acid **23**.*

During the characterisation of compound **23** it was interesting to note that two sets of quartets were observed in the 1H NMR spectrum at δ 4.27 ppm and δ 4.54 ppm (Figure 3.3 at 20 °C). This is attributed to the observance, on the NMR timescale [169], of two conformers at the amide nitrogen, which suggests the formation of a pseudo-stereocentre at the nitrogen due to impeded pyramidal inversion, resulting in restricted rotation [130].

This restricted rotation can also be observed by the splitting associated with the Boc protecting group at δ 1.39 ppm. Repeating the 1H NMR experiment at a series of increasing temperatures (20 °C (r.t.) \rightarrow 60 °C) resulted in peak coalescence at 60 °C for each of the α -protons and Boc signals, respectively. This suggests that a reasonable amount of energy was required to allow for rapid nitrogen pyramidal inversion or rotation and individual diastereomeric effects to no longer be

observed [170, 171]. Peak coalescence for the α -proton is shown in the insets on the left hand side of the ^1H NMR spectra, Figure 3.4.

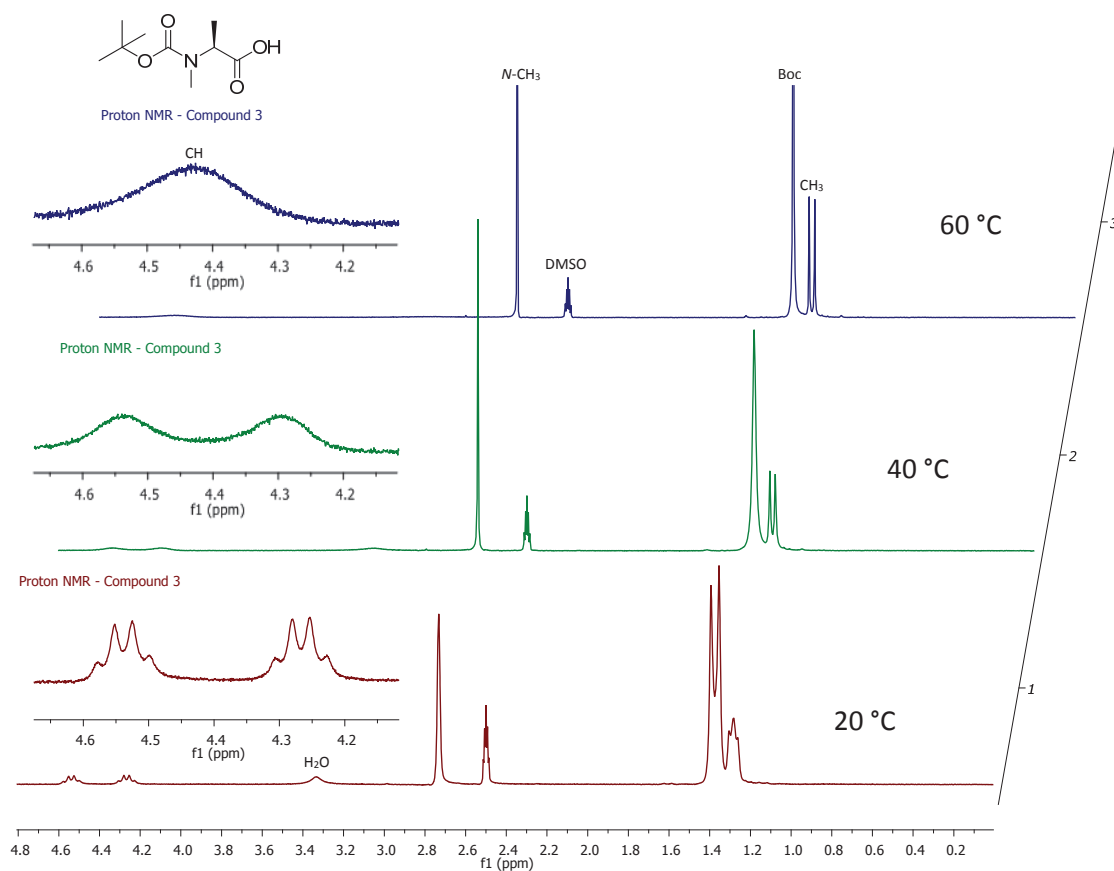
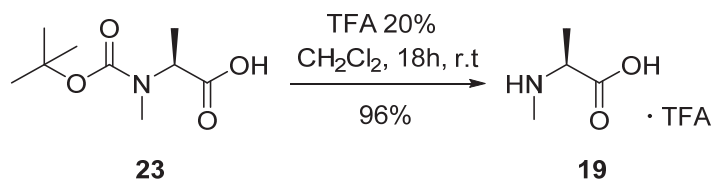


Figure 3.4: ^1H NMR spectra of compound **23** at various temperatures: 20 °C (r.t.), 40 °C and 60 °C. Inset shows expanded region between the range δ 4.1 – 4.7 ppm.

The final step of the synthesis involved the deprotection of compound **23**, by simply stirring with a 20% trifluoroacetic acid in dichloromethane at room temperature, overnight. A 96% yield of the target *N*-methylalanine **19** (isolated as the trifluoroacetate salt) was achieved in the deprotection step, shown in Scheme 3.9. Significantly for the clandestine drug chemist community, an immediate precursor for the synthesis of ephedrine and pseudoephedrine has been easily produced in an overall yield > 75%.



Scheme 3.9: Deprotection of tertiary amine to form target compound **19**.

Although a pathway to *N*-methylalanine **19** was completed, research by Renato *et al.* [146] also examined the reductive methylation of primary and secondary amines using aqueous formaldehyde and zinc. As such, the methodology reported [146] was trialled with L-alanine **15** as an alternative approach (Table 3.3).

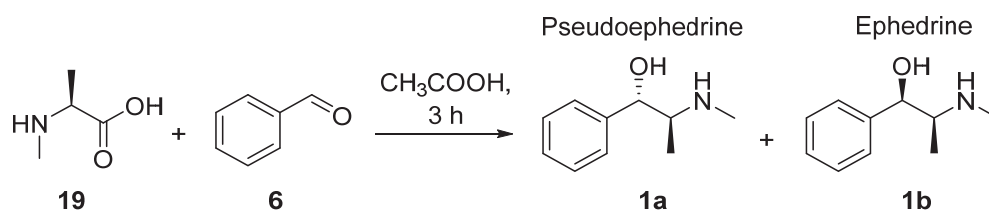
Table 3.3: Reductive methylation of primary amine L-alanine.

Entry	Reagents	Time
1	NaOH, Phosphoric Acid	6 h
2	NaOH, Phosphoric Acid	18 h
3	Monosodium Phosphate	18 h

Initially 16 mL of phosphoric acid was added to 200 mL of de-ionised water, followed by the addition of sodium hydroxide (237 mmol, 2.1 equivalents). Then L-alanine **15** (112 mmol, 1.0 equivalents) was added to the solution in a single portion and finally 10 mL of 37% formaldehyde was added dropwise and stirred for 6 hours and 18 hours. Unfortunately, no *N*-methylalanine **19** was observed in the ^1H NMR spectra of the reported method in any of the three entries from Table 3.3.

Attention turned to the reaction between *N*-methylalanine **19** and benzaldehyde **6**. To build on the research carried out by Painter *et al.* [136], numerous trials of

the reaction were completed for future chemical mapping which will be discussed in Chapter 5. *N*-methylalanine (Compound **19**) can be used as a precursor for the synthesis of a mixture of ephedrine and pseudoephedrine (Compound **1a** and **1b**). It can be produced by the reaction of *N*-methylalanine with benzaldehyde using the Akabori-Momotani reaction as described by Painter *et al.* [136], illustrated in Scheme 3.10.

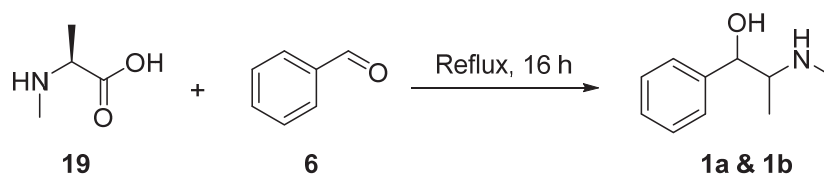


Scheme 3.10: Synthesis of ephedrine/pseudoephedrine.

To date, there is no sign of ephedrine/pseudoephedrine (**1a** and **1b**) being prepared from *N*-methylalanine **19** in this way on any significant scale. In fact, Painter *et al.* [136] only identified trace amounts by GC-MS analysis. However, given the potential for use of the Akabori reaction to prepare a range of precursor materials by using substituted benzaldehydes, it is of great interest. If a ready source of *N*-methylalanine **19** were to be available, it would not be unexpected to find this reaction being explored by illicit laboratories due to its simplicity.

Initially, benzaldehyde **6** (2.0 equivalents) was added slowly to a stirring solution of toluene, triethylamine (1.1 equivalents) and *N*-methylalanine **19** (1.0 equivalent). The solution was stirred to reflux for an hour before 5 v/v % acetic acid was added and then left to stir for a further 15 hours. A number of repeat reactions were performed with parameters altered as per Table 3.4, to test the robustness of this reaction. All produced ephedrine/pseudoephedrine only in small amounts.

Table 3.4: Ephedrine/Pseudoephedrine synthesis from benzaldehyde and N-methylalanine.



Entry	Benzaldehyde Equivalents	Base	Solvent	Acetic Acid v/v (%)	LC-MS trace (Ephedrine)
1	2.0	Et ₃ N	Toluene	5	Yes
2	0.5	None	Toluene	5	Yes
3	2.0	Et ₃ N	Toluene	50	Yes
4	0.5	None	Toluene	50	Yes
5	2.0	Et ₃ N	neat	5	Yes
6	0.5	None	neat	5	Yes
7	2.0	None	DMSO	0	Yes
8	0.5	None	DMSO	0	Yes

Although ephedrine/pseudoephedrine (**1a** and **1b**) were detected in all experiments (Entries 1 – 8), It is important to note, LC-MS confirmed the formation of at least 5 other unknown compounds (m/z 148.1036, m/z 228.1353, m/z 162.0886, m/z 254.1528, m/z 280.169) from the reaction, excluding the ephedrine/pseudoephedrine peak (m/z 166.12263) and there were numerous products observed in the ¹H NMR spectrum. Further purification and optimisation was not necessary and outside this scope of work, as a plausible synthetic route to pseudoephedrine has been confirmed. It is actually quite important that purification is not carried out as a chemical fingerprint cannot be identified (further discussed in Chapter 5), without the presence of its associated impurities.

3.4 CONCLUSION

The methodology presented here may be easily transferable to a clandestine laboratory environment and potentially be used to synthesis pseudoephedrine. The *N*-methylalanine pathway requires readily accessible reagents and only basic glassware to be carried out. Although some care must be taken with the use of sodium hydride for the methylation step of Boc protected L-alanine, this would not be restrictive to a clandestine operation and other bases might also prove useful. Based on the synthesis presented here it is possible for alanine to become a molecule of interest for clandestine drug laboratories involved in the manufacture of methamphetamine, as it has been confirmed as an alternative route to ephedrine/pseudoephedrine.

The work presented in this chapter has been published in a restricted police journal as: **L.M. Andrighetto**, F.M. Pfeffer, J.R. Pearson, P.G. Stevenson, S.M. Hickey, G.J. Barbante, X.A. Conlan, Three step synthesis of *N*-methylalanine – A precursor to ephedrine, pseudoephedrine, and methamphetamine, *Journal of the Clandestine Laboratory Investigating Chemists Association*, 24, 33-37 (2014).

CHAPTER 4:

IN-SILICO OPTIMISATION OF 1D-HPLC AND
2D-HPLC USING DRYLAB[®] SIMULATION
SOFTWARE

CHAPTER OVERVIEW

This chapter incorporates a brief literature summary of the analytical techniques used to analyse methamphetamine samples, highlighting the need of two-dimensional HPLC (2D-HPLC) for comprehensive separation and identification of complex samples. This section explores the use of simulation software DryLab®, and its application for *in-silico* optimisation of a model methamphetamine sample in 1D-HPLC and 2D-HPLC separations. An excellent match between DryLab® predicted separations and actual separations were observed. The 2D-HPLC method developed was then applied to a real methamphetamine seizure sample, identifying the systems limit of detection in both first and second dimensions. A detailed explanation of the advantages and disadvantages of 2D-HPLC and how they can improve modern chromatographic chemical fingerprinting is discussed in detail.

4.1 Introduction

The current limitations of methamphetamine impurity profiling have been recently described by Stojanovska *et al.* [26] who stated that '*future research is needed to address the knowledge gaps in regards to the manufacture of drugs of current interest*'. Globally, Australia has one of the highest recorded consumption rates of methamphetamine with an estimated 1/20 residents having tried it for recreational purposes and 395,000 reported users in 2010 [172]. Gas and liquid chromatography coupled to mass spectrometry (GC-MS and LC-MS), infrared spectroscopy (IR) and capillary electrophoresis (CE) have traditionally been the primary analytical techniques used to generate chemical information from methamphetamine seizure samples [173]. Other techniques have been used to study methamphetamine samples such as nuclear magnetic resonance spectroscopy (NMR) [62], ion mobility spectrometry [174], isotope ratio mass spectrometry (IRMS) [175], and high performance liquid chromatography (HPLC) [176, 177]. However, the capacity to rapidly generate comprehensive chemical fingerprints of seized methamphetamine, and its impurities, is of upmost importance to Australian law enforcement agencies in order to track and identify clandestine laboratories and only multidimensional chromatography affords this.

The relative concentrations of associated pathway impurities in the synthetic route are somewhat variable and can be dependent on the clandestine laboratory environment [148]. This variability, when coupled with the extensive range of cutting agents commonly used in the production of methamphetamine, forms a chemical matrix that can be elucidated by law enforcement agencies to individualise seizure samples [178].

The advent of two-dimensional high performance liquid chromatography (2D-HPLC) has enhanced an analyst's ability to develop separation procedures for the analysis of components in complex forensic [47], industrial [179], biomedical [180], and pharmaceutical [181] samples. Comprehensive two-dimensional gas chromatography with time of flight mass spectrometry has been used by forensic chemists to profile complex drug samples [182, 183]. In forensic field studies

multi-dimensional gas chromatography has been used to monitor volatile compounds of interest such as molecules from decaying bodies [184]; however, this study was limited by the inability of the separation to deal with the immensely complex sample background. Despite the complex nature of samples in forensic science 2D-HPLC has not had as large uptake due to the time limits traditionally associated with sample analysis and the complexity of data handling [185]. However, in addition to forensic science, 2D-HPLC has been used to elucidate cannabinoids in hemp [73] and alkaloids in Chinese medicine [186]. A targeted form of 2D-HPLC has been investigated in this thesis that can isolate ephedrine and pseudoephedrine from methamphetamine excipient standard mixtures, however the comprehensive chemical information on a seizure sample has not been determined.

In order for 2D-HPLC to be fully exploited for detailed forensic investigations fundamental aspects of the separation process need to be optimised. This is driven by the fact that conventional 1D-HPLC is limited by the number of theoretical plates (resolving power) available, the heterogeneity of the column material and the potential disruption of analytes due to viscous fingering [187]. Viscous fingering is defined as a flow instability phenomenon caused by two different solvent viscosities being forced together through a porous medium, for example, when a heart-cut from the first dimension is injected into the second dimension [188]. It is important to note that viscous fingering is likely to be more problematic in 2D-HPLC when the concentrations between dimensions is more extreme and the injection volumes are large [74]. The use of two chromatography columns in 2D-HPLC dramatically increases the resolving power of complex samples when different separation mechanisms are used in each dimension [189, 190], as demonstrated in Figure 4.1.

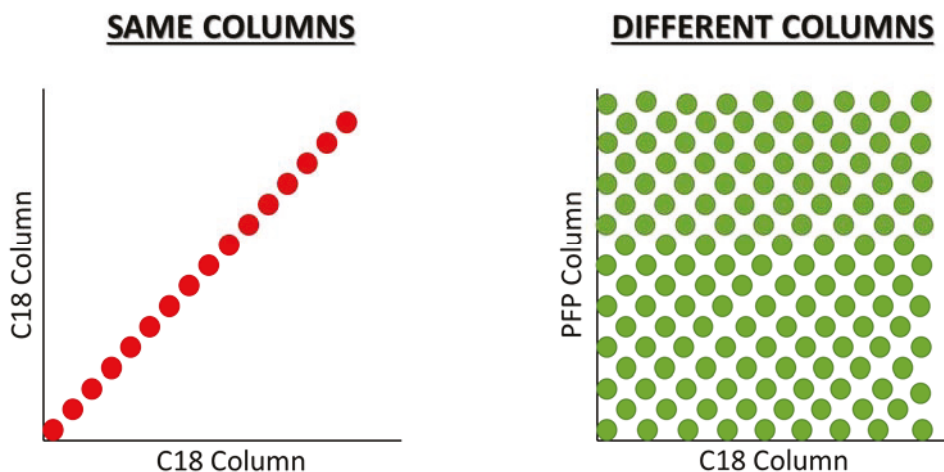


Figure 4.1: Potential separation space of 2D-HPLC when using different columns with different retention mechanisms compared to using the same columns.

There are a range of experimental factors that influence a chromatographic separation (solvent type, temperature, flow rate etc.). However, the most important variable is the stationary phase and should be the first aspect addressed in any optimisation process [191].

Several techniques have been explored to optimise the 2D-HPLC separation space including the analysis of relative retention profiles of a library of HPLC columns. However, due to the complexity of samples requiring a multidimensional separation this method proved to be problematic as representative standards cannot be easily found [192]; also, these types of approaches are typically very time consuming due to the number of injections and the flow rate of the second dimension [193].

The importance of this aspect has been highlighted by Stevenson and co-workers [189] who have developed a fundamental study highlighting the significance of C18 and C1 stationary phases, for the separation of PAH's in a model system. This stresses the importance of selectivity for complex real world samples such as those in the forensic sciences. Gilar and co-workers [194] developed a robust method for calculating the orthogonality and separation space utilisation of two columns in a 2D-HPLC analysis. This method was used to calculate the $f_{coverage}$, also

known as orthogonality (O) for the 2D-HPLC peak capacity equation [195] by dividing the separation space by a number of bins equal to the number of separated components to provide the fractional surface coverage. Peak capacity, n_c , is directly proportional to orthogonality (O) as per Equation 1.

$$\text{Equation 1: } n_{c,2D} = \frac{n_{c,1} \times n_{c,2} \times f_{coverage}}{\langle \beta \rangle}$$

where, $n_{c,2D}$ is the practical 2D-HPLC peak capacity,

$n_{c,i}$ is the peak capacity in both separation dimensions,

$f_{coverage}$ is the proportional amount of separation space utilisation, and

$\langle \beta \rangle$ is the under-sampling correction factor.

The utilisation of separation space, which can be calculated by Equation 2: where $\sum bins$ is the number of occupied bins and P_{max} is the total number of bins.

$$\text{Equation 2: } O = \frac{\sum bins - \sqrt{P_{max}}}{0.63 \times P_{max}}$$

The stationary phase has the greatest impact on peak capacity, however the solvent should not be neglected as it can act as a major driver on retention processes for example the π - π interactions that are observed between acetonitrile and C18 stationary phases [191]. The mobile phase associated with a two-dimensional separation needs to be carefully considered to avoid solvent mismatch which may lead to issues such as viscous fingering as identified by Shalliker and Guiochon [196]. The selection of appropriate stationary phases, mobile phases, and analysis time need to be considered in the optimisation of 2D-HPLC experiments. Traditionally, 2D-HPLC method development has taken

considerable time and there exists a real need for a simplified optimisation approach.

This chapter introduces the DryLab® software package [89] in order to efficiently optimise the gradient profile for a rapid separation of key components in a model methamphetamine seizure sample. This will allow the superior resolving power of 2D-HPLC to screen seizure samples and create a chemical fingerprint of production impurities and cutting agents.

The interaction between the solute and the stationary phase in chromatography is well known and has been reported by Horváth and co-workers [85] with equation 3:

$$\text{Equation 3:} \quad K = \frac{[SL]}{[S][L]}$$

Where K, is the equilibrium constant,

S, is the solute molecules,

L, is the hydrocarbonaceous ligands,

SL, is the solvophobic interactions

It is with this main equation, that the DryLab® program is able to simulate, predict and optimise both one-dimensional and two-dimensional HPLC separations.

Two-dimensional HPLC has the capacity to separate complex mixtures *via* two independent retention mechanisms, which allows for the resolution of otherwise co-eluting species [197]; 2D-HPLC has not previously been used for impurity profiling of methamphetamine samples. Simulation software has been used for the first time on methamphetamine seizure samples in order to rapidly optimise an HPLC separation. This type of optimisation will ultimately lead to improved chemical fingerprinting of clandestine drug seizure samples.

4.2 Experimental

There are two major experiments in this chapter and as such will be listed sequentially.

Standards and Samples - Experiment 1

All standards (methamphetamine, ephedrine, pseudoephedrine, paracetamol, caffeine, benzyl alcohol, dimethyl sulfone, benzaldehyde, phenyl-2-propanone (P2P) and diphenylacetone) were obtained from Sigma-Aldrich (Castle Hill, NSW, Australia) and the National Measurement Institute, Australian Government (Port Melbourne, Vic, Australia). High performance liquid chromatography grade acetonitrile (ACN) and methanol was obtained from Ajax Finechem (Taren Point, NSW, Australia); deionized water (Continental water systems, Vic, Australia) was filtered through a 0.45 μm membrane filter (Sigma-Aldrich) prior to use. Stock solutions of all standards were prepared by dissolving in a solution of 5% aqueous ACN at a concentration of 1 mg mL^{-1} and were diluted 5-fold with 5% aqueous ACN prior to injection.

High Performance Liquid Chromatography - Experiment 1

An Agilent Technologies (Mulgrave, VIC., Australia) 1260 2D-chromatograph was used for all separations, including: auto injector; capillary pump; binary pump; column thermostat; 2 position 8 port switching valve; and two diode array detectors (one in each dimension, which recorded at 254 nm). Two chromatography columns were used: the first dimension column constituted of an Agilent Poroshell 120 EC-C18 (4.6 \times 100 mm, 2.7 μm particle diameter); the second dimension a Phenomenex (Lane Cove, NSW, Australia) Kinetex C18 (100 Å pore diameter, 4.6 \times 100 mm, 2.6 μm particle diameter). All analysis was completed at 1 mL min^{-1} and 1 μL of all model drug solutions were injected in triplicate to ensure reproducibility. Two-dimensional HPLC was completed in the on-line heart-cutting mode, whereby a single 20 μL aliquot of the first dimension (switched at 4.31 min) was transferred to the second dimension *via* a sample loop

and an 8 port 2 position switching valve; valve timing was controlled with by the HPLC control software.

DryLab® Optimization - Experiment 1

The DryLab® user manual requires screening data of each component from two injections with different gradient times (20 and 60 min, respectively) to optimise the separation's gradient profile [99]. Each standard was injected individually into a linear gradient over the aforementioned times with an initial mobile phase of 5% aqueous ACN that increased to 95% aqueous ACN. Retention time, heights and areas for each injection was recorded and subsequently entered into DryLab®. The gradient profile of the chromatogram generated by DryLab® was then manually adjusted in order to produce the optimum representative separation in the least amount of time and was applied to the analysis of the model seizure sample.

Model Seizure Samples - Experiment 1

Stock solutions of all standards were prepared by dissolving in a solution of 5% aqueous ACN at a concentration of 1 mg mL⁻¹ and were diluted 5-fold with 5% aqueous ACN. A 100 µL aliquot of each standard was put into a 2 mL HPLC Vial. According to the optimised simulation the model seizure mixture was separated carried out in triplicate with 1 µL injections and a flow rate of 1 mL min⁻¹ with a gradient time of 15.57 min. The initial conditions were 5% aqueous ACN to 95% aqueous ACN over 11.57 minutes with a detection wavelength of 254 nm. The second dimension was completed in isocratic mode with a mobile phase of 85% aqueous methanol until all peaks were eluted; separation was recorded at 254 nm and 210 nm. Both columns were thermostated at 30 °C within the column heater.

Chemicals - Experiment 2

Milli-Q water was obtained in-house (Continental Water Systems, Victoria, Australia); HPLC grade ACN was purchased from Sigma-Aldrich Pty Ltd (Castle Hill, NSW, Australia).

Standards and Samples - Experiment 2

Paracetamol, caffeine, benzaldehyde, aspirin, creatine, procaine, *N*-methylalanine, and diphenylacetone were obtained from Sigma-Aldrich. Methamphetamine, pseudoephedrine, ephedrine and phenyl-2-propanone (P2P) were obtained from and the National Measurement Institute, Australian Government (Port Melbourne, Vic., Australia). Stock solutions of all standards were prepared by dissolving in a solution of 5% aqueous ACN at a concentration of 1 mg mL⁻¹ and were diluted 10-fold with a 5% ACN in water solution and mixed prior to injection. All methamphetamine seizure samples were provided by Victoria Police Forensic Services Department (Macleod, Victoria, Australia).

Chromatography Columns - Experiment 2

Five HPLC columns were trialled for the selectivity study of a model seizure sample (Table 4.1)

Table 4.1: Trialled HPLC columns.

	Brand	Type	Size	Dimensions	Part Number
Column 1	Phenomenex	Kinetex PFP 100 A	2.6 µm	4.6 x 100 mm	00D-4477-E0
Column 2	Phenomenex	Kinetex Phenyl-Hexyl 100 A	2.6 µm	4.6 x 100 mm	00D-4495-E0
Column 3	Agilent	Poroshell 120 EC-C18	2.7 µm	4.6 x 100 mm	695975-902
Column 4	Agilent	Poroshell 120 Bonus RP	2.7 µm	4.6 x 100 mm	695968-901
Column 5	Phenomenex	Kinetex Biphenyl	2.6 µm	2.1 x 100 mm	00D-4622-AN

2D-HPLC - Experiment 2

Chromatographic analysis was performed with an Agilent 1260 system (Agilent Technologies, Mulgrave, Victoria, Australia), incorporating a quaternary pump with solvent degasser, an auto-sampler and a DAD module which monitored the absorbance at 254 nm. Chromatographic data was obtained and processed with Agilent ChemStation software. All injections were 60 µL and carried out in triplicate. The first dimension column was a Phenomenex Kinetex PFP 100Å (4.6 × 100 mm, 2.6 µm particle diameter) and the second dimension a Phenomenex Onyx Monolithic C18 (4.6 × 100 mm). The first dimension gradient was completed

at a flow rate of 0.1 mL min^{-1} with an initial mobile phase of 5% aqueous ACN that increased to 30% aqueous ACN over 100 minutes and then increased to 100% ACN for a further 10 minutes. The second dimension gradient was completed at 5 mL min^{-1} with an initial mobile phase of 5% aqueous ACN that increased to 80% aqueous ACN for 1 minute. The comprehensive two-dimensional separation had an overall completion time of 110 minutes. Two-dimensional HPLC was completed in on-line comprehensive mode with a modulation time of 1.5 minutes, whereby a fraction volume of $75 \text{ }\mu\text{L}$ was transferred to the second dimension *via* a sample loop and an 8 port 2 position switching valve; valve timing was controlled with by the HPLC control software.

Measurements for bins, plate heights, plate numbers and peak variances were performed with Wolfram Mathematica 10.3 (distributed by Hearn Scientific, South Yarra, Victoria, Australia) using algorithms written in-house.

LC-MS - Experiment 2

High resolution mass spectrometry (HRMS) was performed using an Agilent 6210 MSD TOF mass spectrometer with the following settings: gas temperature ($350 \text{ }^{\circ}\text{C}$), vaporizer ($28 \text{ }^{\circ}\text{C}$), capillary voltage (3.0 kV), cone voltage (40 V), nitrogen flow rate (5 L min^{-1}), nebuliser (15 psi).

4.3 Results and Discussion

4.3.1 1D-HPLC using DryLab®

DryLab® [198] is a software tool that allows scientists to optimise several chromatographic variables *in-silico* to rapidly optimise a HPLC separation. It does this by taking the results obtained from an analyte run at two different gradient times, t_G , to obtain values of k_0 and S for each solute [199] When pre-elution and post-elution of the solutes can be ignored these parameters can be obtained by solving a set of simultaneous equations [199]:

$$t_{g,1} = \frac{t_0}{b_1} \log(2.3k_0b_1 + 1) + t_0 + t_D$$

$$t_{g,2} = \frac{t_0}{b_2} \log(2.3k_0b_2 + 1) + t_0 + t_D$$

where

$$b = \frac{V_0 \Delta \Phi S}{t_G F}$$

and $t_{g,1}$ and $t_{g,2}$ are the retention times for the first and second dimensions, respectively; $\Delta \Phi$ is the change in proportion of the strong mobile phase component, Φ , during the gradient; t_0 is the time required to elute an un-retained marker and t_D is the dwell time of the system, i.e. the time required for concentration changes in the mobile phase to leave the pump and enter the head of the column. Using the above equations it is relatively easy to simulate how subtle changes to the gradient can change the elution order and resolution of a HPLC separation. The software has the capacity to optimise 3 different experimental parameters simultaneously, which is very helpful when designing a rapid 2D-HPLC separation, rapidly identifying co-eluting peaks. DryLab® facilitates this process by generating a resolution map to identify the optimal gradient time, which can then be further manipulated by adding extra gradient steps in the gradient editor. Targeted 2D-HPLC, known as heart-cutting, is a protocol whereby only select portions of co-eluting peaks are transferred to the second dimension; this is important for rapid 2D-HPLC when a comprehensive analysis is superfluous. It is significant that the simulation software could predict co-elution and identify when this occurs so that the target analysis could be streamlined.

A model seizure sample of methamphetamine with commonly associated side products and cutting agents was prepared for *in-silico* optimisation [47]. Specifically a sample mixture containing: methamphetamine, ephedrine, pseudoephedrine, nicotinamide, paracetamol, caffeine, benzyl alcohol, dimethyl sulfone, benzaldehyde, P2P and diphenylacetone was prepared. Initially, each standard was run individually at a 20 minute gradient and a 60 minute gradient to train the algorithms and the corresponding retention times and peak heights were recorded and entered into the software. DryLab® then provided the optimal separation conditions for baseline separation of all the compounds, illustrated in Figure 4.2. Note that nicotinamide was not retained and eluted in the void volume. Note: Peak D/E (i.e. ephedrine and pseudoephedrine) co-eluted and could not be separated according to the simulations.

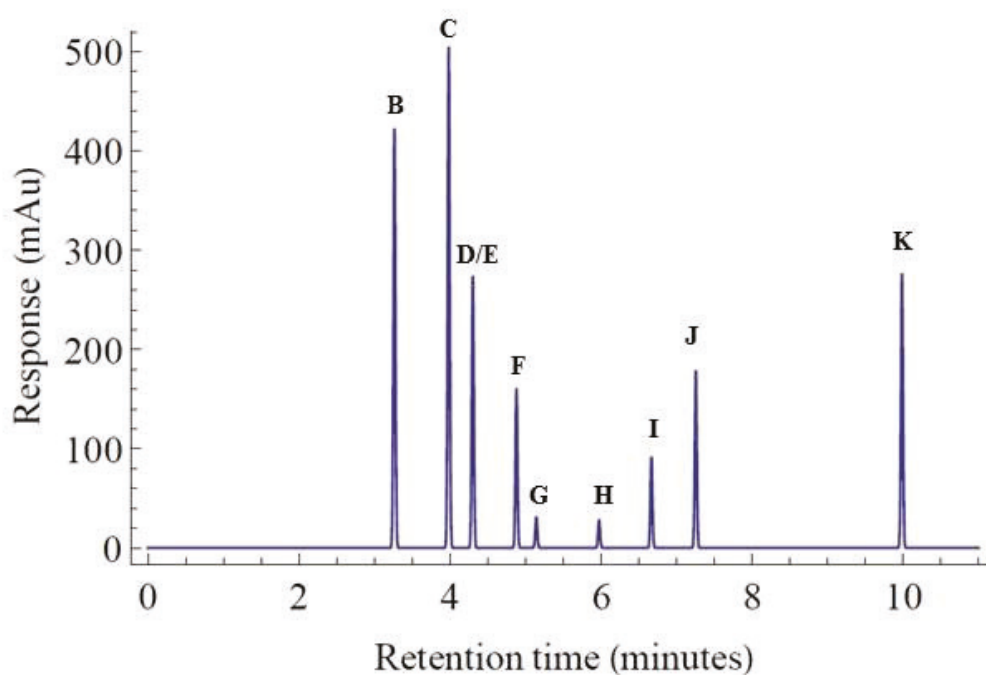


Figure 4.2: Optimised DryLab® prediction **B** – Paracetamol, **C** – Caffeine, **D/E** – Ephedrine/Pseudoephedrine, **F** – Methamphetamine, **G** – Benzyl Alcohol, **H** – Dimethyl Sulfone, **I** – Benzaldehyde, **J** – Phenyl-2-propanone, **K** – Diphenylacetone.

To test the accuracy of the simulation software, a mixed solution containing all of compounds **A-K** were made and the DryLab® optimal conditions were trialled in an actual separation that is shown in Figure 4.3.

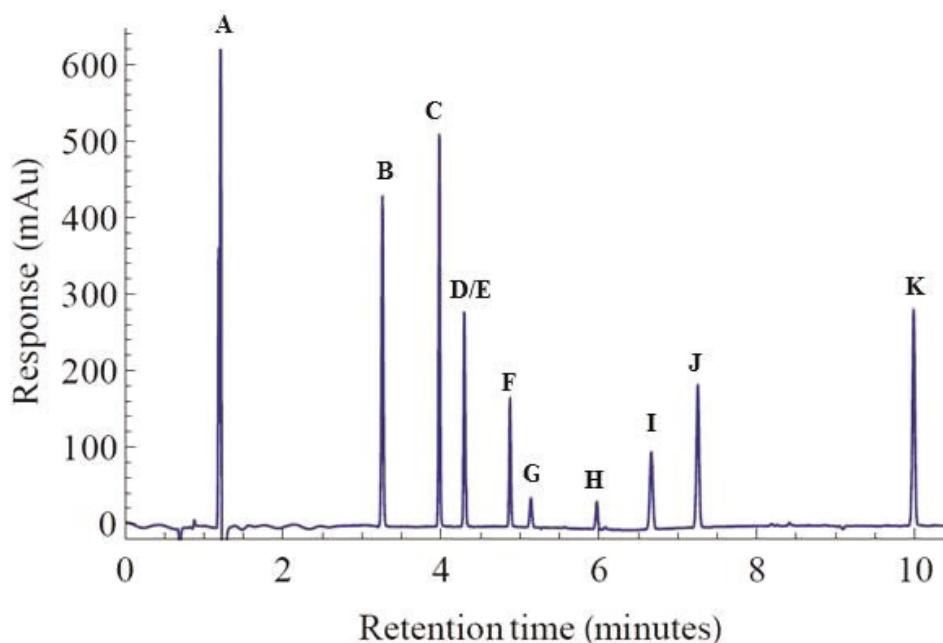


Figure 4.3: Separation of the model methamphetamine sample.

A – Nicotinamide (**B** – **K** as for Figure 4.1).

It is important to note that the optimal separation provided a relatively fast gradient time (i.e. t_G) of 11.57 minutes to resolve all the peaks of interest, with the exception of the ephedrine and pseudoephedrine diastereomers (peak **D/E**), which co-eluted, however, the actual time taken to elute all 10 compounds was only 9.7 minutes prior to the completion of the gradient. As predicted, peak **A** – nicotinamide – eluted in the void volume. This separation was completed with an ACN mobile phase and a C18 HPLC column. The model seizure sample was analysed in triplicate with experimental parameters matching those provided by the software. The direct overlay of the model methamphetamine sample and the DryLab® prediction, shows excellent matching of peaks (Figure 4.4). It is important

to note that the limitations on DryLab® modelling is based on the theoretical peak capacity of the chromatography column.

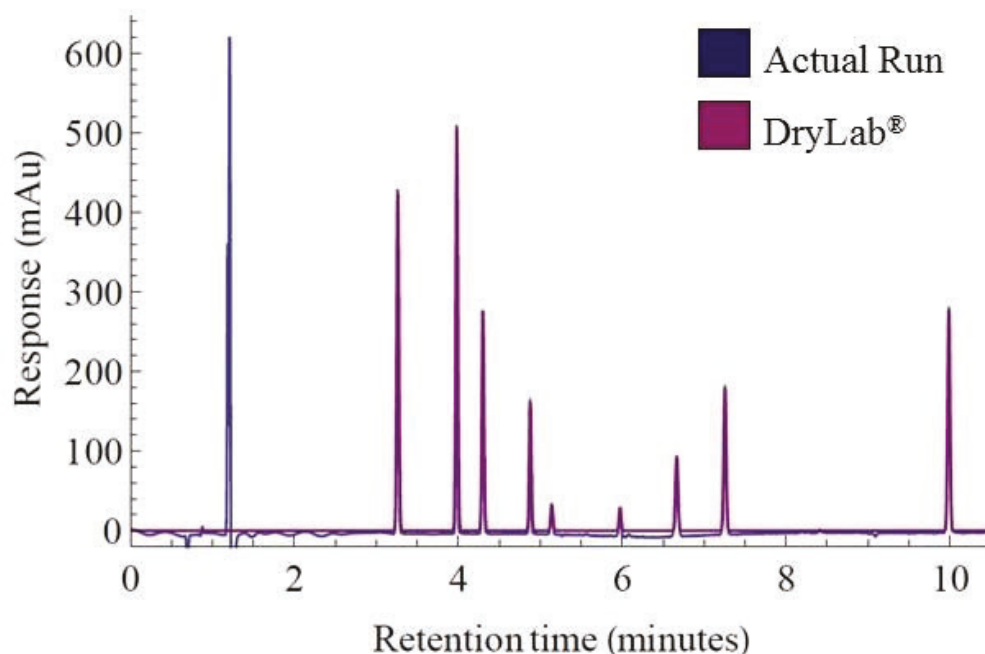


Figure 4.4: Overlay of optimised DryLab® prediction and separation of the model methamphetamine sample.

Importantly, the co-elution of the ephedrine and pseudoephedrine were observed in the real separation, as predicted by the simulation software. Co-elution of diastereomers is a common problem in chromatography, and is a great challenge for the identification of the precursor involved in the synthesis of methamphetamine. Ephedrine and pseudoephedrine were resolved from the other compounds and each other with a simple 2D-HPLC separation protocol. The peak (**D/E**) at a retention time of 4.31 minutes in the first dimension was transferred to a second dimension with a 20 μ L sample loop and an 8 port, 2 position, switching valve. The second dimension was operated with an isocratic methanol/H₂O mobile phase (85% MeOH) on a C18 column, the different selectivities afforded by the solvents polarity was sufficient to allow the resolution of all model compounds. The second dimension separation is illustrated in Figure 4.5.

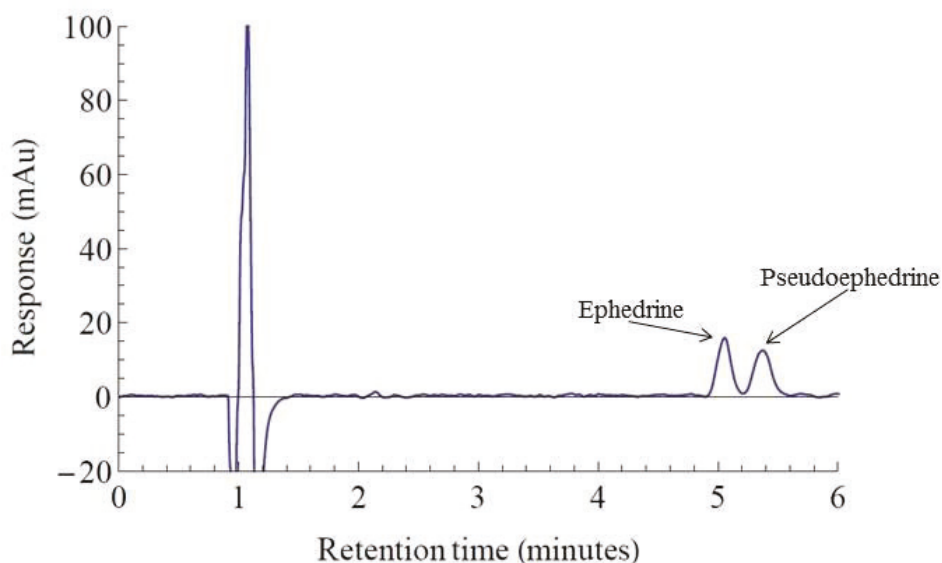


Figure 4.5: Second dimension separation of ephedrine and pseudoephedrine (both $1.3 \times 10^{-3}M$) from the overlapping peak (D/E).

The ephedrine and pseudoephedrine have been baseline resolved with retention times of 5.05 and 5.38 minutes respectively in the second dimension. This is an important finding for three reasons:

1. The diastereomers have been separated;
2. A simple C18:C18 two dimensional separation was sufficient for baseline resolution of the analytes. It is important to note that the separation in this case is driven by the difference in the mobile phases across the two dimensions. While C18:C18 limits the ability to generate a large separation space this make the system much simpler to apply. For more complex samples different stationary phases would be required as highlighted in Chapter 5.
3. The total analysis time for the separation of all model compounds in both dimensions, including discrimination between ephedrine and pseudoephedrine, was completed in 10.31 minutes (4.31 min first dimension + 6.00 min second dimension).

4.3.2 2D-HPLC using DryLab®

As the DryLab® simulation software has worked extremely well with conventional one dimensional HPLC, attention turned to using DryLab® as a tool for the optimisation of a full comprehensive two-dimensional separation. Within this study a full comprehensive 2D separation was developed by slowing the first dimension flow rate down significantly (0.1 mL min^{-1}) and transferring 4 fractions per minute into the second dimension.

A model seizure sample was prepared containing known concentrations of methamphetamine and 11 other common precursors and cutting agents: pseudoephedrine, ephedrine, phenyl-2-propanone (P2P), paracetamol, caffeine, benzaldehyde, aspirin, creatine, procaine, *N*-methylalanine, and diphenylacetone. After a column selectivity study was performed (which will be discussed in chapter 5), a combination of the PFP and EC-C18 stationary phases was found to provide the greatest surface space utilisation with an f_{coverage} of 0.18 (see Figure 4.6). To facilitate a rapid separation towards the goal of 'fit-for-purpose' analysis the monolithic [200] C18 column was trialled in place of the particle packed column; an f_{coverage} of 0.18 was maintained. The first dimension was completed at a flow rate of 0.1 mL min^{-1} to allow for a modulation frequency of 3 transfers of each first dimensional peak to the second dimension. Therefore, the second dimension must be performed very fast so that the second analysis can be done in a time equal to the period of fraction collection minus the fraction transfer time [70] a speed that can only be afforded by the monolithic column.

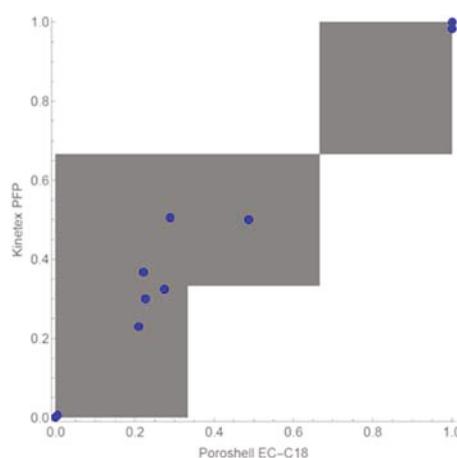


Figure 4.6: Bins plot (Poroshell C18 \times Kinetex PFP) of two dimensional HPLC separation of the model methamphetamine seizure sample.

With this in mind, a fully comprehensive two-dimensional separation was completed with a total analysis time of 115 minutes, the separation is illustrated in Figure 4.7. The retention times predicted by DryLab® are shown by the white circles, which have been overlaid on the actual two dimensional separation (Figure 4.7).

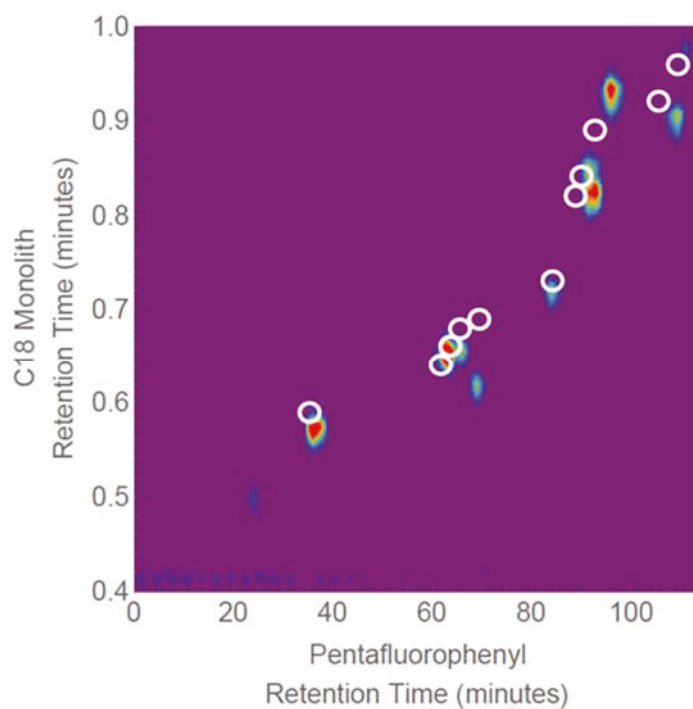


Figure 4.7: Overlaid DryLab® and actual two dimensional separation of the model methamphetamine seizure sample.

Likewise, a more detailed 3D representation of the actual two-dimensional separation, highlighting the intensities of each compound was created and shown in Figure 4.8.

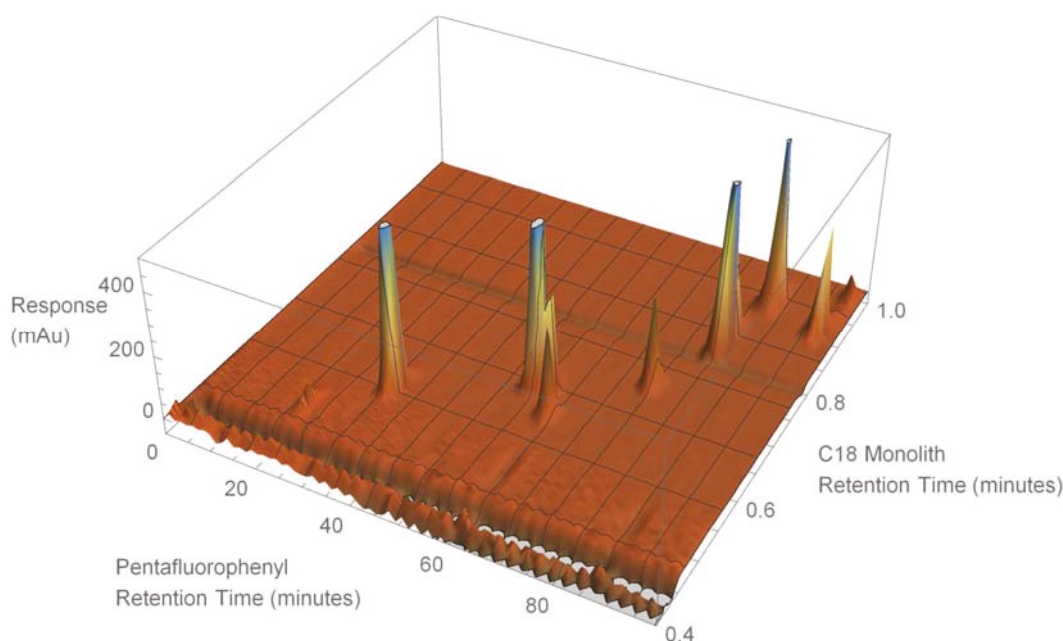


Figure 4.8: 3D representation of a model methamphetamine seizure sample two-dimensional separation.

This is the first time *in-silico* software has been used to predict a two dimensional separation of methamphetamine samples and indeed forensically relevant samples at large. This is of great significance for the development of 2D-HPLC protocols, a process that historically takes considerable time. The total method development time for separation presented in Figure 4.8 was less than two hours with *in-silico* aided optimisation. This is significantly less than the time required for typical optimisation of individual sample injections [47]. The results of 2D-HPLC separation prediction was impressive as all components of interest were closely matched. This is not a trivial outcome due to the complex nature of the separation mechanisms involved allowing the user to have high confidence in the *in-silico* prediction.

4.3.3 2D-HPLC of a real methamphetamine seizure sample

In order to determine the effectiveness of this process 12 real methamphetamine seizure samples provided by Victoria Police Forensic Services Department were analysed using the developed method. Several components were observed in all of the seizure samples; a characteristic chromatogram is presented in Figure 4.9.

The two major components in Figure 4.9 are methamphetamine (first dimension retention time ($R_{t,1}$) of 83.4 min, second dimension retention time ($R_{t,2}$) of 0.72 min) and pseudoephedrine ($R_{t,1} = 68.1$ min, $R_{t,2} = 0.66$ min) that were determined by comparing the retention times against known standards. With only two detected component peaks this sample is particularly clean; this is not uncommon in crystal methamphetamine samples. Trace amounts of excipients were not observed in this or any of the other eleven samples.

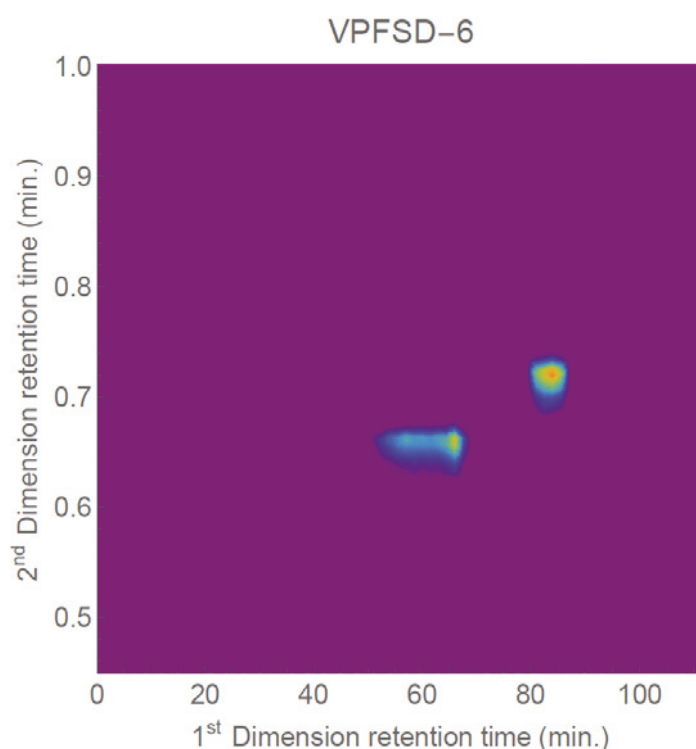


Figure 4.9: Victoria Police Forensic Services Department (VPFSD) methamphetamine seizure sample.

As high resolution mass spectrometry is a significantly more sensitive technique than UV detection using HPLC [201], LC-MS was used to analyse all twelve seizure samples also in the search for other excipients. The associated masses of all 12 random seizure samples are shown in Table 4.2. As there were a few more compounds detected using LC-MS, it highlights the fact that there are some detection limit issues when looking for trace amounts of excipients using a UV detector. However, it is important to note that for 8 out of the 12 random seizure

samples, three or less compounds were detected, again highlighting the clean nature of these samples in Victoria.

Table 4.2: Molecular weights detected in methamphetamine (MA) seizure samples including pseudoephedrine (PE).

SAMPLE	<i>m/z</i>	<i>m/z</i>	<i>m/z</i>	<i>m/z</i>	<i>m/z</i>
VPFSD-1	MA	144.9872	168.0204	-	-
VPFSD-2	MA	144.9872	168.0204	-	-
VPFSD-3	MA	179.0111	335.2257	-	-
VPFSD-4	MA	165.0756	-	-	-
VPFSD-5	MA	PE	148.1124	198.0980	383.1165
VPFSD-6	MA	PE	148.1128	198.0980	335.2248
VPFSD-7	MA	PE	335.2255	-	-
VPFSD-8	MA	335.2280	-	-	-
VPFSD-9	MA	335.2273	-	-	-
VPFSD-10	MA	335.2256	-	-	-
VPFSD-11	MA	PE	133.0875	148.1118	198.0966
VPFSD-12	MA	PE	198.0961	226.1589	383.1153

The determination of excipients is of particular importance for chemical fingerprinting and is useful when analysing intermediate synthetic samples found in clandestine laboratories.

4.3.4 2D-HPLC of a synthesised intermediate sample to methamphetamine

To assess the level of chemical complexity that can be assessed with 2D-HPLC an intermediate sample from a methamphetamine synthesis in the laboratory was analysed and is presented in Figure 4.10.

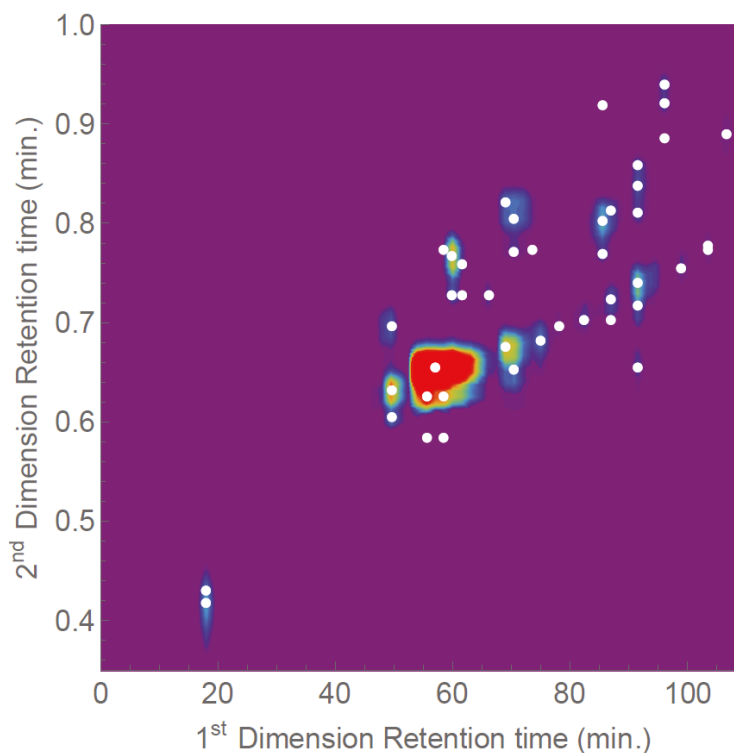


Figure 4.10: Synthesised intermediate sample to methamphetamine.

More than forty components were detected based on peak maxima, determined by examining the derivatives of the curves using algorithms described by Stevenson *et al.* [202]. The components in the intermediate sample are highlighted by white dots in Figure 4.10, thus emphasising the forensic significance of fingerprinting intermediate seizure samples to build a comprehensive database of the chemical pathways in a clandestine laboratory. For example, if dirty glassware were found at a clandestine laboratory, this technology can be used to trace back to the use of exact precursors which may be enough to determine exactly what processes have been used.

The distribution of the components in the model system and the real intermediate sample generally appear in the top right hand quadrant of the two dimensional separation, due to the non-polar nature of the components present. While the other three quadrants are not fully exploited here, it is important for any analyst to use the full separation procedure in case some unknown polar excipients are present and to counter any future novel syntheses that may present more polar

components. While this will add to the overall separation time, it is of greater importance to the forensic community to have a comprehensive analysis so one universal method can be used regardless of the synthetic route, location, purity and precursors.

An $f_{coverage}$ of 0.49 was found when the surface space usage of the intermediate separation was completed, far exceeding that of the standard mixture ($f_{coverage}$ of 0.18). While every attempt was made to replicate a typical seizure sample, the optimisation of the model sample did not accurately reflect the separation space used by the actual intermediate sample (Figure 4.10). This highlights the issues faced when selecting columns for 2D-HPLC and the importance of creating a universal separation that can cope with complex mixtures.

It is important to consider the analytical figures of merit for this type of two dimensional separation, in order to determine if transferring peaks between dimensions has any influence on the detection limit. To achieve this several key excipients (paracetamol, caffeine, methamphetamine, pseudoephedrine, procaine and aspirin) were selected and the limit of detection (LOD) in the second dimension ($LOD_{1D-HPLC}$) was calculated and recorded in Table 4.3. The limit of detection were calculated multiplying the slope of the calibration curve by 3.3 and dividing by the standard error [203]. The LOD of these compounds was in the range of 3×10^{-5} M, which was comparable to literature values [204-206].

Table 4.3: 2D-HPLC Limit of Detections.

EXCIPIENT	Rt (min)	R ²	Calibration Equation	LOD _{1D-HPLC} (M)	LOD _{2D-HPLC} (M)
Methamphetamine	2.46	0.9999	$y = 1 \times 10^6x - 8.8$	2.7×10^{-5}	4.6×10^{-4}
Pseudoephedrine	1.55	0.9999	$y = 1 \times 10^6x + 8.2$	2.3×10^{-5}	4.0×10^{-4}
Aspirin	4.26	0.9998	$y = 918340x - 29.1$	5.4×10^{-5}	9.3×10^{-4}
Caffeine	2.07	0.9985	$y = 2 \times 10^6x - 12.8$	2.9×10^{-5}	5.2×10^{-4}
Paracetamol	0.76	0.9988	$y = 755343x - 0.61$	3.4×10^{-5}	5.9×10^{-4}
Procaine	1.23	0.9997	$y = 220286x + 10.6$	1.2×10^{-4}	2.0×10^{-3}

The ideal modulation frequency when transferring analytes between dimensions in 2D-HPLC is 3–4 fractions per peak [207]. To ensure this frequency is maintained for peaks in adjacent fractions, the amount of transferred analyte must at least match the second dimension's limit of detection ($LOD_{2nd-dimension}$). In this work a modulation frequency of 3 fractions per peak was maintained whereby a minimum of 5.8% of the first dimension peak (fractions 1 and 3 – derived by dividing the area of a Gaussian peak with an area of 1 into 3 evenly spaced segments) were transferred, with the assumption that the peak maxima is centred in the 4σ peak width. To maintain detected 3 fractions per peak the minimum amount of transferred material was 5.8% of the total peak area with a concentration at least equal to the $LOD_{2nd-dimension}$ after separation. Thus, the total concentration of compound injected (i.e. the $LOD_{2D-HPLC}$) is calculated by Equation 3, which is transposed in two steps below:

$$5.8\% LOD_{2D-HPLC} = 100\% LOD_{2nd-Dimension} \quad (\text{Equation 3})$$

$$LOD_{2D-HPLC} = 100\% / 5.8\% LOD_{2nd-Dimension}$$

$$LOD_{2D-HPLC} = 17.2 \times LOD_{2nd-Dimension}$$

As such, the $LOD_{1D-HPLC}$ (single dimension) must be multiplied by 17.2. Following the same procedure the effect will become significantly more pronounced as the modulation frequency increases, for example if a modulation frequency of 4 fractions per peak was used the $LOD_{2D-HPLC}$ is equal to $107.9 \times LOD_{2nd-dimension}$. Table 4.2 lists the LODs (one and two-dimensions) of standards for 6 common excipients in the manufacture of methamphetamine and is in the order of 5×10^{-4} M.

4.4 Conclusion

The use of *in-silico* optimisation of two-dimensional separations for the analysis of methamphetamine seizure samples has been shown to have a significant impact on the experimental development time. The greatest challenge in 2D-HPLC method development has typically been the time required to identify the columns required to provide the greatest separation space utilisation. This was overcome here with Drylab[®] optimisation software. This improvement in analysis time also reduces the organic solvent load produced and directly impacts the laboratory waste generated. Importantly the Drylab[®] optimised *in-silico* separations matched closely with the model and synthetic samples allowing the analyst to have confidence in the predicted separation parameters despite the complex nature of the separation mechanisms involved. A 2D-HPLC separation was completed that isolated more than 40 individual chemical compounds from an intermediate methamphetamine sample. This knowledge can be used by the forensic analyst to create a chemical fingerprint of the seizure, which can theoretically be linked back to a clandestine laboratory.

The work presented in this chapter has been published in the following two papers:

L.M. Andrighetto, P.G. Stevenson, J.R. Pearson, L.C. Henderson, X.A. Conlan, DryLab[®] optimised two-dimensional high performance liquid chromatography for differentiation of ephedrine and pseudoephedrine based methamphetamine samples, *Forensic Science International*, 244, 302-305 (2014).

L.M. Andrighetto, N.K Burns, L.C. Henderson, C.J Bowen, J.R. Pearson, P.G. Stevenson and X.A. Conlan, *In-silico* optimisation of two-dimensional HPLC for the determination of Australian methamphetamine seizure samples, *Forensic Science International*, 266, 511-516 (2016).

CHAPTER 5:

COLUMN SELECTIVITY STUDY AND
CHEMICAL MAPPING

CHAPTER OVERVIEW

This chapter brings together all the key concepts around the multidisciplinary approach (synthetic and analytical chemistry) that has been developed in this thesis for methamphetamine chemical fingerprinting. This chapter examines a comprehensive column selectivity study where a novel selection protocol is developed, using OpenMS® (open source LC-MS data handling software). The methodology developed in this chapter identifies the two most orthogonal columns in order to provide the user with the best separation of complex samples of interest.

This section will also include the chemical mapping of a full synthetic pathway to methamphetamine from easily accessible ingredients such as benzaldehyde and nitroethane. A comparative study between LC-MS and LC-UV Visible data was carried out simultaneously for the mapping of the synthetic route of the clandestine product. This enabled a comprehensive impurities table to be generated which has been discussed regarding the direct impact they will have towards real world forensic analysis of seizure samples. An alternative approach for the identification of synthetic route and precursors was also trialled, with a preliminary study using targeted principal component analysis.

5.1 Introduction

As briefly discussed in Chapter 4, conventional HPLC although widely used as a chromatography tool, has a limited separation potential when analysing complex samples. Two-dimensional HPLC offers significant potential and is utilised in order to separate out compounds *via* two different retention mechanisms afforded by the two stationary phases [70]. The ability to separate complex samples is considerably improved by using 2D-HPLC due to the significant increase in theoretical peak capacity [70]. Ideally, for the full benefits of multi-dimensional separations to be realised, the stationary phase properties of the selected columns should be as different as possible [70]. The process of assessing this is often labour intensive and very time consuming, requiring a trial-and-error approach or injecting numerous standards to test every possible stationary phase combination [192, 193].

In order to improve the separation power and best utilise the separation space, the two most orthogonal columns must be selected allowing for the best chromatography [70]. The separation potential of a 2D-HPLC system is established by the peak capacity which put simply is the chromatographic resolving power. The peak capacity determines the separation potential of a system [194] and is proportional to the fractional coverage defined by Watson *et al.* [208] according to Equation 4:

$$f_{coverage} = \frac{\sum bins}{P^2} \quad (\text{Equation 4})$$

where $f_{coverage}$ is the proportional surface coverage that ranges from 0 to 1,

$\sum bins$ is the number of bins that contain peaks, and

P^2 is the total number of available bins.

The $f_{coverage}$ is directly related to the two-dimensional peak capacity, highlighting in Equation 5 that the greater the $f_{coverage}$, the better use of separation space and better overall 2D-HPLC separation [194]:

$$n_{c,2D} = \frac{n_{c,1} \times n_{c,2} \times f_{coverage}}{\langle \beta \rangle} \quad (\text{Equation 5})$$

where, $n_{c,2D}$ is the practical 2D-HPLC peak capacity,

$n_{c,i}$ is the peak capacity in both separation dimensions,

$f_{coverage}$ is the proportional amount of separation space utilisation, and

$\langle \beta \rangle$ is the under-sampling correction factor.

The under-sampling correction factor is directly proportional to the modulation frequency per peak from the first dimension to the second, as described by Li and co-workers [195]. This is achieved through a given number of bins used to divide the separation space, $\Sigma bins$, that is equal to the number of peaks; the area of all normalised bins containing peaks is then totalled giving P^2 [190]. Using this method, the $f_{coverage}$ is calculated as a number between 0 and 1, where 0 is no separation and 1 represents full use of the available separation space.

The separation space is maximised using orthogonal column stationary phases however identifying the best two columns can be a lengthy and challenging task when the retention profiles of each column needs to be compared individually [192]. It is extremely difficult to match peaks based on area when changing column type, as the elution order and peak profile will almost certainly change when optimising using the sample itself [192]. A way around this is to inject individual standards one at a time onto each column [199] however this is extremely time consuming and inefficient.

An alternative method to monitor the peaks across each separation is by their molecular weight with the aid of mass spectrometry [209]. Mass spectrometry is often coupled with liquid chromatography, gas chromatography, or capillary electrophoresis to obtain more chemical information about a sample [210]. Liquid chromatography – mass spectrometry is superior to HPLC with UV-absorbance detection when analysing complex samples as it provides the user with not only retention time but also molecular weight and isotopic information, and can be

useful when using the selected ion mode or extracted ion mode for constituent monitoring [201]. Liquid chromatography – mass spectrometry has been used in this column selectivity study to monitor the same component peaks across 17 different columns and provide as much information about the peaks as possible.

Raw high resolution LC-MS data is incredibly large, complex and care needs to be taken when handling the data so that the analyst can achieve the best outcomes. Software like XCMS™ [211], OpenMS® [212], ProteoWizard [213], mspire [214], MzJava [215], MzMine [216] and Pyteomics [217] have all been used for the analysis of LC-MS and LC-MS/MS data [218] and have been utilised in a range of fields (proteomics [217], metabolomics [219], and lipids [220]) differing in supported formats.

In this investigation OpenMS® (version 1.11.1), an open source program designed to interpret and analyse mass spectrometry data, was explored to see if the software can assist in identifying the best column combination for an optimised 2D-HPLC separation. OpenMS® was prioritised over other programs due to its flexible nature, large range of supported formats and user friendly characteristics [221]. This program offers filters that can be applied allowing for the extraction of information the user deems important, such as particular peaks of interest, exact mass measurements, mass ranges, etc. There are a many modules that can be designed for the analysis of a complex data set, including elimination of noise and peak picking operations [218].

Once the best two columns were chosen, further statistical analysis were then trialled on methamphetamine-type samples. Principal Component Analysis (PCA) was also used to see if it was possible to predict the synthetic pathway used to make the methamphetamine (from pseudoephedrine or P2P). Principal Component Analysis is a statistical procedure applied to multivariate data which identifies and isolates samples based on the degree of variance (ie. how similar or different one sample is from another) [222]. It involves an orthogonal transformation so that the new axes lies along the maximum variance in the data, converting correlated into uncorrelated data [223]. Principal Component Analysis can reveal the variables that differentiate a sample from another and can be used

to predict what groups unknown samples are most similar to. It is important to note that the covariance matrix method of PCA was used in this analysis. As such the eigenvalues and eigenvectors are calculated from the covariance matrix equation. Initially, the covariance is calculated using equation 6:

$$Cov_{xy} = \sum_{i=1}^n (x_i - \bar{x}) (y_i - \bar{y}) / (n - 1) \quad (\text{Equation 6})$$

Where Cov_{xy} , is the covariance of a system,

x_i , is the individual value of sample x ,

\bar{x} , is the mean of sample x ,

n , is the sample size.

The covariance is represented in a matrix form shown in equation 7:

$$\text{Covariance Matrix} = \begin{pmatrix} Cov_{x,x} & Cov_{x,y} \\ Cov_{y,x} & Cov_{y,y} \end{pmatrix} \quad (\text{Equation 7})$$

With the covariance matrix in hand, a transposition is performed as outlined in equation 8. This transposition when represented in the three dimensional space allows for the eigenvector to be calculated. The eigenvectors with the largest value has the strongest correlation to the data set. When this data is plotted between principle components the data sets that are correlated can be directly observed.

$$\text{Covariance Matrix} = XX^T = [x_1 - \bar{x}, x_2 - \bar{x} \dots x_n - \bar{x}] \begin{bmatrix} (x_1 - \bar{x})^T \\ (x_2 - \bar{x})^T \\ (x_n - \bar{x})^T \end{bmatrix}$$

(Equation 8)

This type of predictive modelling was developed by Henry Hotelling and it was first reported in the literature in 1933 [224]. Principal component analysis is a well-developed technique that has been used in many analytical applications such as

analysis of coffee beans [225], drugs in rats [226], heavy metals in food [227], drugs in smuggled packages [228], photochemical reactions [229], fermented food products like cow's milk and cheese [230], profiling of tobacco [231] and olive oils [232]. Principal Component Analysis on LC-MS data has some challenges due to the large data sets generated and the need for careful data alignment due to potential misinformation generated from precursor ions in MS-MS. Typically data is binned and this reduces the quality of information gained through high resolution data [233].

A major difficulty in the optimisation of 2D-HPLC operating conditions is the selection of the most orthogonal columns. This chapter will discuss a new approach to efficiently selecting the best column combination for 2D-HPLC analysis of any complex sample followed by a short pilot study, carrying out PCA on methamphetamine type samples. Seventeen columns were used to separate a model methamphetamine sample using LC-MS. OpenMS[®] was then used to evaluate the data from each column and identify which two columns when used together will provide the best use of separation space. Using the selected two columns, PCA was trialled as a complementary method of swiftly identifying routes of manufacture.

5.2 Experimental

Chemicals and samples

Deionised water was obtained in-house (Continental Water Systems, Victoria, Australia) and filtered through a 0.45 µm membrane filter (Sigma-Aldrich Pty Ltd, Castle Hill, NSW, Australia) prior to use. HPLC grade acetonitrile (ACN) was purchased from Ajax Finechem Pty Ltd (Taren Point, NSW, Australia). Trifluoroacetic acid was purchased from Sigma-Aldrich. All standards (methamphetamine, ephedrine, pseudoephedrine, paracetamol, caffeine, benzyl alcohol, dimethyl sulfone, benzaldehyde, phenyl-2-propanone (P2P) and diphenylacetone) were obtained from Sigma-Aldrich (Castle Hill, NSW, Australia) and the National Measurement Institute, Australian Government (Port Melbourne, Vic., Australia).

Liquid Chromatography Mass Spectrometry (LC-MS)

Mass spectrometry analysis was performed with an Agilent Technologies 6210 LC-MSD TOF system (Agilent Technologies, Mulgrave, Victoria, Australia). It was equipped with an Agilent technologies 1200 series solvent degasser, binary pump and an Agilent technologies 1100 series ALS. Positive ion polarity was used in conjunction with nitrogen drying gas (5 L min^{-1}) and nitrogen nebuliser gas (30 psi). The model methamphetamine sample was injected ($10 \mu\text{L}$) into a linear gradient over 40 minutes with an initial mobile phase of 5% aqueous ACN that increased to 100% ACN. All analyses were run at a flow rate of 0.5 mL min^{-1} . Chromatographic data was obtained and processed with Agilent ChemStation software. The 17 columns that comprised the stationary phase library for this study are listed in Table 5.1.

Table 5.1: Columns trialled in study.

	Brand	Type	Size	Dimensions	Part Number
Column 1	Agilent	Poroshell 120 EC-C8	$2.7 \mu\text{m}$	$4.6 \times 100 \text{ mm}$	695975-906
Column 2	Agilent	Poroshell 120 EC-CN	$2.7 \mu\text{m}$	$4.6 \times 100 \text{ mm}$	695975-905
Column 3	Phenomenex	Kinetex PFP 100 A	$2.6 \mu\text{m}$	$4.6 \times 100 \text{ mm}$	00D-4477-E0
Column 4	Phenomenex	Kinetex Phenyl-Hexyl 100 A	$2.6 \mu\text{m}$	$4.6 \times 100 \text{ mm}$	00D-4495-E0
Column 5	Phenomenex	Synergi Fusion - RP 80A	$4 \mu\text{m}$	$4.6 \times 150 \text{ mm}$	00F-4424-E0
Column 6	Phenomenex	Synergi Hydro - RP 80A	$4 \mu\text{m}$	$4.6 \times 150 \text{ mm}$	00F-4375-E0
Column 7	Phenomenex	Luna C5 100A	$5 \mu\text{m}$	$4.6 \times 50 \text{ mm}$	00B-4043-E0
Column 8	Phenomenex	Luna NH2 100A	$5 \mu\text{m}$	$4.6 \times 100 \text{ mm}$	00D-4378-E0
Column 9	Phenomenex	Luna HILIC 200A	$5 \mu\text{m}$	$4.6 \times 150 \text{ mm}$	00F-4450-E0
Column 10	Cosmosil	πNAP	$2.5 \mu\text{m}$	$4.6 \times 100 \text{ mm}$	08084-51
Column 11	Cosmosil	5PBB-R	$5 \mu\text{m}$	$4.6 \times 150 \text{ mm}$	05697-21
Column 12	Cosmosil	5NPE	$5 \mu\text{m}$	$4.6 \times 150 \text{ mm}$	37904-01
Column 13	Agilent	Poroshell 120 EC-C18	$2.7 \mu\text{m}$	$4.6 \times 100 \text{ mm}$	695975-902
Column 14	Agilent	Poroshell HPH-C18	$2.7 \mu\text{m}$	$4.6 \times 100 \text{ mm}$	695975-702
Column 15	Agilent	Poroshell 120,SB-C18	$2.7 \mu\text{m}$	$4.6 \times 100 \text{ mm}$	685975-902
Column 16	Agilent	Poroshell 120 Bonus RP	$2.7 \mu\text{m}$	$4.6 \times 100 \text{ mm}$	695968-901
Column 17	Agilent	Pursuit XRs 3 Diphenyl	$3 \mu\text{m}$	$4.6 \times 100 \text{ mm}$	A6021100X046

Liquid Chromatography Mass Spectrometry (LC-MS) for chemical mapping of synthetic pathway.

Mass spectral analysis was performed with a Thermo Fisher Q-Exactive Plus UPLC Ultimate 3000/orbitrap system (Thermo Fisher Scientific, Scoresby, Victoria, Australia). It was equipped with a Dionex Ultimate 3000 (HPG-3400RS) UPLC pump. Positive ion polarity was used in conjunction with nitrogen drying gas (7 L min^{-1}) and nitrogen nebuliser gas (30 psi). When using the Phenomenex Kinetex PFP Column, the samples were injected ($10 \mu\text{L}$) into a linear gradient over 22 minutes with an initial mobile phase of 5% aqueous ACN that increased to 30 % ACN over 20 minutes, then increased to 100% ACN which was held for a further 2 minutes. All analyses were run at a flow rate of 0.5 mL min^{-1} . When using the Onyx C18 monolith column, the samples were injected ($10 \mu\text{L}$) into a linear gradient over 10 minutes with an initial mobile phase of 5% aqueous ACN that increased to 80% ACN. Mass spectrometry data were obtained and processed with Thermo Fisher 'Xcalibur' software.

Two-dimensional high performance liquid chromatography

An Agilent Technologies (Mulgrave, Vic., Australia) 1290 2D chromatograph was used for all separations, including: an auto sampler; solvent degasser; capillary pump; binary pump; quaternary pump; column thermostat; 2 position 8 port switching valve; and two diode array detectors (one in each dimension, which recorded at 254 nm). The 2D-HPLC separations were performed using $80 \mu\text{L}$ injections and a controlled temperature of 25°C . The first dimension gradient was completed at a flow rate of 0.1 mL min^{-1} with an initial mobile phase of 5% aqueous ACN that increased to 30% aqueous ACN over 100 minutes and then increased to 100% ACN for a further 10 minutes. The second dimension gradient was completed at 5 mL min^{-1} with an initial mobile phase of 5% aqueous ACN that increased to 80% aqueous ACN for 1 minute. The comprehensive two-dimensional separation had an overall completion time of 110 minutes. Two-dimensional HPLC was completed in on-line comprehensive mode with a modulation time of 1.5 minutes (Kinetex PFP & Onyx Monolithic C18) and 3.0 minutes (Kinetex PFP & Synergi Hydro), whereby a fraction volume of $75 \mu\text{L}$ was transferred to the second

dimension *via* a sample loop (500 μL) and an 8 port 2 position switching valve; valve timing was controlled with by the HPLC control software.

Data Processing

The chromatographic data obtained from the LC/MS was analysed with OpenMS[®] 1.11.1 [212, 221]. The OpenMS[®] pipeline included a file converter (convert .mzdata to .mzml), file filter (parameters such as intensity, retention times and m/z values were optimised), re-sampler (LC-MS map is transformed into a resampled map), noise filter SGolay (smooth peaks and eliminate peaks caused by noise), peak picker wavelet (peaks are selected), feature finder metabo (filters repeated masses) and data collection. All parameters within these tools were default except in the file filter where m/z values were specified to be 50-300 and intensity values were 1,000–30,000,000. The output files from OpenMS[®] consisted of a list of retention times for features that were common amongst the investigated HPLC columns. This data was processed with Wolfram Mathematica 10.3 (distributed by SHI UK, Milton Keynes, England) to match these retention times and predict the relative retention behaviour using algorithms written in-house to calculate the most orthogonal columns. Two-dimensional contour plots were prepared with Wolfram Mathematica 10.3.

Principal Component Analysis (PCA)

PCA was carried out on 22 random methamphetamine seizure samples provided by the Victoria Police Forensic Services Centre. This pilot study was processed using a specialised Thermo Fisher Scientific software by the name of 'SIEVE™', which is a LC-MS data processing program. The data was scaled and normalised using the internal SIEVE™ mechanism. A mass range was set as m/z 166.0-166.2 in order to carry out a targeted PCA of pseudoephedrine. The analysis time (0 – 15 minutes), m/z range (166.0 – 166.2), m/z tolerance (10 ppm), minimum intensity threshold (2.0×10^7), peak scans (5), signal to noise ratio (3:1) and m/z step size (10) were the parameters chosen for the targeted PCA.

5.3 Results and Discussion

5.3.1 Column Selectivity Study using OpenMS®

When comparing column combinations individually, selecting two columns that provide the greatest separation space is a labour intensive process. As such, monitoring the molecular masses using LC-MS has the potential to rectify the problem of differentiating peak elution times when comparing all 17 columns.

Initially, the model methamphetamine sample described in Chapter 4 was run on all 17 columns (single dimensional), with the aid of LC-MS as a detection system. It is important to note that a model methamphetamine sample was used in the column selection process with OpenMS®, as dataset training was designed to cope with all of the potential precursors and cutting agents related to methamphetamine. As previously discussed in chapter 4, a real methamphetamine seizure sample is typically very clean, only consisting of methamphetamine a couple of other chemicals. Therefore, the column selectivity study was carried out with a significantly more complex model sample to ensure universal application for law enforcement agencies.

The model methamphetamine sample was injected (5 µL) at a flow rate of 0.5 mL min⁻¹ into a linear gradient over 40 minutes with an initial mobile phase of 5% aqueous ACN that increased to 100% ACN. The resulting data files were uploaded to OpenMS® which was then used to identify the $f_{coverage}$ of all the column combinations in a 2D-HPLC separation. This allowed a large variety of columns (272 combinations) to be compared in a significantly reduced time (20 minutes of processing) in comparison to the traditional trial-and-error process which for this number of columns would take more than 181 hours. This is significant in an analytical laboratory as it results in time, energy, solvent and cost savings [234].

The 9 step information pipeline that was used by OpenMS® in this work is illustrated in Figure 5.1, which outlines the data processing pipeline utilised to identify the most orthogonal columns.

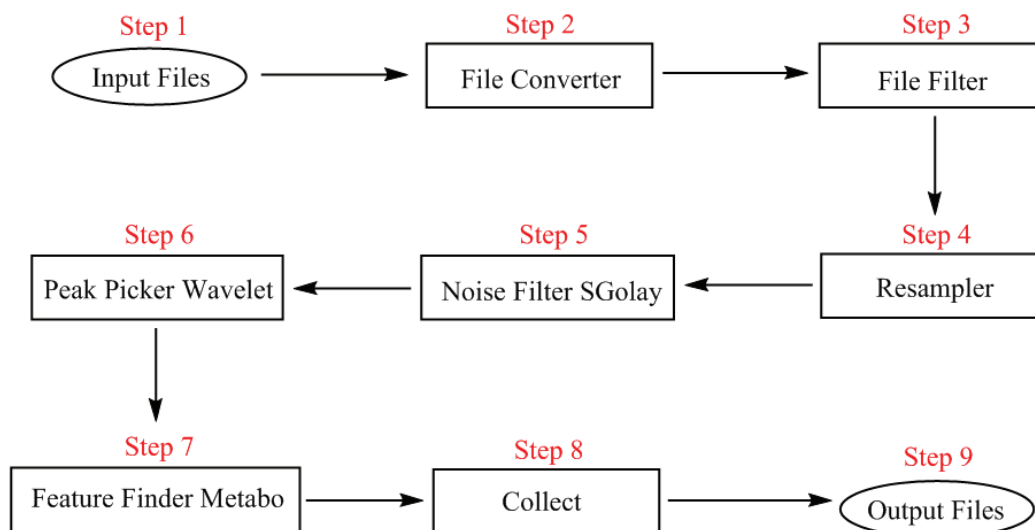


Figure 5.1: OpenMS® pipeline used for the data analysis.

The function of each sequential step is described below:

- **Step 1** – Upload individual column data files (.mzdata format).
- **Step 2** – Convert file from .mzdata to .mzml format for OpenMS® processing.
- **Step 3** – Extract peak intensities (1,000 – 30,000,000) and set m/z range (50-300) of interest [212].
- **Step 4** – Filters are applied by transposing the original LC-MS map into a resampled map.
- **Step 5** – Noise filter is applied to smooth the baseline and remove peaks caused by noise [16].
- **Step 6** – Picks peaks out of the noise-filtered and baseline-reduced data that satisfies the applied filters.
- **Step 7** – Data reducing filter that removes additional small traces of identical molecular weight, leaving only the main signal.
- **Step 8** – All the individual filtered files are collected and joined into a single data file.
- **Step 9** – Export as OpenMS® data file (.toppas format) [212].

The results from the pipeline were then processed using Mathematica and algorithms designed in house by Stevenson *et al.* [78, 202]. Table 5.2 lists the expected $f_{coverage}$ for each column combination based on the pipeline described for OpenMS®.

Table 5.2: f_{coverage} of different column combinations columns 1-17.

Column	1	2	3	4	5	6	7	8	9	10	11	12	13	14	15	16	17
1	-	0.31	0.25	0.25	0.31	0.31	0.25	0.31	0.25	0.25	0.19	0.25	0.31	0.25	0.25	0.19	0.31
2	0.31	-	0.25	0.25	0.31	0.31	0.25	0.19	0.19	0.25	0.38	0.19	0.25	0.31	0.38	0.31	0.31
3	0.25	0.25	-	0.38	0.31	0.44	0.38	0.25	-	0.31	0.31	0.25	0.31	0.31	0.19	0.19	0.38
4	0.25	0.25	0.38	-	0.25	0.38	0.19	0.19	0.25	0.31	0.25	0.31	0.31	0.25	0.25	0.31	0.25
5	0.31	0.31	0.31	0.25	-	0.25	0.25	0.25	-	0.25	0.25	0.31	0.31	0.19	0.38	0.25	0.31
6	0.31	0.31	0.44	0.38	0.25	-	0.31	0.38	-	0.38	0.25	0.25	0.25	0.19	0.31	0.38	0.25
7	0.25	0.25	0.38	0.19	0.25	0.31	-	-	-	0.25	0.38	0.25	0.38	0.38	0.38	0.25	-
8	0.31	0.19	0.25	0.19	0.25	0.38	-	-	0.19	0.25	0.25	0.25	0.13	0.25	0.25	0.31	-
9	0.25	0.19	-	0.25	-	-	-	0.19	-	-	-	-	0.25	-	-	-	-
10	0.25	0.25	0.31	0.31	0.25	0.38	0.25	0.25	-	-	0.25	0.19	0.25	0.31	0.38	0.31	-
11	0.19	0.38	0.31	0.25	0.25	0.25	0.38	0.25	-	0.25	-	0.31	0.25	0.19	0.31	0.25	0.38
12	0.25	0.19	0.25	0.31	0.31	0.25	0.25	0.25	-	0.19	0.31	-	0.25	0.28	0.13	0.38	0.25
13	0.31	0.25	0.31	0.31	0.31	0.25	0.38	0.13	0.25	0.25	0.25	0.25	-	0.25	0.25	0.38	0.31
14	0.25	0.31	0.31	0.25	0.19	0.19	0.38	0.25	-	0.31	0.19	0.28	0.25	-	0.31	0.25	0.28
15	0.25	0.38	0.19	0.25	0.38	0.31	0.38	0.25	-	0.38	0.31	0.13	0.25	0.31	-	0.38	0.31
16	0.19	0.31	0.19	0.31	0.25	0.38	0.25	0.31	-	0.31	0.25	0.38	0.38	0.25	0.38	-	0.44
17	0.31	0.31	0.38	0.25	0.31	0.25	-	-	-	-	0.38	0.25	0.31	0.28	0.31	0.44	-

An algorithm based on the aforementioned $f_{coverage}$ equations 1 & 2, was used to predict the fractional surface coverage when combined in a hypothetical 2D-HPLC analysis. From the seventeen columns tested with the model methamphetamine sample, the two sets of column combinations that displayed the greatest predicted $f_{coverage}$ (0.44) with the best separation was identified as:

- **Column 3** (Phenomenex Kinetex PFP) & **Column 6** (Phenomenex Synergi Hydro).
- **Column 16** (Poroshell 120 Bonus RP) & **Column 17** (Pursuit XRs 3 Diphenyl).

An $f_{coverage}$ of 0.44 is comparable to literature values of impressive multi-dimensional separations in a range of scientific fields [192, 234]. Burns *et al.* reported their best $f_{coverage}$ as 0.43 from their 2D-HPLC blind column selection study on opiates [234]. Likewise, Bassanese *et al.* reported an orthogonality and $f_{coverage}$ of approximately 0.35 from their work on the two-dimensional separation of extracted antioxidants from coffee [192].

Columns 3 (Kinetex PFP) and 6 (Synergi Hydro) have very different chemical properties and retention mechanisms, with the greatest potential to utilise the most separation space available when used in combination. The Kinetex PFP column (Figure 5.2) consists of pentafluorophenyl groups bonded to the core-shell silica through C-C bonds, with TMS (trimethylsilyl) non-polar endcapping.

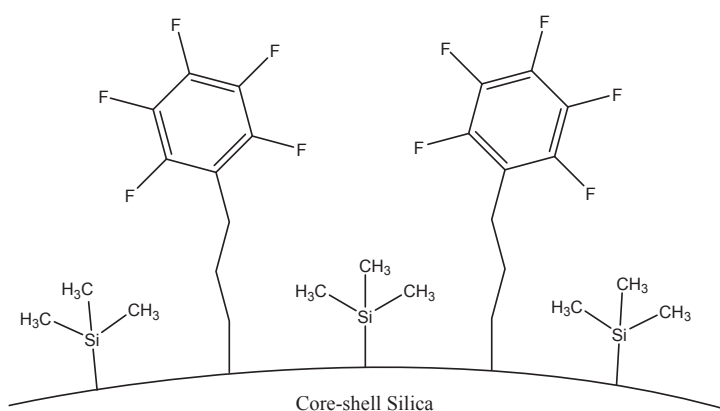


Figure 5.2: Stationary phase of the Phenomenex Kinetex PFP column.

This stationary phase is excellent at separating aromatic compounds and halogenated compounds due to their π - π interactions, with the electronegative fluorine groups offering high selectivity for cationic compounds [235]. All of the compounds present (except *N*-methylalanine and creatine) in this model methamphetamine sample (created in chapter 4) are aromatic compounds, correlating well with the column selection identified by OpenMS® protocol. Mirali *et al.* developed a fast extraction and separation method for phenolic compounds in lentil seeds using the same stationary phase [236]. The phenolic compounds extracted from the lentil seeds such as aminosalicic acid (an antibiotic) and salicin (a β -glucoside) are all polar aromatic compounds which efficiently separate using the Kinetex PFP column. The Kinetex PFP column has also been used within the literature for similar compounds that in all cases contained both an aromatic portion and a polar region such as a hydroxyl moiety. Other research groups have used the same stationary phase with impurity profiling of drugs [237] and in the chemical screening of polyphenols in beer hops [238].

The Synergi Hydro is a C18 column with polar endcapping (Figure 5.3) consisting of C18 alkyl chains bonded to the silica surface, resulting in methylene selectivity and effective separation of hydrophobic compounds through π - π interactions [235].

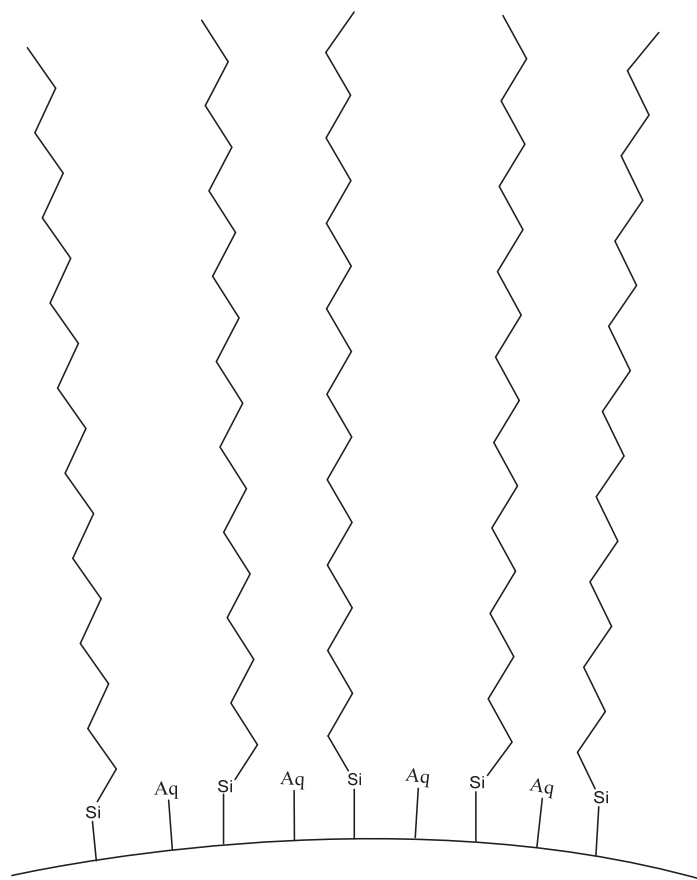


Figure 5.3: Surface (stationary phase) of Synergi Hydro column (C18 with polar end-capping).

The main separation properties are identical to that of a standard C18 with a slight variation in the secondary retention mechanism (unknown polar endcapping) which provides improved retention of hydrophobic compounds. Extremely polar compounds are sometimes not retained and generally don't separate well using conventional C18 columns [239], whereas the polar endcapping on the surface improves the retention of those types of compounds [235]. This column has also been used in the literature to separate amino acids [240], prescribed pharmaceuticals [241] and metabolites in baby food [242], all separating compounds of similar properties.

The second set of columns which had a predicted f_{coverage} of 0.44 was the Agilent Poroshell 120 Bonus RP and the Agilent Pursuit XRs 3 Diphenyl. The Poroshell Bonus RP (shown in Figure 5.4) consists of sterically-protected diisopropyl-C14 alkyl groups covalently bonded through an embedded amide linkage group to the silica and is also triple endcapped [243].

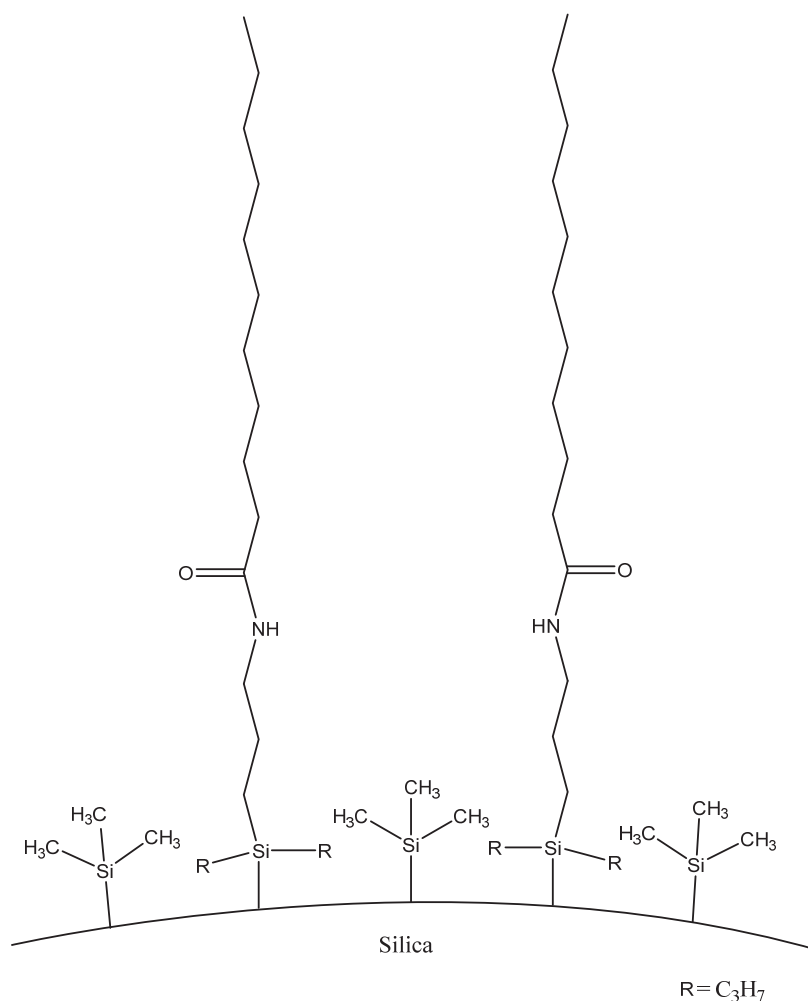


Figure 5.4: Surface (stationary phase) of Poroshell Bonus RP (with triple endcapping).

The embedded amide group is extremely polar that helps to deactivate unwanted silanol interactions, making this stationary phase ideal for the separation of basic, neutral and highly ionisable compounds [243]. The selectivity of this column is suited to every compound present in the model methamphetamine sample and

has been used by researchers for the determination of prohibited drugs in hair [244] and antibacterial drugs [245], which also investigate polar aromatic compounds.

In contrast to the previous column, the Agilent Pursuit XRs 3 Diphenyl stationary phase (Figure 5.5) consists of two phenyl groups which are covalently bonded to porous silica particles [246]. This column is endcapped and designed to efficiently separate aromatic compounds by utilising strong dipole-dipole hydrogen bonding and π - π interactions [246]. It has been reported being used on the separation of opiates [234], antibodies [247], and bitter aromatic compounds in whole wheat bread [248].

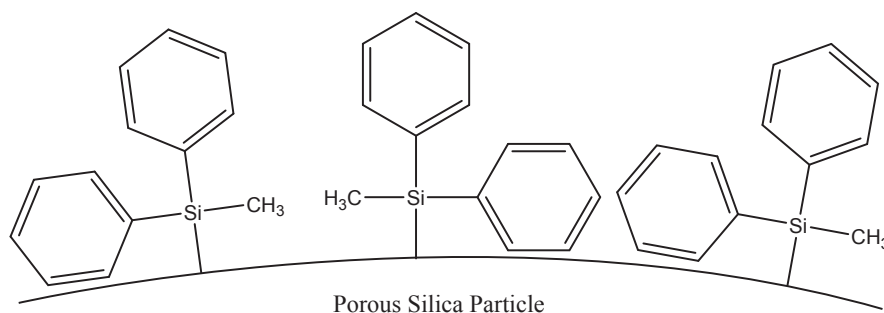


Figure 5.5: Surface (stationary phase) of Agilent Pursuit XRs 3 Diphenyl (with endcapping).

After exploring the different chemical properties of the stationary phases (columns) with the highest predicted $f_{coverage}$, based on the compounds being analysed it was evident that the columns chosen by OpenMS® can be justified by the retention mechanisms of all 4 columns. Interestingly the Column 9 (Luna HILIC) did not work well for this sample set and is generally utilised for solely polar compounds and affords the user the ability to inject samples in strong organic solvents [249]. This phase is in contrast to the retention mechanisms highlighted to be useful here and this shows the importance of doing a comprehensive column selectivity study in order to best understand full implications of stationary phases on a sample.

In order to visualise the predicted setting on a real sample an actual two-dimensional separation (Figure 5.6) was performed using the Column 3 and Column 6 combination.

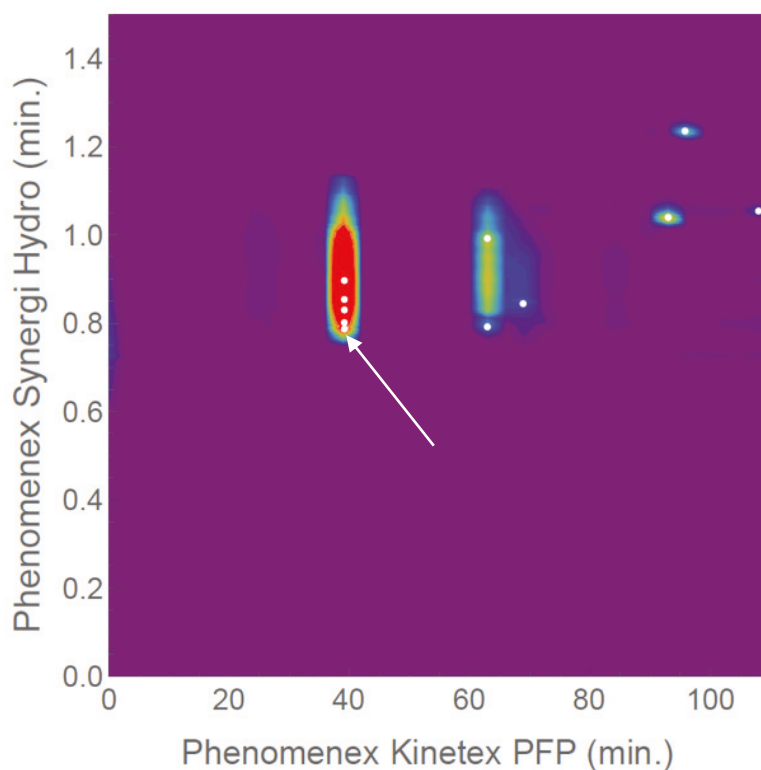


Figure 5.6: Comprehensive two-dimensional separation of model sample using the largest $f_{coverage}$ as determined by OpenMS® (white dots represent peak maxima – UV Detection).

From the two-dimensional plot, it was observed that there was a need for improved separation of a cluster of peaks (shown in Figure 5.6 with a white arrow), that does not increase analysis time significantly. As the Kinetex PFP column provided the best first dimension separation out of all columns (Figure 5.7), it was chosen (based on visual inspection) as the initial stationary phase.

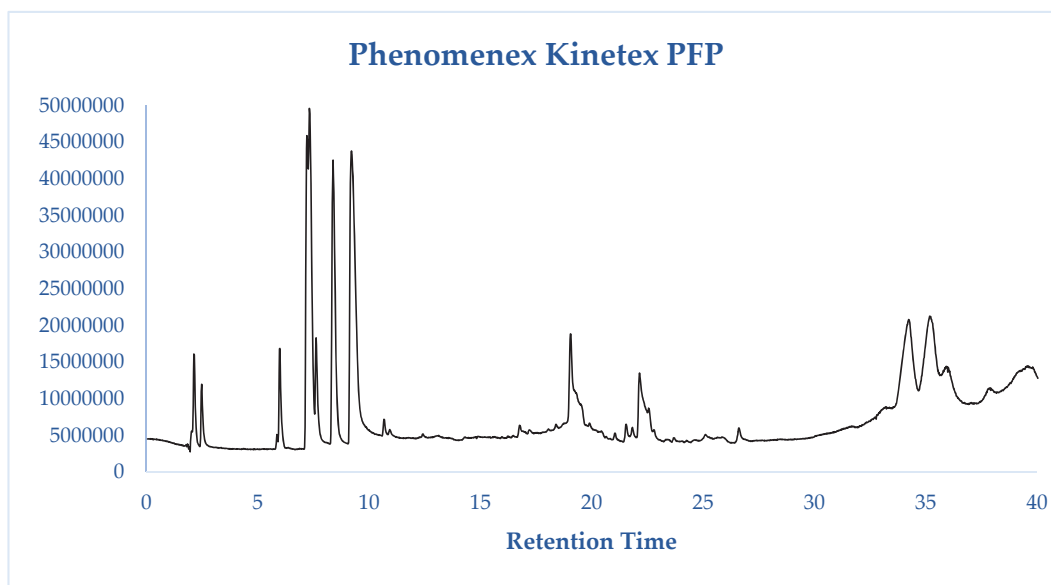


Figure 5.7: LC-MS Total Ion Chromatogram of model methamphetamine sample using Kinetex PFP column.

The chromatography produced by the Kinetex PFP column is ideal for the first dimension as the peaks are well spread out over the gradient time with several baseline resolved peaks. Compared to the other columns trialled from Table 1, it is an impressive separation considering the injection volume (80 μL) which overloads the stationary phase. However, this is required to ensure a sufficient concentration can be detected in the second dimension after the switching valve transfer and sample dilution within the mobile phase.

Attention turned to selecting a column in the second dimension that can support much faster flow rates for improved analysis time. As the Synergi Hydro is a C18 column with polar endcapping (Figure 5.3), the main separation properties are identical to that of a standard C18 with a slight variation in the secondary retention mechanism (polar endcapping).

As such, Table 5.2 was consulted again and the third best predicted f_{coverage} (0.31) with the Kinetex PFP column was the C18 columns (13 and 14) so the decision was made to substitute a solid-core C18 column for a Monolithic C18 column which has the same retention mechanisms but can withstand flow rates of up to 5 mL

min⁻¹ with reduced backpressure. The C18 column separates on the basis of analyte size and methylene selectivity *via* interactions between the analyte and a chain of 18 carbons [250]. The C18 surface is widely used in modern chromatography and thus has many applications [251].

Therefore, a comprehensive two-dimensional separation was carried out using the Phenomenex Kinetex PFP 100Å (4.6 × 100 mm, 2.6 µm particle diameter) in the first dimension and the Phenomenex Onyx Monolithic C18 (4.6 × 100 mm) in the second dimension (Figure 5.8). In fact with the use of the monolith column, the second dimension modulation time was able to be reduced from 3.0 minutes to 1.5 minutes over a 1.0 minute gradient and gave a significantly improved separation. When compared to the previous two-dimensional separation (Figure 5.6), the compounds are considerably more distributed and make better use of the potential separation space. It is also important to note that comprehensive 2D-HPLC requires the second dimension to be significantly shorter than the first dimension, allowing the compounds to elute in the second dimension before another peak is transferred [70], which is satisfied using the monolithic C18 column.

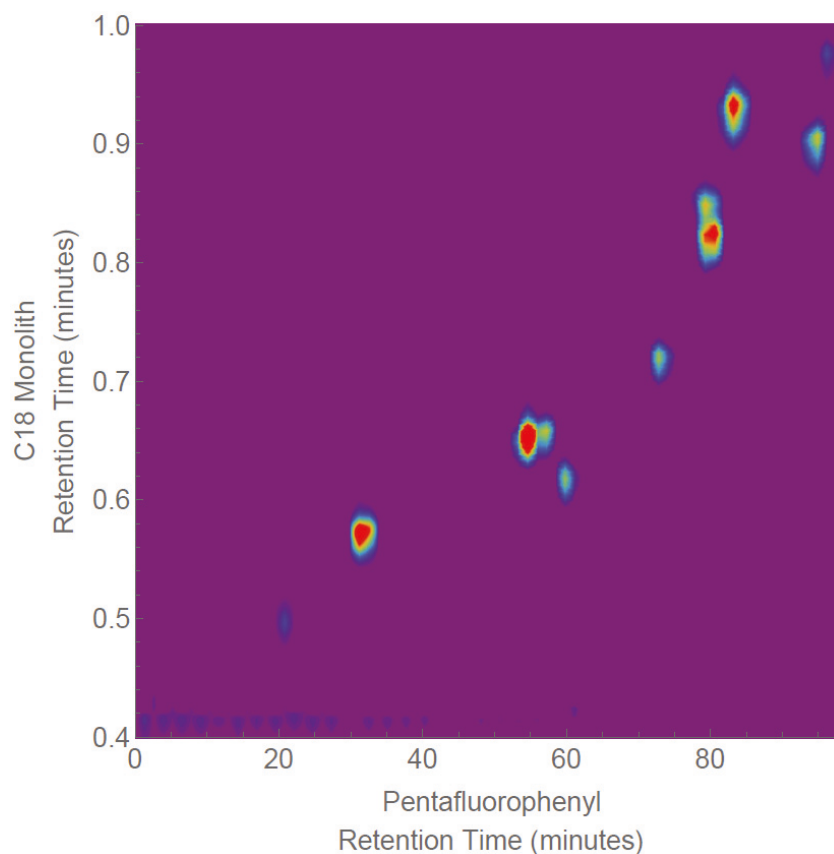


Figure 5.8: Two-dimensional separation using the Kinetex PFP and Onyx C18 Monolithic columns.

5.3.2 Chemical mapping of impurities for a pathway to methamphetamine

Now with an optimised two-dimensional separation in hand that is sculptured around the compounds of interest (methamphetamine and its common associated precursors/cutting agents), attention turned to the chemical mapping of an un-purified synthetic pathway to methamphetamine, carried out previously in Chapter 2, demonstrated in Figure 5.9.

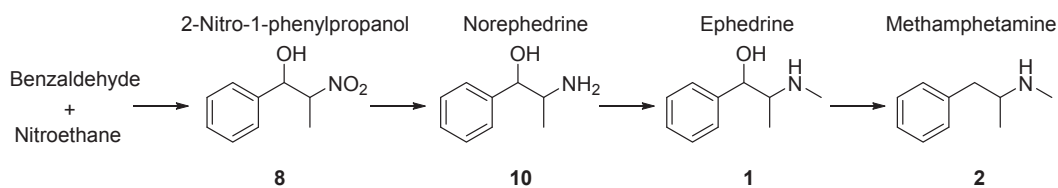


Figure 5.9: Synthetic pathway from benzaldehyde and nitroethane to methamphetamine.

A sample was taken from each step of the synthetic pathway for two-dimensional separation and mass spectrometry analysis. The same columns and conditions from that of Figure 5.8, were used to carry out a two-dimensional separation of each synthetic step.

Mass spectrometry is a significantly more sensitive detection system than UV [201], so the same columns and scaled conditions (relative retention) were run individually using LC-MS with subsequent coordinates plotted (white dots) over the 2D-HPLC separation denoting the peaks identified by mass spectrometry that were not observed in the UV. As LC-MS is a more widely used technique for the analysis of drugs, it was used as a comparison for the 2D-HPLC profiling of synthetic routes to methamphetamine, to ensure the sensitivity was sufficient to be used by law enforcement agencies. The original first dimension (110 minute at 0.1 mL min^{-1}) and second dimension (1 minute at 5 mL min^{-1}) had their run times and gradients scaled to the optimal flow rate of 0.5 mL min^{-1} for LC-MS analysis, resulting in a 22 minute and a 10 minute run time, respectively. As such, any mass detected with a retention time greater than 22 minutes in the LC-MS run was excluded from the 2D plot. The data generated from the mass spectrometry was significant and in order to focus on the key constituents a peak intensity limit of 1×10^7 counts was determined to allow for the identification of the main components. Once the platform technology developed here is taken up by other research groups it would be worth lowering this limit in order to monitor minor constituents and this may be of greater use once this technology is used on large sets of real world seizure samples.

There were masses detected outside of the scaled gradient range (> 22 minutes) which highlights the need for longer analysis times for a full comprehensive chemical fingerprint. Again, highlighting that future method developments for drug detection should be carried out using LC-MS instead of UV as it provides the analyst with considerably more information.

This is supported by Barbarin *et al.* [201] who has published a comparison study on drug detection using LC-UV and LC-MS, evaluating the ability of both techniques to detect unknown impurities. Their findings showed that although

chemical noise was higher when using full scan LC-MS, low level impurities were much better detected. Therefore, LC-MS was carried out in conjunction with 2D LC-UV as a direct comparison for each synthetic step in order to develop the best method for the chemical mapping of methamphetamine impurities.

The first sequential sample analysed was benzaldehyde and as expected the two-dimensional separation shown in Figure 5.10 is quite clean showing an extremely large peak at coordinates (first dimension x = 95, second dimension y = 0.95) and a small peak at coordinates (first dimension x = 90, second dimension y = 0.85). The horizontal signal (second dimension y = 0.35) is caused by the solvent front across each dimension and is not significant to the chemical profiling. However, 6 other impurities were detected using LC-MS, 3 of which were included in the 2D-HPLC chromatogram (bottom left of Figure 5.10). Benzaldehyde eluted outside of the relative scaled retention and as such was not included on the 2D-HPLC chromatogram. Comparatively, 7 different masses were detected using mass spectrometry while only 2 were detected using UV detection, proving the importance of MS when it comes to chemical profiling.

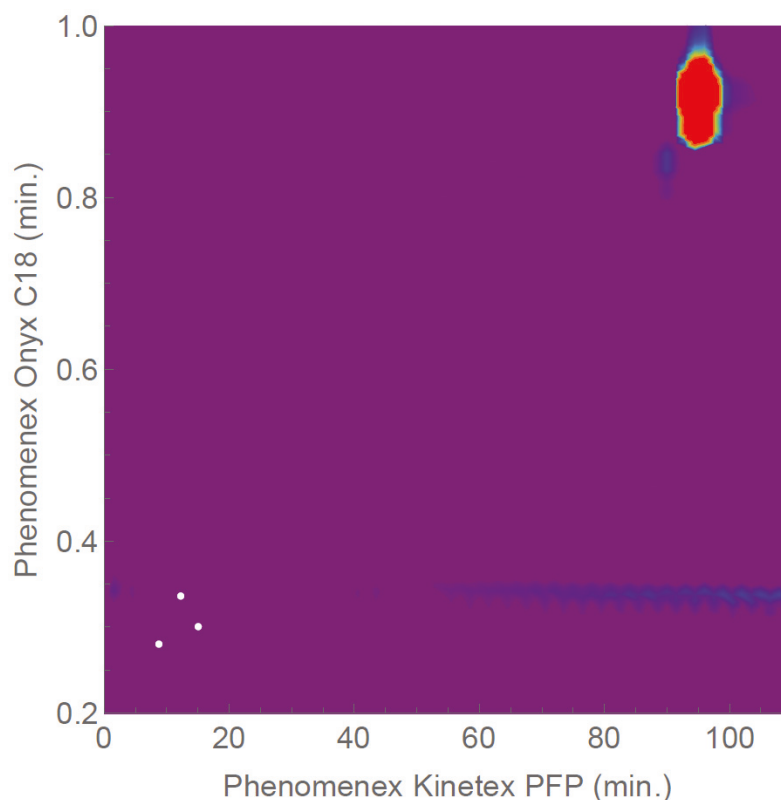
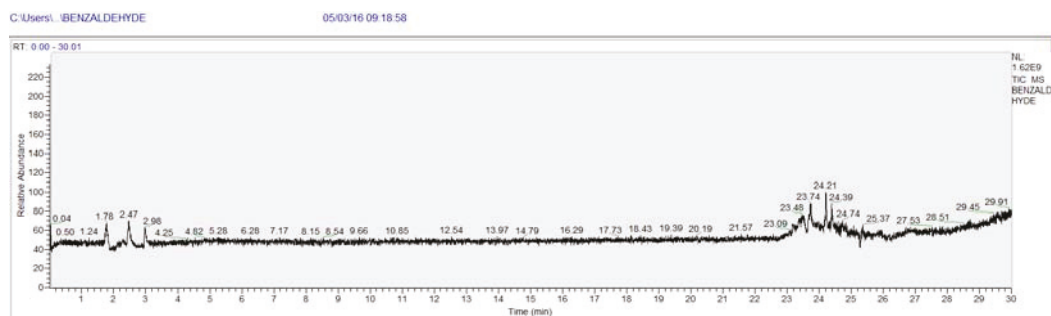


Figure 5.10: Two-dimensional HPLC separation and two-dimensional LC-MS separation (white dots) of benzaldehyde (m/z 107.04912 $[M+H]^+$).



Rt 1.78 = 158.96411, Rt 2.47 = 85.05938, Rt 2.98 = 61.02906, Rt 23.09 = 107.04912, Rt 23.74 = 199.16943, Rt 24.21 = 279.15909, Rt 24.39 = 315.25305.

Figure 5.11: Scaled first dimension LC-MS chromatogram and retention time masses of benzaldehyde using Kinetex PFP column at 0.5 mL min^{-1} .

Nitroethane was then run using both systems as well, showing that LC-MS detected 4 masses including nitroethane (Figure 5.13), 3 of which are illustrated in Figure 5.12, where only one compound was detected with the UV-visible detector.

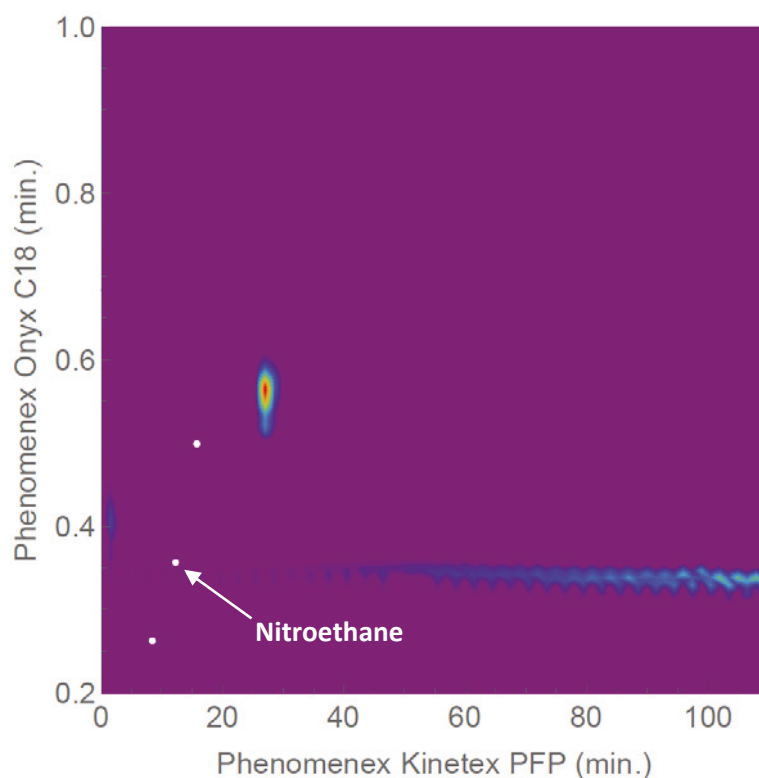
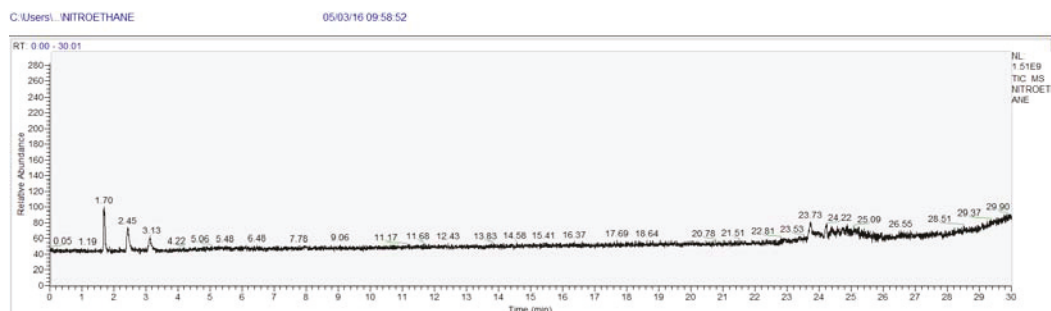


Figure 5.12: Two-dimensional HPLC separation and two-dimensional LC-MS separation (white dots) of nitroethane (m/z 76.03982 $[M+H]^+$).



Rt 1.70 = 182.98523, Rt 2.45 = 76.03982, Rt 3.13 = 84.08125, Rt 23.73 = 217.17992

Figure 5.13: Scaled first dimension LC-MS chromatogram and retention time masses of nitroethane using Kinetex PFP column at 0.5 mL min⁻¹.

The nitroaldol synthesis of 2-nitro-1-phenylpropanol **8** is the first step that involves the reaction of 2 relatively pure compounds, increasing the probability of by-product formation. As shown in Figure 5.14, the 2D-HPLC system detected 4 different compounds displayed as blue or red markings whereas LC-MS detected 8 different compounds (6 included from Figure 5.15).

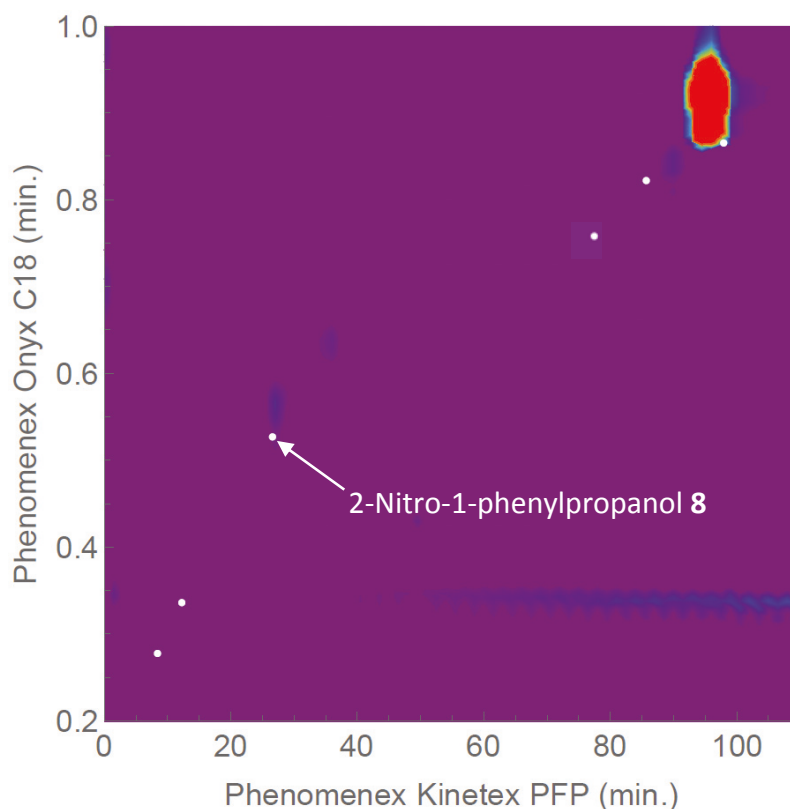
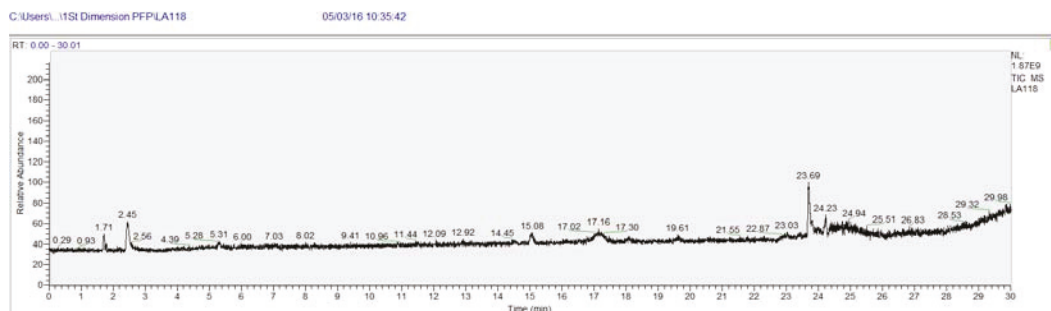


Figure 5.14: Two-dimensional HPLC separation and two-dimensional LC-MS separation (white dots) of 2-nitro-1-phenylpropanol **8** (m/z 182.08116 $[M+H]^+$).



Rt 1.71 = 158.96413, Rt 2.45 = 85.05936, Rt 5.31 = 182.08116, Rt 15.08 = 174.09138, Rt 17.16 = 192.10187,
Rt 19.61 = 248.16016, Rt 23.69 = 174.09132, Rt 24.23 = 164.07059

*Figure 5.15: Scaled first dimension LC-MS chromatogram and retention time masses of 2-nitro-1-phenylpropanol **8** using Kinetex PFP column at 0.5 mL min^{-1} .*

Within the LC-MS separation (Figure 5.15), m/z 164.07059 was found at a retention time of 24.23 minutes which is proposed to be phenyl-2-nitropropene (Figure 5.16); an intermediate product characteristic to this reaction as discussed in chapter 2. This is significant because it shows that the reaction has not gone to completion and it now can be used as a characteristic impurity for this reaction pathway.

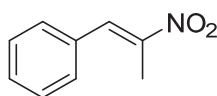


Figure 5.16: Intermediate phenyl-2-nitropropene with m/z 164.07059.

The next step analysed was the reduction of 2-Nitro-1-phenylpropanol **8** to form norephedrine **10**. The sample is more complex with notably more impurities, with 12 different masses detected using LC-MS, shown in Figure 5.18. In contrast, UV-visible detector found 4 intense peaks and 3 weak peaks; making a total of 7 compounds located (Figure 5.17).

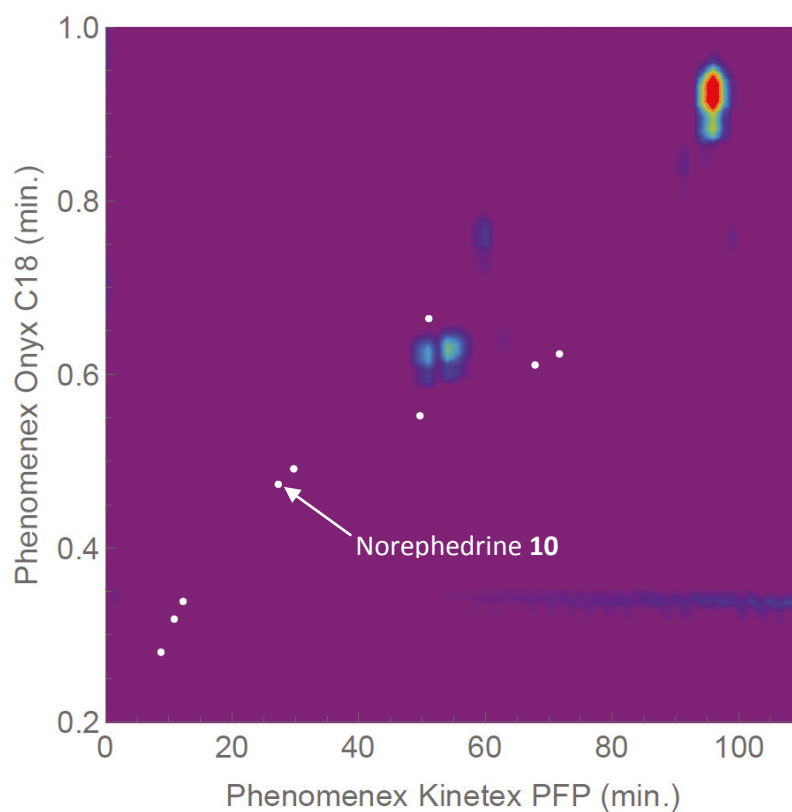
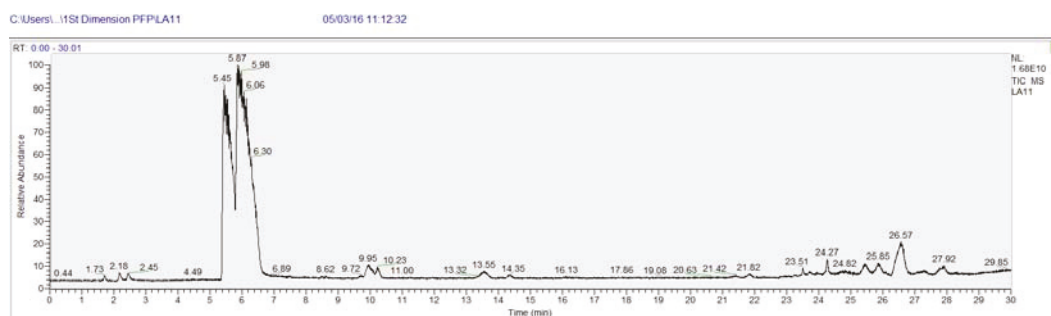


Figure 5.17: Two-dimensional HPLC separation and two-dimensional LC-MS separation (white dots) of norephedrine **10** (m/z 152.10696 $[M+H]^+$).

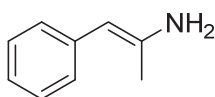


Rt 1.73 = 158.96409, Rt 2.18 = 60.04504, Rt 2.45 = 85.05933, Rt 5.45 = 152.10696, Rt 5.98 = 134.09642, Rt 9.95 = 180.13828, Rt 10.23 = 176.10699, Rt 13.55 = 178.12268, Rt 14.35 = 173.10735, Rt 21.82 = 256.13321, Rt 24.27 = 238.12268, Rt 25.44 = 307.18042.

Figure 5.18: Scaled first dimension LC-MS chromatogram and retention time masses of norephedrine **10** using Kinetex PFP column at 0.5 mL min^{-1} .

After analysis of the masses detected by LC-MS in Figure 5.18, it was proposed that the m/z 134.09642 is the product of the previous intermediate (Figure 5.16) undergoing a reduction of the nitro functional group to a primary amine (Figure 5.19 – Structure **A**).

Structure **A**



m/z 134.09642

Figure 5.19: Proposed Structure **A**.

It is important to note that m/z 158.96409 and m/z 85.05933 impurities were carried through to the norephedrine **10** sample from 2-nitro-1-phenylpropanol **8**.

When analysing the next step in the pathway; the methylation of norephedrine **10** to pseudoephedrine/ephedrine **1**, one can see yet another rise in the number of peaks detected. This suggests that the deeper in to the synthetic pathway we get, the more impurities and by-products are formed, making the sample quite complex as shown in Figure 5.20. This is significant as this method allows the analyst to detect what synthetic pathway was used.

The UV-visible detector found 9 compounds, whereas LC-MS detected 19 masses listed in Figure 5.21, in which 18 masses were overlaid on the 2D-plot (Figure 5.20).

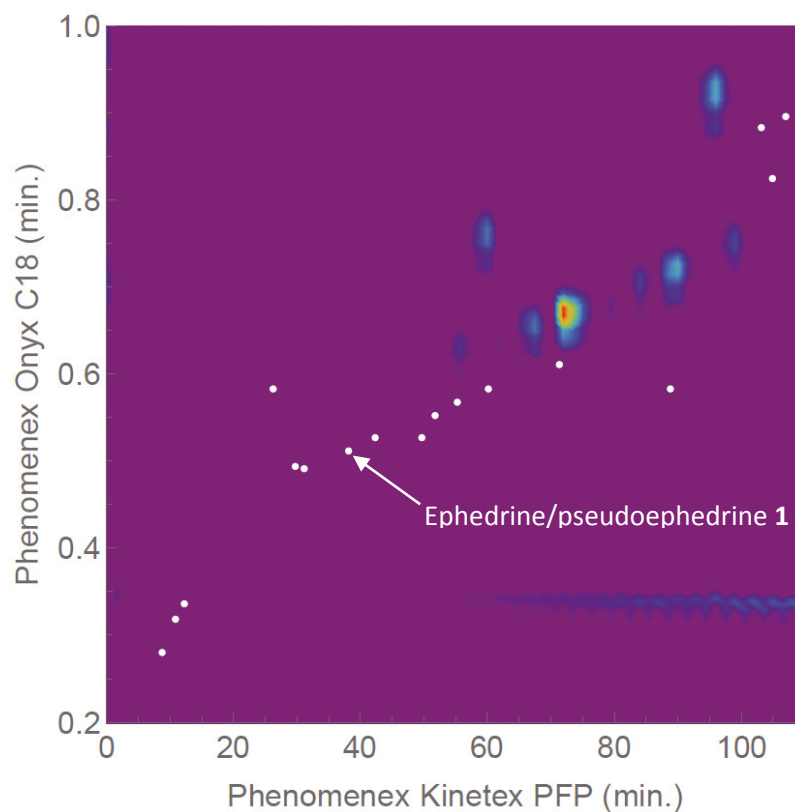
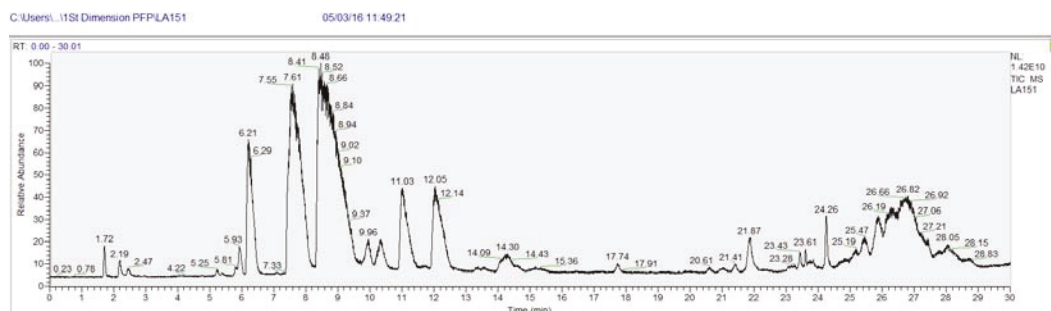


Figure 5.20: Two-dimensional HPLC separation and two-dimensional LC-MS separation (white dots) of ephedrine/pseudoephedrine **1** (m/z 166.12267 $[M+H]^+$).



Rt 1.72 = 158.96130, Rt 2.19 = 60.04502, Rt 2.47 = 85.05933, Rt 5.25 = 178.12270, Rt 5.93 = 152.10701, Rt 6.21 = 134.09645, Rt 7.61 = 166.12267, Rt 8.48 = 180.13824, Rt 9.96 = 180.13826, Rt 10.35 = 196.13326, Rt 11.03 = 194.15399, Rt 12.05 = 178.12265, Rt 14.30 = 192.13828, Rt 17.74 = 136.11210, Rt 20.61 = 206.11758, Rt 21.01 = 284.16443, Rt 21.41 = 256.13309, Rt 21.87 = 256.13312, Rt 24.26 = 238.12254.

Figure 5.21: Scaled first dimension LC-MS chromatogram and retention time masses of ephedrine/pseudoephedrine **1** using Kinetex PFP column at 0.5 mL min^{-1} .

As the methylation of norephedrine is not controlled by protecting groups, it is expected that methylation will occur at different sites of the molecule resulting in

Structures **B**, **C** and **D** from Figure 5.22. However, Structure **E** (amphetamine) and Structure **F** (*N*-acetylmethamphetamine) appear to be common impurities identified by other research groups in the ephedrine pathway to methamphetamine [26, 116, 252-254].

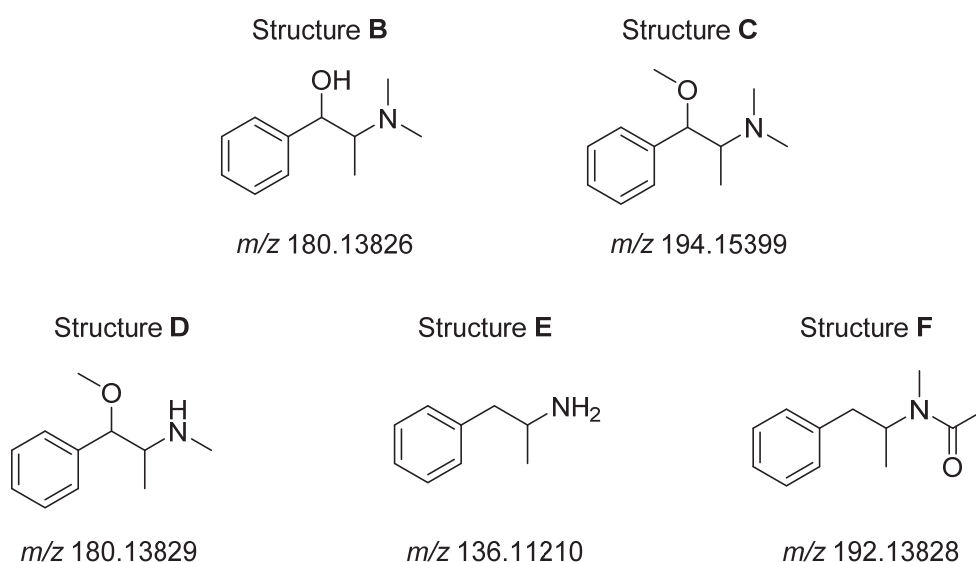


Figure 5.22: Proposed Structures **B – F**.

It is important to note that m/z 158.96409, m/z 60.04504, m/z 85.05933, m/z 152.10696, m/z 134.09642, m/z 180.13828, m/z 178.12268, m/z 256.13321, m/z 238.12268 were all carried through to ephedrine/pseudoephedrine **1** from norephedrine **10**.

The final step in a full synthetic pathway to methamphetamine looks at the reduction of pseudoephedrine/ephedrine **1** to methamphetamine **2**. Following the same trend, the number of masses detected using LC-MS has increased to 21 (Figure 5.24), in which 15 are illustrated (white dots) in Figure 5.23 along with the 7 compounds being found by the UV-visible detector.

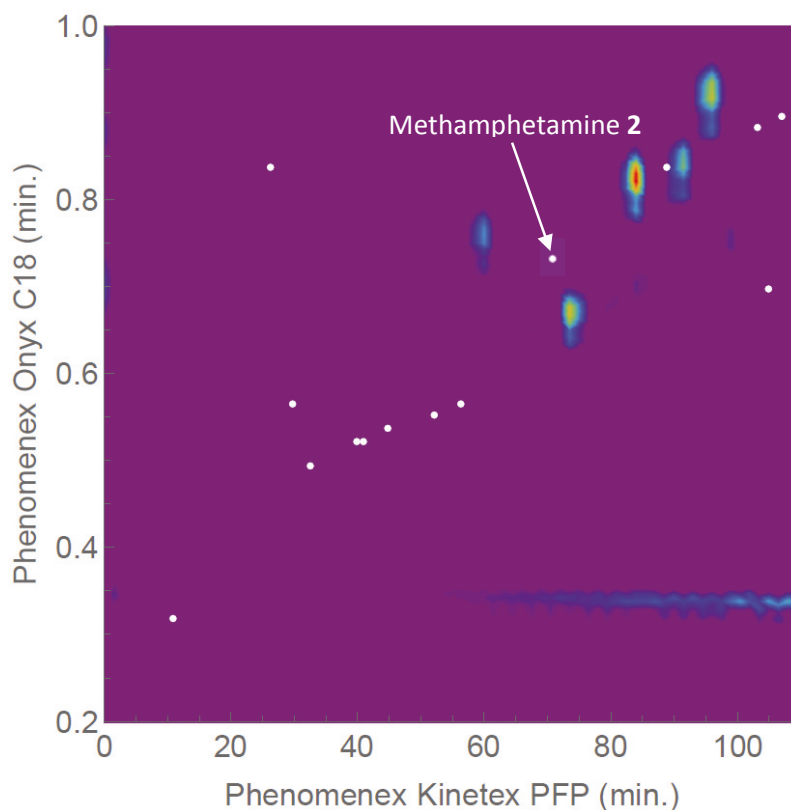
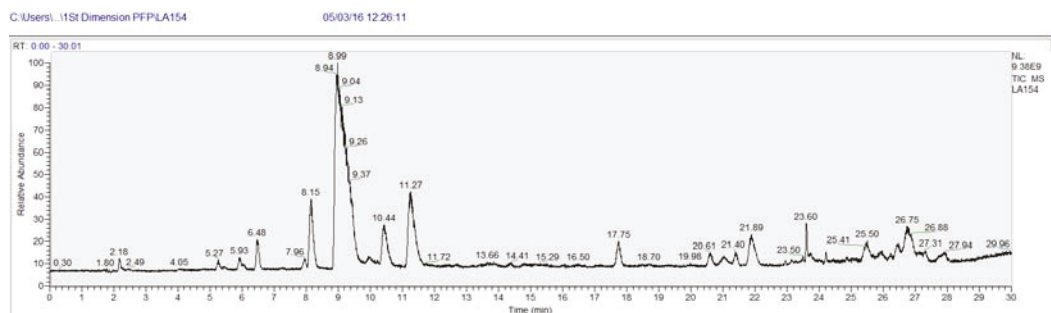


Figure 5.23: Two-dimensional HPLC separation and two-dimensional LC-MS separation (white dots) of methamphetamine **2** (m/z 150.12771 $[M+H]^+$).



Rt 2.18 = 60.04504, Rt 5.27 = 178.12273, Rt 5.93 = 194.11763, Rt 6.48 = 134.09654, Rt 7.96 = 166.12274, Rt 8.15 = 166.12271, Rt 8.15 = 148.11215, Rt 8.94 = 180.13840, Rt 10.44 = 196.13332, Rt 11.27 = 194.15410, Rt 13.45 = 164.14346, Rt 14.61 = 150.12771, Rt 17.75 = 136.11207, Rt 20.61 = 206.11740, Rt 21.01 = 284.16434, Rt 21.40 = 256.13300, Rt 21.89 = 256.13300, Rt 23.60 = 240.13814, Rt 25.50 = 307.18024, Rt 26.12 = 282.18520, Rt 26.75 = 284.20090.

Figure 5.24: Scaled first dimension LC-MS chromatogram and retention time masses of methamphetamine **2** using Kinetex PFP column at 0.5 mL min^{-1} .

The literature was consulted for known impurities and by-products found in methamphetamine samples and then compared to the masses detected in Figure

5.24. Structures **G – K** from Figure 5.25 are well documented impurities found in methamphetamine seizure samples [26, 116, 252-254], that were also found in the methamphetamine **2** sample (Structure **G** = dimethylamphetamine, Structure **H** = pseudoephedrine, Structure **I** = *n,n*-di-(*b*-phenylisopropyl)formamide, Structure **J** = amphetamine, Structure **K** = 1,2-dimethyl-3-phenyl aziridine).

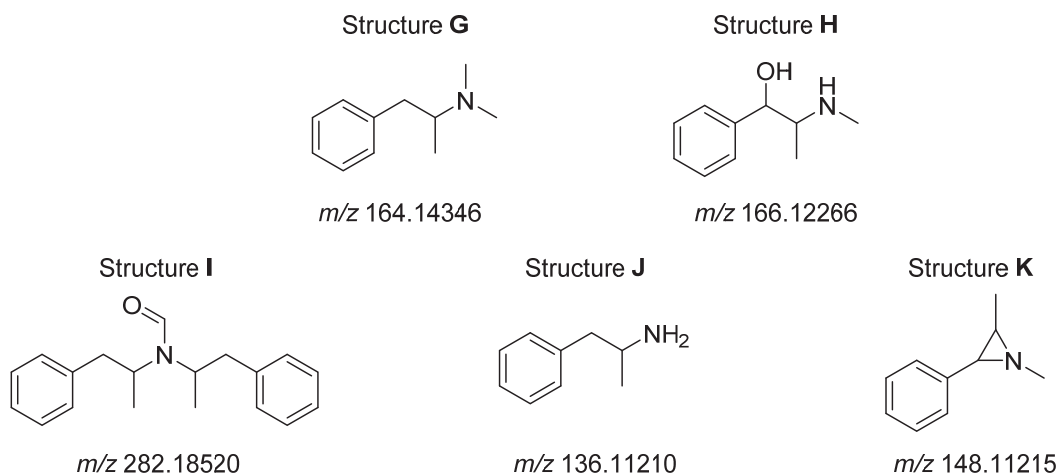
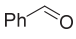
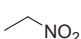
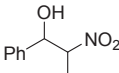
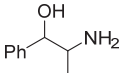
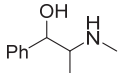
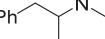


Figure 5.25: Proposed Structures **G – K**.

There were 11 masses that were carried through to the product methamphetamine **2** from ephedrine/pseudoephedrine **1** (m/z 60.04502, m/z 178.12270, m/z 134.09645, m/z 166.12267, m/z 180.13824, m/z 196.13326, m/z 194.15399, m/z 178.12265, m/z 136.11210, m/z 206.11758, m/z 256.13309).

A summary of LC-MS detected masses (rounded to whole integers) in each pathway step to methamphetamine is displayed in Table 5.3.

Table 5.3: The mapping of impurity masses for entire pathway to methamphetamine.

					
Benzaldehyde	Nitroethane	8	10	1	2
-	-	-	<i>m/z</i> 60	<i>m/z</i> 60	<i>m/z</i> 60
<i>m/z</i> 61	-	-	-	-	-
-	<i>m/z</i> 76	-	-	-	-
-	<i>m/z</i> 84	-	-	-	-
<i>m/z</i> 85	-	<i>m/z</i> 85	<i>m/z</i> 85	<i>m/z</i> 85	-
<i>m/z</i> 107	-	-	-	-	-
-	-	-	<i>m/z</i> 134	<i>m/z</i> 134	<i>m/z</i> 134
-	-	-	-	<i>m/z</i> 136	<i>m/z</i> 136
-	-	-	-	-	<i>m/z</i> 148
-	-	-	-	-	<i>m/z</i> 150
-	-	-	<i>m/z</i> 152	<i>m/z</i> 152	-
<i>m/z</i> 158	-	<i>m/z</i> 158	<i>m/z</i> 158	<i>m/z</i> 158	-
-	-	<i>m/z</i> 164	-	-	<i>m/z</i> 164
-	-	-	-	<i>m/z</i> 166	<i>m/z</i> 166
-	-	-	<i>m/z</i> 173	-	-
-	-	<i>m/z</i> 174	-	-	-
-	-	-	<i>m/z</i> 176	-	-
-	-	-	<i>m/z</i> 178	<i>m/z</i> 178	<i>m/z</i> 178
-	-	-	<i>m/z</i> 180	<i>m/z</i> 180	<i>m/z</i> 180
-	<i>m/z</i> 182	<i>m/z</i> 182	-	-	-
-	-	<i>m/z</i> 192	-	<i>m/z</i> 192	-
-	-	-	-	<i>m/z</i> 194	<i>m/z</i> 194
-	-	-	-	<i>m/z</i> 196	<i>m/z</i> 196
<i>m/z</i> 199	-	-	-	-	-
-	-	-	-	<i>m/z</i> 206	<i>m/z</i> 206
-	<i>m/z</i> 217	-	-	-	-
-	-	-	<i>m/z</i> 238	<i>m/z</i> 238	-
-	-	-	-	-	<i>m/z</i> 240
-	-	<i>m/z</i> 248	-	-	-
-	-	-	<i>m/z</i> 256	<i>m/z</i> 256	<i>m/z</i> 256
<i>m/z</i> 279	-	-	-	-	-
-	-	-	-	-	<i>m/z</i> 282
-	-	-	-	<i>m/z</i> 284	<i>m/z</i> 284
-	-	-	-	-	<i>m/z</i> 284
-	-	-	<i>m/z</i> 307	-	<i>m/z</i> 307
<i>m/z</i> 315	-	-	-	-	-

There are 13 masses (m/z 60, m/z 134, m/z 136, m/z 164, m/z 166, m/z 178, m/z 180, m/z 194, m/z 196, m/z 206, m/z 256, m/z 284, m/z 307) detected in the final methamphetamine product that can also be detected in previous steps. As such if analysts can identify or detect any of these masses, it may be their presence is indicative that this pathway was used to manufacture methamphetamine and its associated precursors can be identified. Such information may assist law enforcement in their investigations allowing them to identify intermediate samples within a clandestine laboratory in order to expedite a prosecution. It is important to note the presence of ephedrine/pseudoephedrine **1** (m/z 166) was detected in the final methamphetamine sample and confirms that the pathway used in this case involved the use of ephedrine/pseudoephedrine as a monitored precursor. From an application perspective tables such as these will be of great value to investigators and they could be generated to inform other synthetic pathways.

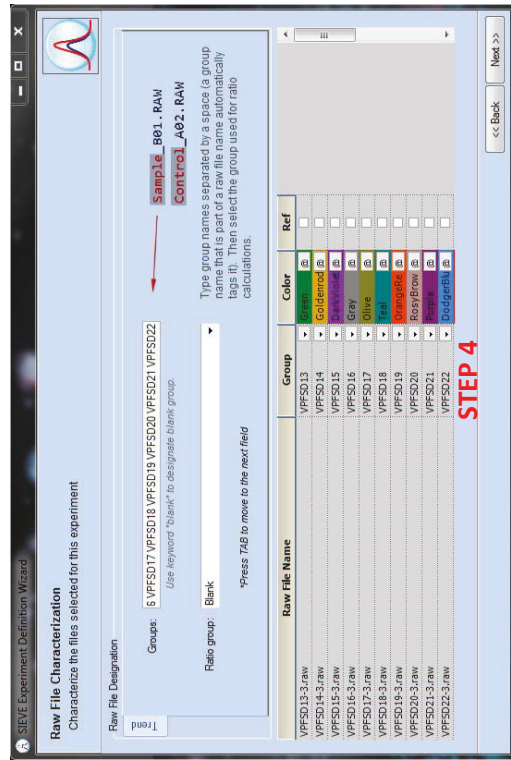
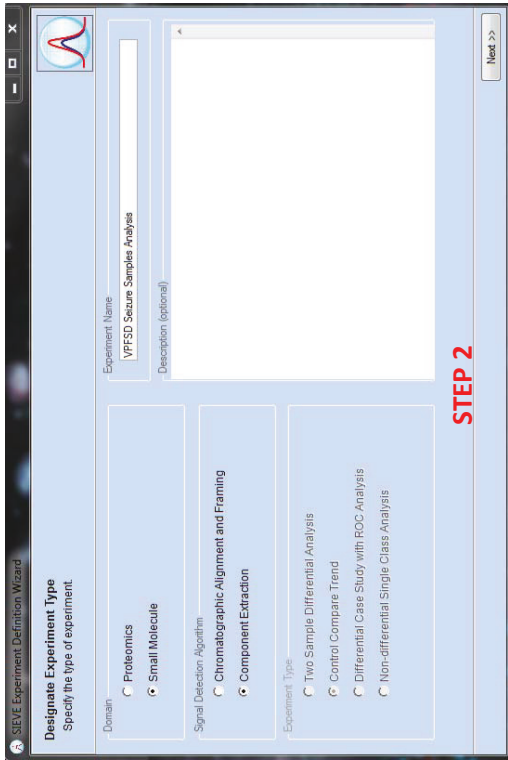
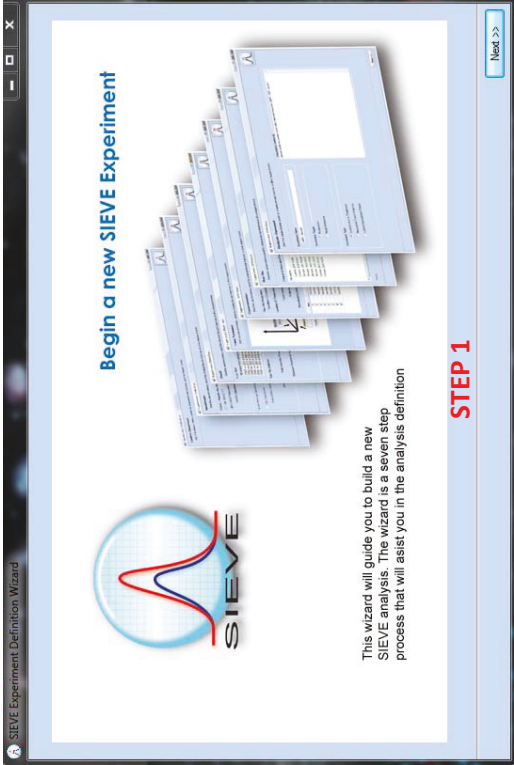
5.3.3 Preliminary PCA Study

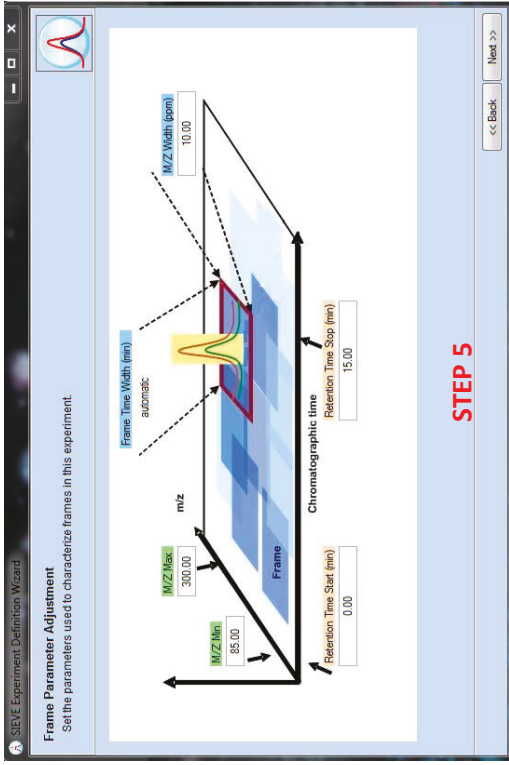
The presence of either pseudoephedrine or P2P in a final methamphetamine seizure sample is an extremely useful tool to identify a synthetic route, as almost all manufacture processes use one or the other. Due to this distinct difference in synthetic foundation, an alternate method of synthetic route identification was attempted, that would potentially be capable of analysing hundreds of methamphetamine seizure samples simultaneously.

As such, PCA analysis was carried out on all 22 seizure samples (VPFSD 1 – 22) provided by Victoria Police Forensic Services Centre, as a preliminary study. A Thermo Fisher Scientific program by the name of 'SIEVE™' [255] was used to process the LC-MS data produced from the Thermo Fisher High Resolution Mass Spectrometer (Q-Exactive Plus), for simplicity of being in the same file format. Pseudoephedrine targeted PCA was produced by SIEVE™ in a pilot study, setting the m/z range to 166.0-166.2 to separate samples purely based on the presence of ephedrine/pseudoephedrine.

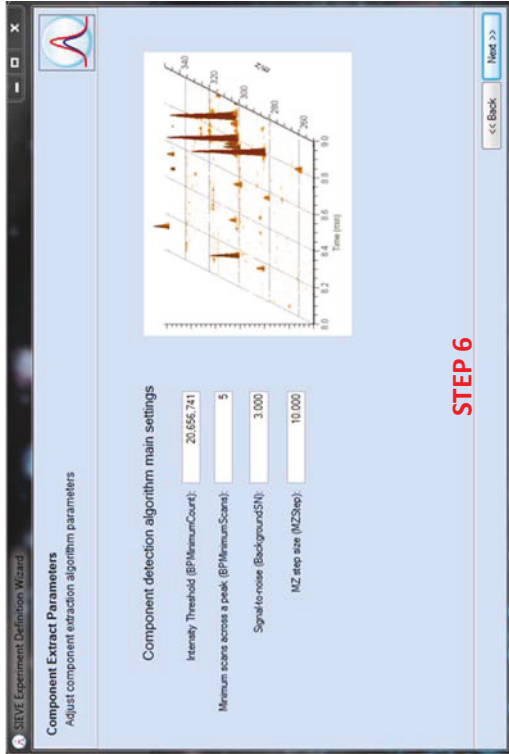
The operation of SIEVE™ is extremely simple, user friendly and incorporates a wizard that guides the user through a 7 step analysis process, shown in Figure 5.27.

- **Step 1** – Open the program and create ‘New Experiment’.
- **Step 2** – Select type of experiment (small molecule) and detection algorithm (component extraction). Then name your experiment for future reference.
- **Step 3** – Copy and paste Thermo Fisher LC-MS files for analysis. Then run a scan of the raw files to ensure compatibility.
- **Step 4** – Raw file characterisation is carried out. That is, replicates are named and grouped together while the blank run is set as the reference. Here is where the user can select what colour will be linked to what sample.
- **Step 5** – Desired parameters like retention time (0 – 15 minutes), m/z range (166.0 – 166.2) and m/z tolerance (10 ppm) are set.
- **Step 6** – This is where the component extraction algorithm parameters are adjusted. Minimum intensity threshold (2.0×10^7 counts), peak scans (5), signal to noise ratio (3:1) and m/z step size (10) can all be manipulated for a targeted analysis.
- **Step 7** – The final step involves clicking ‘Finish’ and waiting for the program to carry out the statistical analysis and produce the results including a normalisation of the data and peak alignment.





STEP 5



STEP 6



STEP 7

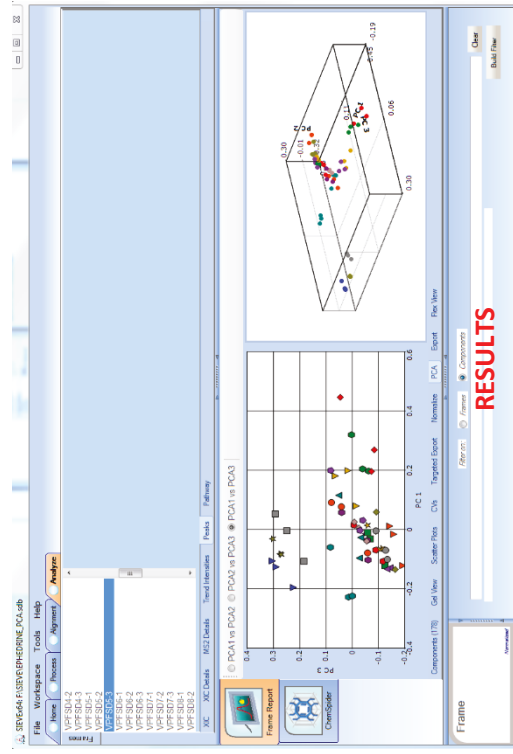


Figure 5.27: SIEVE™ 7 step wizard process.

Analysis of all seizure samples (1-22) was carried out and precursor amounts were recorded in Table 5.3. Extracted ion chromatograms (EIC) for pseudoephedrine (m/z 166.12) and P2P (m/z 135.08) were carried out on all seizure samples individually and the results were also recorded in Table 5.3. A reporting limit of 2.0×10^7 peak intensity count was set in SIEVE™ based on the visual detection of the pseudoephedrine peak. That is, an intensity under that threshold cannot be seen on the LC-MS chromatogram and was excluded and classed as trace amounts.

Table 5.3: Contents of Seizure Samples (VPFSD-1 – 22).

Seizure Sample	Methamphetamine	Pseudoephedrine (Peak Intensity Counts)	P2P (Peak Intensity Counts)
VPFSD-1	✓	3.10×10^4 - Trace	✗
VPFSD-2	✓	4.94×10^5 - Trace	✗
VPFSD-3	✓	8.32×10^6 - Trace	✗
VPFSD-4	✓	2.55×10^6 - Trace	✗
VPFSD-5	✓	3.51×10^8	✗
VPFSD-6	✓	5.73×10^8	✗
VPFSD-7	✓	4.68×10^5 - Trace	✗
VPFSD-8	✓	3.57×10^6 - Trace	✗
VPFSD-9	✓	2.88×10^6 - Trace	✗
VPFSD-10	✓	2.20×10^6 - Trace	✗
VPFSD-11	✓	6.44×10^8	✗
VPFSD-12	✓	7.56×10^5 - Trace	✗
VPFSD-13	✓	✗	2.51×10^4 - Trace
VPFSD-14	✓	✗	2.07×10^4 - Trace
VPFSD-15	✓	✗	1.74×10^4 - Trace
VPFSD-16	✓	✗	2.48×10^4 - Trace
VPFSD-17	✓	2.90×10^5 - Trace	✗
VPFSD-18	✓	2.55×10^8	✗
VPFSD-19	✓	1.21×10^5 - Trace	✗
VPFSD-20	✓	1.45×10^6 - Trace	✗
VPFSD-21	✓	1.31×10^6 - Trace	✗
VPFSD-22	✓	4.64×10^5 - Trace	✗

There were only 4 seizure samples (VPFSD – 5, 6, 11 & 18) that satisfied the limit and are bolded in the table. For example, VPFSD-18 contained the smallest

intensity count (2.55×10^8) out of the bolded seizure samples but a clear pseudoephedrine peak (retention time: 1.34 minutes) can be easily identified in the Total Ion Chromatogram (TIC) and in the Extracted Ion Chromatogram (EIC), shown in Figure 5.28.

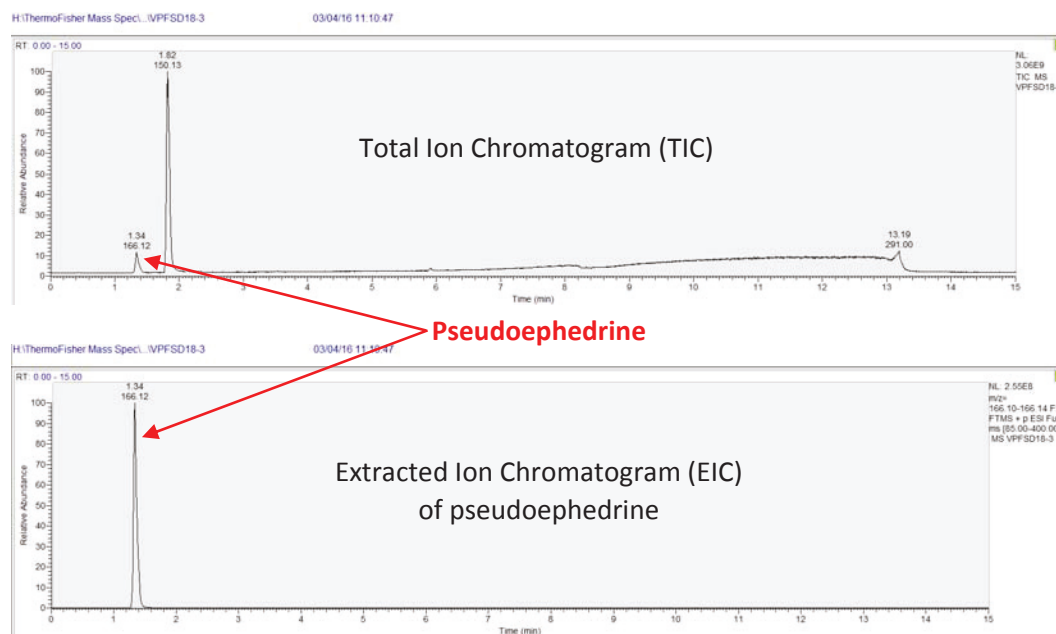


Figure 5.28: TIC and EIC (pseudoephedrine - 2.55×10^8) of VPFS018-3 seizure sample.

By contrast, VPFS018-3 has the highest intensity count for pseudoephedrine (8.32×10^6) that is below the reporting limit (2.0×10^7 counts) and as such, pseudoephedrine cannot be seen in the TIC but is definitely present in the EIC, as shown in Figure 5.29.

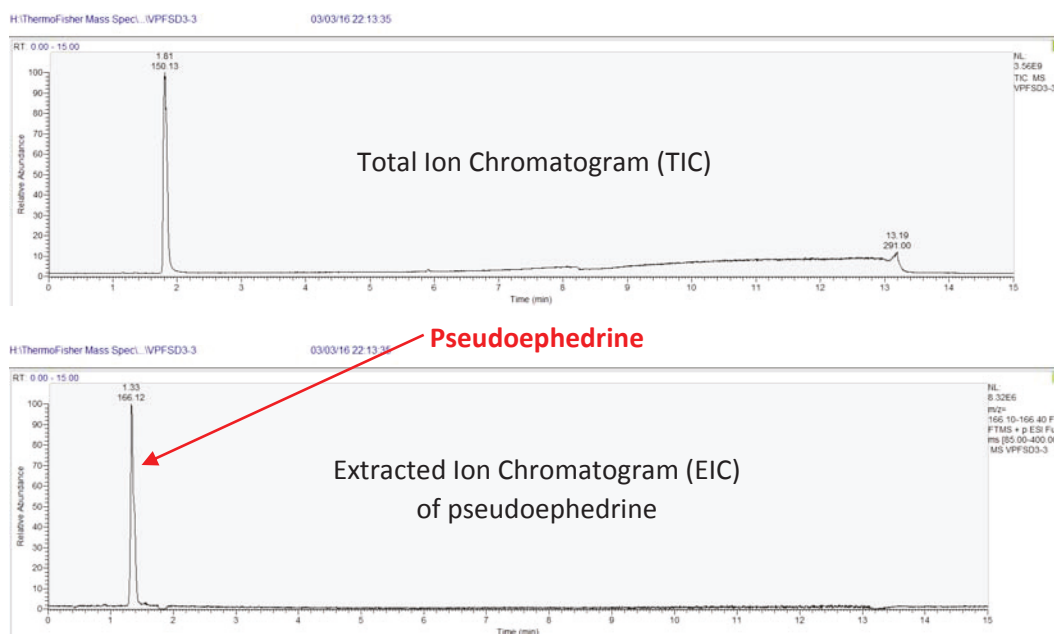


Figure 5.29: TIC and EIC (pseudoephedrine – 8.32×10^6) of VPFS-3 seizure sample.

This work aimed to develop the platform technology to be used as a fast, precursor screening method for large sample quantities. If this preliminary study can separate reportable amounts of precursor from trace or absent amounts, then it can be used as a future template to rapidly screen precursors, after a database of pathway standards has been created. By altering the intensity threshold and searching for a library of characteristic pathway impurities a robust system can be developed to identify a manufacture route by analysing a methamphetamine seizure sample.

Principal component analysis was carried out in triplicate using SIEVE™ (Figure 5.30) and a clear distinction of reportable amounts of pseudoephedrine was observed; proving this as a promising technique for future development. A three-dimensional PCA model was created to help visually identify the extent of separation. After consulting Table 5.30, it appears that the greater the peak intensity of pseudoephedrine, the further away samples are placed from the main cluster. This is significant because the use of ephedrine targeted PCA is clustering samples together based on concentration and can be manipulated to target masses of interest.

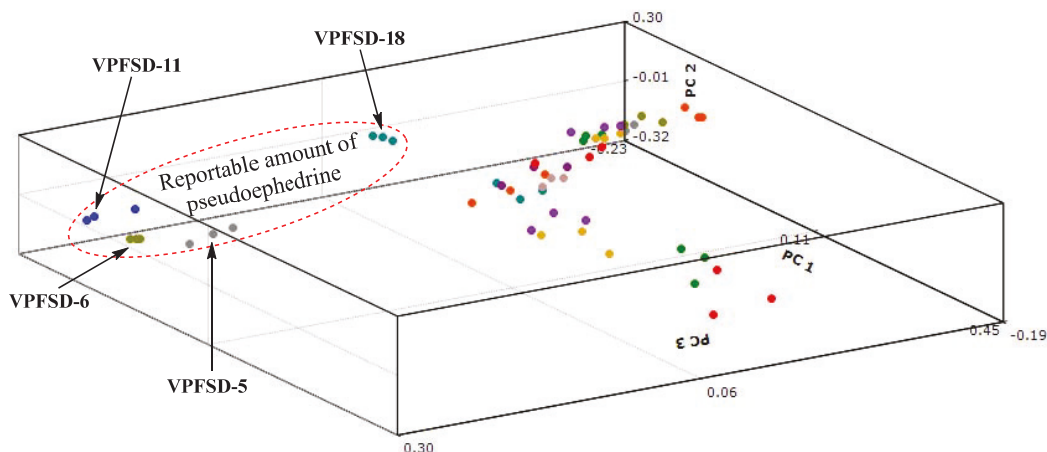


Figure 5.30: 3D PCA plot of 22 methamphetamine seizure samples.

Currently this type of multidisciplinary approach using PCA and analytical data is not routinely used by Victoria Police and clearly promise is shown here. The approach described here would be directly applicable to case work if the Victoria Police increased their technological capacity to include high resolution LC-MS or tandem MS for routine operations. The Ice taskforce identified the improvements in infrastructure required to target methamphetamine policing and this work helps support the case. This is a targeted form of PCA and for this to be fully realised with large real world sample sets a full validation process is required. This work was validated through a two-step process, firstly a blind analysis of the samples was performed. Due to the fact that the data set was small and the unique nature of the seizure samples meant that gaining a larger set in a short time frame was challenging and as such, secondly validation was confirmed *via* direct chemical interrogation from Victoria Police sources. This was a pilot study designed to highlight the potential capacity of PCA as a tool for determination of synthetic manufacture routes. It is important to note that for full development for casework, large data sets and full validation is required.

As discussed in Chapter 1, the Australian Ice Taskforce published a report of all the expert findings in 2015. The executive summary highlights [17]:

- Ice use in Australia is at extremely high levels and is increasing.
- The market remains strong despite efforts by law enforcement agencies to disrupt the supply.
- It has created a distinct problem for society due to its powerful stimulant and addiction properties.
- Methamphetamine is the only drug that is both imported and locally manufactured in significant quantities, making the response by law enforcement agencies incredibly complex.
- Efforts to supply must be more coordinated and targeted.
- Better data, more research and regular reporting will strengthen Australia's response.

As such it is evident that by creating the platform technology, it will allow future scientists, statisticians and law enforcement agencies to work collectively in developing a more advanced multidimensional system to track the origins of methamphetamine manufacture. This is significant as it forces different fields of expertise to tackle this ice epidemic together as a nation.

5.4 Conclusion

Current methods to identify the most orthogonal columns are time consuming and labour intensive. The use of LC-MS to monitor molecular masses over different stationary phases has significantly improved this selection protocol. This allows columns to be blindly selected for unknown sample components without comparing each column pair individually. Injecting multiple standards for each column is still extremely time consuming, whereas all standards can be combined, requiring only one injection for each column. This method improves analysis time significantly and spares sample amount and solvent required thus reducing the cost.

This column selection protocol was used to acquire the most orthogonal columns for methamphetamine type compounds. They were then applied to analyse each step of a full synthetic pathway to methamphetamine, taking full advantage of two-dimensional separation space. A comparison study between LC-UV and LC-MS was carried out to determine the best method of mapping impurities from methamphetamine manufacture.

Finally, synthetic chemistry, *in-silico* optimised 2D-HPLC, comprehensive selectivity studies, high resolution LC-MS and comprehensive data analysis for chemical mapping was developed. This significantly improving the ability to rapidly screen precursors and associated synthetic pathways from methamphetamine seizure samples.

The work presented in this chapter has been published as: N.K Burns †, **L.M Andrighetto †**, S.D Purcell, N.W Barnett, J. Denning, P.S Francis, X.A Conlan and P.G. Stevenson, Blind column selection protocol for two-dimensional high performance chromatography, *Talanta*, 154, 85-91 (2016) DOI: 10.1016/j.talanta.2016.03.056. **(Co-first author)**.

CHAPTER 6:

CONCLUDING REMARKS AND FUTURE WORK

6.1 Concluding Remarks

The work presented here fits into a broader research program within the analytical chemistry group at Deakin University and this has formed a large part of the progress in the area of multidimensional chromatography and chemical mapping. This is the first to apply an approach that utilises synthetic chemistry to inform the chromatographic separation development processes. Significant advancement has been achieved in methamphetamine seizure sample profiling and the technology platform developed is of great interest to the Victoria Police Forensic Services. This work has a very high chance of having a real and direct impact on drug profiling in Victoria and will complement the targeted approach currently in use to better inform court proceedings and project prioritisation. This work has also informed a parallel research program here run by one of my publication [234] co-authors Niki Burns who is developing protocols for process monitoring of commercial opiate streams. The fundamental approach taken here has been critical to the application of opiate monitoring which has led to the recent development of PCA analysis of 2D-HPLC data. Throughout this project care was taken to develop a platform technology that could be transposed to other industries and it is greatly satisfying to see my approach used for process chemistry applications. Recently the lead supervisor from this project Dr Xavier Conlan has directly used my protocol to develop a research grant (Australian Rotary Health) around mapping methamphetamine seizure samples towards informing clinical mental health research. As part of this proposal an agreement was made between Deakin University and the Victoria Police Forensic Services Department enabling access for Deakin researchers to methamphetamine seizure samples. This highlights how my work has already lead significantly to enhancing the research potential within Deakin University.

6.2 Future Work

Chemistry is constantly evolving and there is a limitless amount of future research to be undertaken in the chemical mapping of illicit drugs. The work presented in this thesis can be expanded and a few suggestions are provided below.

Chapter 2 and Chapter 3 investigated viable synthetic routes to methamphetamine from easily accessible materials; benzaldehyde, nitroethane and L-alanine. The reaction between benzaldehyde and nitroethane produced different products simply by altering the type of base used. Coincidentally, both resulting products can be used in different pathways (P2P and Ephedrine) to methamphetamine manufacture. There were 5 different bases used in Chapter 2 and a range of different bases should be trialled for a superior comprehensive analysis. Likewise alternative protecting groups and synthetic pathways could also be investigated to develop more efficient methods.

Chapter 4 investigated the *in-silico* optimisation of one-dimensional and two-dimensional separations using a simulation software called DryLab®. Future work may include trialling more columns and new columns to the market to test and improve the robustness of this program. A range of alternative complex sample types and solvents should be investigated to improve on the algorithms created for accurate simulations, incorporating and multivariable analysis. Likewise, a laboratory study should be undertaken to determine exactly how much time, money, waste, solvent, wages, maintenance parts and service contracts are being saved through the use of *in-silico* optimisation, to promote reduced environmental waste.

Chapter 5 investigated the chemical mapping of methamphetamine seizure samples using, optimised 2D-HPLC, LC-MS and targeted principal component analysis. Future work to further develop this platform technology would include synthesising and mapping all the different known pathways to methamphetamine (> 15 pathways). Essentially creating an enormous database which incorporates every step of every synthetic pathway, so that an automated system can quickly analyse, categorise and inform law enforcement agencies as to what route and

precursors were used in each methamphetamine seizure sample. The preliminary study was carried out using high resolution mass spectrometry and typical parameters, so the generation of a low resolution database would be of particular interest for universal analysis as low resolution data is commonly used in forensic laboratories. As targeted PCA was used, non-targeted PCA should be developed to process seizure samples to fully exploit the potential of this process. The chemical mapping process carried out in Chapter 5 should be repeated with the L-alanine pathway to methamphetamine, as discussed in Chapter 3. Importantly, the database will need to be constantly updated long term as new and alternative synthetic pathways are created to overcome the use of controlled substances.

REFERENCES

- [1] Hashimoto K. New Research on Methamphetamine Abuse. New York: *Nova Science Publishers, Inc.*; **2007**.
- [2] Weisheit R, White WL. Methamphetamine : Its History, Pharmacology and Treatment. Minneapolis: *Hazelden Publishing*; **2009**.
- [3] Zhu S, Kitani Y, Komatsu K. Exploration of Ephedra resource in Mongolia: From field investigation to molecular identification and chemical evaluation. *Journal of Traditional Medicines*. **2012**;29:35-40.
- [4] Anglin MD, Burke C, Perrochet B, Stamper E, Dawud-Noursi S. History of the Methamphetamine Problem. *Journal of Psychoactive Drugs*. **2000**;32:137-41.
- [5] Mullen AJ. The Synthesis and Pharmacology of Ephedrine Analogues: Dublin City University; **1991**.
- [6] abuse NlOD. Drug Facts: Methamphetamine. *U.S. Department of Health and Human Services*; **2014**.
- [7] Sato A. Methamphetamine use in Japan after the Second World War: Transformation of narratives. *Contemporary Drug Problems*. **2008**;35:717-46.
- [8] Information UDoP. United Nations General Assembly Special Session on the World Drug Problem. *United Nations Department of Public Information*; **1998**.
- [9] Moore EA. The amphetamine debate : the use of Adderall, Ritalin, and related drugs for behavior modification, neuroenhancement, and anti-aging purposes: *Jefferson, N.C. : McFarland & Co., 2010.*; **2010**.
- [10] Jackson Co. The Amphetamine Inhaler: A Case Study of Medical Abuse. *Journal of the History of Medicine and Allied Sciences*. **1971**;XXVI:187-96.
- [11] Campbell A. The Australian illicit drug guide : every person's guide to illicit drugs - their use, effects and history, treatment options and legal penalties: *Melbourne : Black Inc., 2001.*; **2001**.
- [12] Rasmussen N. America's First Amphetamine Epidemic 1929–1971: A Quantitative and Qualitative Retrospective With Implications for the Present. *American Journal of Public Health*. **2008**;98:974-85.

- [13] Barley S. The Speed Culture: Amphetamine Use and Abuse in America. *The Journal of the Royal College of General Practitioners*. **1976**;26:209-10.
- [14] Jenkins P. Synthetic panics. [electronic resource] : the symbolic politics of designer drugs: New York : New York University Press, ©1999.; **1999**.
- [15] McPherson SB, Hall HV, Yudko E. Methamphetamine use : clinical and forensic aspects: Boca Raton : CRC Press, 2nd ed.; **2009**.
- [16] Crime UNOoDa. World Drug Report. Vienna **2015**.
- [17] Australia Co. Final Report of the National Ice Taskforce. In: Cabinet DotPMa, editor. Australia: *Australian Government*; **2015**.
- [18] Parliament of Victoria - Law Reform DaCPC. Inquiry into the Supply and Use of Methamphetamine, particularly Ice, in Victoria - Final Report. Parliament House Melbourne **2014**.
- [19] Lloyd B, Turning Point A, Drug C, Ambo Project A, Drug Related Ambulance A. Trends in alcohol and drug related ambulance attendances in Victoria : 2011/12 / Belinda Lloyd. **2013**.
- [20] Hatch P. Ice being used as performance enhancing drug at local football clubs. The Age. Victoria, Australia: *The Age Newspaper*; **2015**.
- [21] Frohmader KS, Lehman MN, Laviolette SR, Coolen LM. Concurrent exposure to methamphetamine and sexual behavior enhances subsequent drug reward and causes compulsive sexual behavior in male rats. *The Journal of neuroscience : the official journal of the Society for Neuroscience*. **2011**;31:16473-82.
- [22] Bell S. Forensic chemistry: Upper Saddle River, N.J. : Pearson Education, 1st ed.; **2006**.
- [23] Sullivan E. Meth: America's Drug Epidemic. *American Library Association*; **2007**. p. 41.
- [24] Erowid. Methamphetamine Vault: Basics. **2001**.
- [25] Comission AC. Illicit Drug Data Report. **2014**.

- [26] Stojanovska N, Fu S, Tahtouh M, Kelly T, Beavis A, Kirkbride KP. A review of impurity profiling and synthetic route of manufacture of methylamphetamine, 3,4-methylenedioxymethylamphetamine, amphetamine, dimethylamphetamine and p-methoxyamphetamine. *Forensic Science International*. **2013**;224:8-26.
- [27] Brzezczko AW, Leech R, Stark JG. The advent of a new pseudoephedrine product to combat methamphetamine abuse. *American Journal of Drug & Alcohol Abuse*. **2013**;39:284-90.
- [28] Cox M, Klass G, Koo CWM. Manufacturing by-products from, and stereochemical outcomes of the biotransformation of benzaldehyde used in the synthesis of methamphetamine. *Forensic Science International*. **2009**;189:60-7.
- [29] Zhang W, Wang Z, Li W, Zhuang B, Qi H. Production of l-phenylacetylcarbinol by microbial transformation in polyethylene glycol-induced cloud point system. *Applied Microbiology and Biotechnology*. **2008**;78:233-9.
- [30] Park JK, Lee KD. Production of L-phenylacetylcarbinol (L-PAC) by encapsulated *Saccharomyces cerevisiae* cells. *Korean Journal of Chemical Engineering*. **2001**;18:363-70.
- [31] Allen A, Stevenson M, Nakamura S, Ely R. Differentiation of Illicit Phenyl-2-Propanone Synthesized from Phenylacetic Acid with Acetic Anhydride Versus Lead (II) Acetate. **1992**.
- [32] Hass HB, Susie AG, Heider RL. Nitro Alkene Derivatives 1. *The Journal of Organic Chemistry*. **1950**;15:8-14.
- [33] Boorman MC. Random Drug Testing of Drivers in Victoria. *Australian Police Journal*. **2007**;61:20-4.
- [34] Di Rago M, Chu M, Rodda LN, Jenkins E, Kotsos A, Gerostamoulos D. Ultra-rapid targeted analysis of 40 drugs of abuse in oral fluid by LC-MS/MS using carbon-13 isotopes of methamphetamine and MDMA to reduce detector saturation. *Analytical and Bioanalytical Chemistry*. **2016**;408:3737-49.
- [35] Joanna Menagh GP. Meth worth \$200m seized after foreign boat intercepted off WA's Mid West coast. ABC News. Melbourne Australia: *ABC News*; **2016**.
- [36] Al-Dirbashi O, Kuroda N, Nakashima K, Menichini F, Noda S, Minemoto M. Enantioselective high-performance liquid chromatography with fluorescence detection of methamphetamine and its metabolites in human urine. *Analyst*. **1998**;123:2333-7.

- [37] Rasmussen S, Cole R, Spiehler V. Methamphetamine in Antemortem Blood and Urine by Radioimmunoassay and GC/MS. *Journal of Analytical Toxicology*. **1989**;13:263-7.
- [38] Huestis MA, Cone EJ. Methamphetamine Disposition in Oral Fluid, Plasma, and Urine. *Annals of the New York Academy of Sciences*. **2007**;1098:104-21.
- [39] Suwannachom N, Thananchai T, Junkuy A, O'Brien TE, Sribanditmongkol P. Duration of detection of methamphetamine in hair after abstinence. *Forensic Science International*. **2015**;254:80-6.
- [40] Lin D.L, Yin R.M, Liu H.C, Wang C.Y, Liu R.H. Deposition Characteristics of Methamphetamine and Amphetamine in Fingernail Clippings and Hair Sections. *Journal of Analytical Toxicology*. **2004**;28:411-7.
- [41] Groeneveld G, de Puit M, Bleay S, Bradshaw R, Francese S. Detection and mapping of illicit drugs and their metabolites in fingermarks by MALDI MS and compatibility with forensic techniques. *Scientific Reports*. **2015**;5:11716.
- [42] Fay J, Fogerson R, Schoendorfer D, Niedbala RS, Spiehler V. Detection of Methamphetamine in Sweat By EIA and GC-MS. *Journal of Analytical Toxicology*. **1996**;20:398-403.
- [43] Smith FP. Detection of amphetamine in bloodstains, semen, seminal stains, saliva, and saliva stains. *Forensic Science International*. **1981**;17:225-8.
- [44] Magni PA, Pacini T, Pazzi M, Vincenti M, Dadour IR. Development of a GC–MS method for methamphetamine detection in *Calliphora vomitoria* L. (Diptera: Calliphoridae). *Forensic Science International*. **2014**;241:96-101.
- [45] Suzuki O, Hattori H, Asano M. Nails as useful materials for detection of methamphetamine or amphetamine abuse. *Forensic Science International*. **1984**;24:9-16.
- [46] Shabir GA. Development and Validation of RP-HPLC Method for the Determination of Methamphetamine and Propranolol in Tablet Dosage Form. *Indian Journal of Pharmaceutical Sciences*. **2011**;73:430-5.
- [47] Andrighetto LM, Stevenson PG, Pearson JR, Henderson LC, Conlan XA. DryLab® optimised two-dimensional high performance liquid chromatography for differentiation of ephedrine and pseudoephedrine based methamphetamine samples. *Forensic Science International*. **2014**;244:302-5.

- [48] Cheng W.C, Mok VK.K, Chan K.K, Li AF.M. A rapid and convenient LC/MS method for routine identification of methamphetamine/dimethylamphetamine and their metabolites in urine. *Forensic Science International*. **2007**;166:1-7.
- [49] Zhang T, Chen X, Yang R, Xu Y. Detection of methamphetamine and its main metabolite in fingerprints by liquid chromatography–mass spectrometry. *Forensic Science International*. **2015**;248:10-4.
- [50] Concheiro M, Simões SMdSS, Quintela Ó, de Castro A, Dias MJR, Cruz A, et al. Fast LC–MS/MS method for the determination of amphetamine, methamphetamine, MDA, MDMA, MDEA, MBDB and PMA in urine. *Forensic Science International*. **2007**;171:44-51.
- [51] Hayakawa K, Imaizumi N, Ishikura H, Minogawa E, Takayama N, Kobayashi H, et al. Determination of methamphetamine, amphetamine and piperidine in human urine by high-performance liquid chromatography with chemiluminescence detection. *Journal of Chromatography A*. **1990**;515:459-66.
- [52] McGeehan J, Dennany L. Electrochemiluminescent detection of methamphetamine and amphetamine. *Forensic Science International*. **2016**;264:1-6.
- [53] Katagi M, Nishikawa M, Tatsuno M, Miyazawa T, Tsuchihashi H, Suzuki A, et al. Direct Analysis of Methamphetamine and Amphetamine Enantiomers in Human Urine by Semi-microcolumn HPLC : Electrospray Ionization Mass Spectrometry. *Eisei kagaku*. **1998**;44:107-15.
- [54] Cody JT, Schwarzhoff R. Fluorescence Polarization Immunoassay Detection of Amphetamine, Methamphetamine, and Illicit Amphetamine Analogues. *Journal of Analytical Toxicology*. **1993**;17:26-30.
- [55] Praisler M, Van Bocxlaer J, De Leenheer A, Massart DL. Chemometric detection of thermally degraded samples in the analysis of drugs of abuse with gas chromatography–Fourier-transform infrared spectroscopy. *Journal of Chromatography A*. **2002**;962:161-73.
- [56] Kuwayama K, Tsujikawa K, Miyaguchi H, Kanamori T, Iwata Y, Inoue H, et al. Identification of impurities and the statistical classification of methamphetamine using headspace solid phase microextraction and gas chromatography–mass spectrometry. *Forensic Science International*. **2006**;160:44-52.
- [57] Miki A, Keller T, Regenscheit P, Dirnhofer R, Tatsuno M, Katagi M, et al. Application of ion mobility spectrometry to the rapid screening of methamphetamine incorporated in hair. *Journal of Chromatography B: Biomedical Sciences and Applications*. **1997**;692:319-28.

- [58] Toske SG, Morello DR, Berger JM, Vazquez ER. The use of $\delta^{13}\text{C}$ isotope ratio mass spectrometry for methamphetamine profiling: Comparison of ephedrine and pseudoephedrine-based samples to P2P-based samples. *Forensic Science International*. **2014**;234:1-6.
- [59] Kimura H, Mukaida M, Mori A. Detection of Stimulants in Hair by Laser Microscopy. *Journal of Analytical Toxicology*. **1999**;23:577-80.
- [60] Guinan T, Della Vedova C, Kobus H, Voelcker NH. Mass spectrometry imaging of fingerprint sweat on nanostructured silicon. *Chemical Communications*. **2015**;51:6088-91.
- [61] Hays P. Proton Nuclear Magnetic Resonance Spectroscopy (NMR) Methods for Determining the Purity of Reference Drug Standards and Illicit Forensic Drug Seizures. **2005**.
- [62] Armellin S, Brenna E, Frigoli S, Fronza G, Fuganti C, Mussida D. Determination of the Synthetic Origin of Methamphetamine Samples by ^2H NMR Spectroscopy. *Analytical Chemistry*. **2006**;78:3113-7.
- [63] Iwamuro Y, Iio-Ishimaru R, Chinaka S, Takayama N, Kodama S, Hayakawa K. Reproducible chiral capillary electrophoresis of methamphetamine and its related compounds using a chemically modified capillary having diol groups. *Forensic Toxicology*. **2010**;28:19-24.
- [64] Rezazadeh M, Yamini Y, Seidi S. Application of a new nanocarbonaceous sorbent in electromembrane surrounded solid phase microextraction for analysis of amphetamine and methamphetamine in human urine and whole blood. *Journal of Chromatography A*. **2015**;1396:1-6.
- [65] Smith JP, Martin A, Sammons DL, Striley C, Biagini R, Quinn J, et al. Measurement of methamphetamine on surfaces using surface plasmon resonance. *Toxicology Mechanisms And Methods*. **2009**;19:416-21.
- [66] Sberveglieri G, Ferrari V, Mohsen Y, Gharbi N, Lenouvel A, Guignard C. Detection of Δ^9 -Tetrahydrocannabinol, Methamphetamine and Amphetamine in air at low ppb level using a Field Asymmetric Ion Mobility Spectrometry microchip sensor. *Procedia Engineering*. **2014**;87:536-9.
- [67] Choodum A, Parabun K, Klawach N, Daeid NN, Kanatharana P, Wongniramaikul W. Real time quantitative colourimetric test for methamphetamine detection using digital and mobile phone technology. *Forensic Science International*. **2014**;235:8-13.

- [68] Gehrke CW, Wixom RL, Bayer E. Chromatography: a Century of Discovery 1900-2000: *Elsevier Science*; **2001**.
- [69] Horvath CG, Preiss B, Lipsky SR. Fast liquid chromatography. Investigation of operating parameters and the separation of nucleotides on pellicular ion exchangers. *Analytical chemistry*. **1967**;39:1422-8.
- [70] Guiochon G, Marchetti N, Mriziq K, Shalliker RA. Implementations of two-dimensional liquid chromatography. *Journal of Chromatography A*. **2008**;1189:109-68.
- [71] Stoll DR, Wang X, Carr PW. Comparison of the Practical Resolving Power of One- and Two-Dimensional High-Performance Liquid Chromatography Analysis of Metabolomic Samples. *Analytical Chemistry*. **2008**;80:268-78.
- [72] Pandohee J, G. Stevenson P, Zhou X-R, J.S. Spencer M, A.H. Jones O. Multi-Dimensional Liquid Chromatography and Metabolomics, Are Two Dimensions Better Than One? *Current Metabolomics*. **2015**;3:10-20.
- [73] Pandohee J, Holland BJ, Li B, Tsuzuki T, Stevenson PG, Barnett NW, et al. Screening of cannabinoids in industrial-grade hemp using two-dimensional liquid chromatography coupled with acidic potassium permanganate chemiluminescence detection. *Journal of Separation Science*. **2015**;38:2024-32.
- [74] François I, Sandra K, Sandra P. Comprehensive liquid chromatography: Fundamental aspects and practical considerations—A review. *Analytica Chimica Acta*. **2009**;641:14-31.
- [75] Cacciola F, Jandera P, Mondello L. Comparison of High-Temperature Gradient Heart-Cutting and Comprehensive LC × LC Systems for the Separation of Phenolic Antioxidants. *Chromatographia*. **2007**;66:661-7.
- [76] Zhang K, Li Y, Tsang M, Chetwyn NP. Analysis of pharmaceutical impurities using multi-heartcutting 2D LC coupled with UV-charged aerosol MS detection. *Journal of Separation Science*. **2013**;36:2986-92.
- [77] Pickrahn S, Sebald K, Hofmann T. Application of 2D-HPLC/Taste Dilution Analysis on Taste Compounds in Aniseed (*Pimpinella anisum* L.). *Journal of Agricultural and Food Chemistry*. **2014**;62:9239-45.
- [78] Stevenson PG, Bassanese DN, Barnett NW, Conlan XA. Improved 2D-HPLC of red wine by incorporating pre-process signal-smoothing algorithms. *Journal of Separation Science*. **2013**;36:3503-10.

- [79] McQueen P, Krokhin O. Optimal selection of 2D reversed-phase–reversed-phase HPLC separation techniques in bottom-up proteomics. *Expert Review of Proteomics*. **2012**;9:125-8.
- [80] Polo-Díez LM, Santos-Delgado MJ, Valencia-Cabrerizo Y, León-Barrios Y. Simultaneous enantiomeric determinations of acid and ester imidazolinone herbicides in a soil sample by two-dimensional direct chiral liquid chromatography. *Talanta*. **2015**;144:375-81.
- [81] Fairchild JN, Horváth K, Guiochon G. Approaches to comprehensive multidimensional liquid chromatography systems. *Journal of Chromatography A*. **2009**;1216:1363-71.
- [82] Marchetti N, Fairchild JN, Guiochon G. Comprehensive Off-Line, Two-Dimensional Liquid Chromatography. Application to the Separation of Peptide Digests. *Analytical Chemistry*. **2008**;80:2756-67.
- [83] Smith DK, Alexander RC. Fumbling the future: How Xerox invented, then ignored, the first personal computer: *iUniverse*; **1999**.
- [84] Tju-lik N, Soon N. Computer simulation of abnormal high-performance liquid chromatograms caused by solvents. *Journal of Chromatography A*. **1985**;329:13-24.
- [85] Horváth C, Melander W, Molnár I. Solvophobic interactions in liquid chromatography with nonpolar stationary phases. *Journal of Chromatography A*. **1976**;125:129-56.
- [86] Bidlingmeyer BA, Deming SN, Price WP, Sachok B, Petrusek M. Retention mechanism for reversed-phase ion-pair liquid chromatography. *Journal of Chromatography A*. **1979**;186:419-34.
- [87] Horvath C, Melander W, Molnar I, Molnar P. Enhancement of retention by ion-pair formation in liquid chromatography with nonpolar stationary phases. *Analytical Chemistry*. **1977**;49:2295-305.
- [88] Snyder LR, Dolan JW, Lommen DC. Drylab® computer simulation for high-performance liquid chromatographic method development. *Journal of Chromatography A*. **1989**;485:65-89.
- [89] Dolan JW, Lommen DC, Snyder LR. Drylab® computer simulation for high-performance liquid chromatographic method development. *Journal of Chromatography A*. **1989**;485:91-112.

- [90] Lewis JA, Lommen DC, Raddatz WD, Dolan JW, Snyder LR, Molnar I. Computer simulation for the prediction of separation as a function of pH for reversed-phase high-performance liquid chromatography. *Journal of Chromatography A*. **1992**;592:183-95.
- [91] Ghrist BFD, Snyder LR. Design of optimized high-performance liquid chromatographic gradients for the separation of either small or large molecules. *Journal of Chromatography A*. **1988**;459:43-63.
- [92] Hancock WS, Chloupek RC, Kirkland JJ, Snyder LR. Temperature as a variable in reversed-phase high-performance liquid chromatographic separations of peptide and protein samples. *Journal of Chromatography A*. **1994**;686:31-43.
- [93] Dolan JW. Temperature selectivity in reversed-phase high performance liquid chromatography. *J Chromatogr A*. **2002**;965:195-205.
- [94] Chloupek RC, Hancock WS, Marchylo BA, Kirkland JJ, Boyes BE, Snyder LR. Temperature as a variable in reversed-phase high-performance liquid chromatographic separations of peptide and protein samples. *Journal of Chromatography A*. **1994**;686:45-59.
- [95] Euerby MR, Scannapieco F, Rieger H-J, Molnar I. Retention modelling in ternary solvent-strength gradient elution reversed-phase chromatography using 30mm columns. *Journal of Chromatography A*. **2006**;1121:219-27.
- [96] Dolan JW, Snyder LR, Djordjevic NM, Hill DW, Saunders DL, Van Heukelem L, et al. Simultaneous variation of temperature and gradient steepness for reversed-phase high-performance liquid chromatography method development. I. Application to 14 different samples using computer simulation. *J Chromatogr A*. **1998**;803:1-31.
- [97] Giaginis C, Theocharis S, Tsantili-Kakoulidou A. Octanol/water partitioning simulation by reversed-phase high performance liquid chromatography for structurally diverse acidic drugs: Effect of n-octanol as mobile phase additive. *J Chromatogr A*. **2007**;1166:116-25.
- [98] Monks KE, Rieger HJ, Molnár I. Expanding the term "Design Space" in high performance liquid chromatography (I). *J Pharm Biomed Anal*. **2011**;56:874-9.
- [99] Krisko RM, McLaughlin K, Koenigbauer MJ, Lunte CE. Application of a column selection system and DryLab software for high-performance liquid chromatography method development. *J Chromatogr A*. **2006**;1122:186-93.
- [100] Shibukawa M, Miyake A, Eda S, Saito S. Determination of the cis–trans Isomerization Barriers of L-Alanyl-L-proline in Aqueous Solutions and at

Water/Hydrophobic Interfaces by On-Line Temperature-Jump Relaxation HPLC and Dynamic On-Column Reaction HPLC. *Analytical Chemistry*. **2015**;87:9280-7.

[101] Stevens FJ. Analysis of protein-protein interaction by simulation of small-zone size exclusion chromatography. Stochastic formulation of kinetic rate contributions to observed high-performance liquid chromatography elution characteristics. *Biophys J*. **1989**;55:1155-67.

[102] Van Heukelem L, Thomas CS. Computer-assisted high-performance liquid chromatography method development with applications to the isolation and analysis of phytoplankton pigments. *Journal of Chromatography A*. **2001**;910:31-49.

[103] Colgan ST, Pollard EB. Normal Phase Separations of Substituted Oxindoles and Isatins with Mobile Phases Containing Crown Ethers. *Journal of Chromatographic Science*. **1991**;29:433-7.

[104] Berridge JC. Simplex optimization of high-performance liquid chromatographic separations. *Journal of Chromatography A*. **1989**;485:3-14.

[105] Kürti. L CB. Strategic Applications of Named Reactions in Organic Synthesis: *Elsevier Academic Press*; **2005**.

[106] Palomo C, Oiarbide M, Laso A. Recent Advances in the Catalytic Asymmetric Nitroaldol (Henry) Reaction. *European Journal of Organic Chemistry*. **2007**;2007:2561-74.

[107] Luzzio FA. The Henry reaction: recent examples. *Tetrahedron*. **2001**;57:915-45.

[108] Sasai H, Suzuki T, Itoh N, Arai S, Shibasaki M. Effects of rare earth metals on the catalytic asymmetric nitroaldol reaction. *Tetrahedron Letters*. **1993**;34:2657-60.

[109] Christensen C, Juhl K, Jorgensen KA. Catalytic asymmetric Henry reactions-a simple approach to optically active [small beta]-nitro [small alpha]-hydroxy esters. *Chemical Communications*. **2001**:2222-3.

[110] Sasai H, Suzuki T, Arai S, Arai T, Shibasaki M. Basic character of rare earth metal alkoxides. Utilization in catalytic carbon-carbon bond-forming reactions and catalytic asymmetric nitroaldol reactions. *Journal of the American Chemical Society*. **1992**;114:4418-20.

[111] Trost BM, Yeh VSC. A Dinuclear Zn Catalyst for the Asymmetric Nitroaldol (Henry) Reaction. *Angewandte Chemie*. **2002**;114:889-91.

- [112] Evans DA, Seidel D, Rueping M, Lam HW, Shaw JT, Downey CW. A New Copper Acetate-Bis(oxazoline)-Catalyzed, Enantioselective Henry Reaction. *Journal of the American Chemical Society*. **2003**;125:12692-3.
- [113] Kogami Y, Nakajima T, Ikeno T, Yamada T. Enantioselective Henry reaction catalyzed by salen-cobalt complexes. *Synthesis*. **2004**;2004:1947-50.
- [114] Alvarez-Casao Y, Marques-Lopez E, Herrera RP. Organocatalytic Enantioselective Henry Reactions. *Symmetry*. **2011**;3:220.
- [115] Xu K, Lai G, Zha Z, Pan S, Chen H, Wang Z. A Highly anti-Selective Asymmetric Henry Reaction Catalyzed by a Chiral Copper Complex: Applications to the Syntheses of (+)-Spisulosine and a Pyrroloisoquinoline Derivative. *Chemistry – A European Journal*. **2012**;18:12357-62.
- [116] Lee J.S, Han E.Y, Lee S.Y, Kim E.M, Park Y.H, Lim M.A. Analysis of the impurities in the methamphetamine synthesized by three different methods from ephedrine and pseudoephedrine. *Forensic Science International*. **2006**;161:209-15.
- [117] Bremer N, Woolery R. The yield of methamphetamine, unreacted precursor and Birch by-product with the lithium-ammonia reduction method as employed in clandestine laboratories. *Newsletter of Midwestern Association of Forensic Scientists*. **1999**:8-16.
- [118] Person EC, Meyer JA, Vyvyan JR. Structural determination of the principal byproduct of the lithium-ammonia reduction method of methamphetamine manufacture. *Journal of forensic sciences*. **2005**;50:1-9.
- [119] Windahl KL, McTigue MJ, Pearson JR, Pratt SJ, Rowe JE, Sear EM. Investigation of the impurities found in methamphetamine synthesised from pseudoephedrine by reduction with hydriodic acid and red phosphorus. *Forensic Science International*. **1995**;76:97-114.
- [120] Caldicott DGE, Pigou PE, Beattie R, Edwards JW. Clandestine drug laboratories in Australia and the potential for harm. *Australian and New Zealand Journal of Public Health*. **2005**;29:155-62.
- [121] Blay G, Domingo LR, Hernández-Olmos V, Pedro JR. New Highly Asymmetric Henry Reaction Catalyzed by CuI and a C1-Symmetric Aminopyridine Ligand, and Its Application to the Synthesis of Miconazole. *Chemistry – A European Journal*. **2008**;14:4725-30.

- [122] Aalberg L, Andersson K, Bertler C, Borén H, Cole MD, Dahlén J, et al. Development of a harmonised method for the profiling of amphetamines: I. Synthesis of standards and compilation of analytical data. *Forensic Science International*. **2005**;149:219-29.
- [123] Gairaud CB, Lappin GR. The Synthesis of Nitrostyrenes. *The Journal of Organic Chemistry*. **1953**;18:1-3.
- [124] Kopylovich MN, Mac Leod TCO, Mahmudov KT, Guedes da Silva MFC, Pombeiro AJL. Zinc(ii) ortho-hydroxyphenylhydrazo-[small beta]-diketonate complexes and their catalytic ability towards diastereoselective nitroaldol (Henry) reaction. *Dalton Transactions*. **2011**;40:5352-61.
- [125] F. McAnda A, D. Roberts K, J. Smallridge A, Ten A, A. Trehwella M. Mechanism of the yeast mediated reduction of nitrostyrenes in light petroleum. *Journal of the Chemical Society, Perkin Transactions 1*. **1998**:501-4.
- [126] Barrett AGM, Spilling CD. Transfer hydrogenation: A stereospecific method for the conversion of nitro alkanes into amines. *Tetrahedron Letters*. **1988**;29:5733-4.
- [127] Brown CA, Ahuja VK. Catalytic hydrogenation. VI. Reaction of sodium borohydride with nickel salts in ethanol solution. P-2 Nickel, a highly convenient, new, selective hydrogenation catalyst with great sensitivity to substrate structure. *The Journal of Organic Chemistry*. **1973**;38:2226-30.
- [128] Ghosh N, Nayak S, Sahoo AK. Gold-Catalyzed Regioselective Hydration of Propargyl Acetates Assisted by a Neighboring Carbonyl Group: Access to α -Acyloxy Methyl Ketones and Synthesis of (\pm)-Actinopolymorphol B⁺. *The Journal of organic chemistry*. **2010**;76:500-11.
- [129] Stoochnoff BA, Benoiton NL. The methylation of some phenols and alcohols with sodium hydride/methyl iodide in tetrahydrofuran at room temperature. *Tetrahedron Letters*. **1973**;14:21-4.
- [130] McMurry J. Organic chemistry: Boston, MA Cengage Learning, Ninth edition.; **2016**.
- [131] Denis A, Renou C. Novel N-demethylation of ketolide: application to the solution phase parallel synthesis of N-desosaminy-substituted ketolides using ion exchange resins. *Tetrahedron Letters*. **2002**;43:4171-4.
- [132] Desai DG, Swami SS, Dabhade SK, Ghagare MG. FeS-NH₄CL-CH₃OH-H₂O: An Efficient and inexpensive system for the reduction of nitroarenes to anilines. *Synthetic Communications*. **2001**;31:1249-51.

- [133] Woo JCS, Cui S, Walker SD, Faul MM. Asymmetric syntheses of a GPR40 receptor agonist via diastereoselective and enantioselective conjugate alkynylation. *Tetrahedron*. **2010**;66:4730-7.
- [134] Flock AM, Krebs A, Bolm C. Ephedrine- and Pseudoephedrine-Derived Thioureas in Asymmetric Michael Additions of Keto Esters and Diketones to Nitroalkenes. *Synlett*. **2010**;2010:1219-22.
- [135] Salouros H, Collins M, George AV, Davies S. Isolation and Identification of Three By-products Found in Methylamphetamine Synthesized by the Emde Route. *Journal of Forensic Sciences*. **2010**;55:605-15.
- [136] Ben Painter PEP. The Akabori-Momotani Reaction: The next Frontier in Illicit Drug Manufacture? *Journal of the Clandestine Laboratory Investigating Chemists Association*. **2012**;22:6-14.
- [137] Chatterjee J, Laufer B, Kessler H. Synthesis of N-methylated cyclic peptides. *Nat Protocols*. **2012**;7:432-44.
- [138] Chatterjee J, Gilon C, Hoffman A, Kessler H. N-Methylation of Peptides: A New Perspective in Medicinal Chemistry. *Accounts of Chemical Research*. **2008**;41:1331-42.
- [139] Aurelio L, Brownlee RTC, Hughes AB. Synthetic Preparation of N-Methyl- α -amino Acids. *Chemical Reviews*. **2004**;104:5823-46.
- [140] Biron E, Chatterjee J, Ovadia O, Langenegger D, Brueggen J, Hoyer D, et al. Improving Oral Bioavailability of Peptides by Multiple N-Methylation: Somatostatin Analogues. *Angewandte Chemie International Edition*. **2008**;47:2595-9.
- [141] Fischer E, Mechel L. Formation of active secondary amino acids from halogen acids and primary amines. *Chem Ber*. **1916**;49:1355-66.
- [142] Das BC, Gero SD, Lederer E. N-methylation of N-acyl oligopeptides. *Biochemical and Biophysical Research Communications*. **1967**;29:211-5.
- [143] Bowman R, Stroud H. N-substituted amino-acids. Part I. A new method of preparation of dimethylamino-acids. *Journal of the Chemical Society*. **1950**:1342-5.
- [144] Ohfuné Y, Kurokawa N, Higuchi N, Saito M, Hashimoto M, Tanaka T. An efficient one-step reductive N-monoalkylation of α -amino acids. *Chemistry Letters*. **1984**;13:441-4.

- [145] Fester U. *Secrets of Methamphetamine Manufacture*. eighth edition ed. Green Bay, Wisconsin: *Festering Publications*; **2009**.
- [146] da Silva RA, Estevam IHS, Bieber LW. Reductive methylation of primary and secondary amines and amino acids by aqueous formaldehyde and zinc. *Tetrahedron Letters*. **2007**;48:7680-2.
- [147] Mothes C, Caumes C, Guez A, Boullet H, Gendrineau T, Darses S, et al. 3-Substituted Prolines: From Synthesis to Structural Applications, from Peptides to Foldamers. *Molecules*. **2013**;18:2307.
- [148] David Doughty MRJ, Ben Painter, Paul E. Pigou. Investigation into the Clandestine Laboratory Synthesis of N-Methylalanine from 2-Halopropionic Acids. *Journal of the Clandestine Laboratory Investigating Chemists Association*. **2016**;26:23-31.
- [149] Aldrich S. **2016**.
- [150] Li J, Sha Y. A Convenient Synthesis of Amino Acid Methyl Esters. *Molecules*. **2008**;13:1111.
- [151] Mastalerz H, Gavai AV, Fink B, Struzynski C, Tarrant J, Vite GD, et al. Pyrrolotriazine-5-carboxylate ester inhibitors of EGFR and HER2 protein tyrosine kinases and a novel one-pot synthesis of C-4 substituted pyrrole-2,3-dicarboxylate diesters. *Canadian Journal of Chemistry*. **2006**;84:528-33.
- [152] De Marco R, Di Gioia ML, Liguori A, Perri F, Siciliano C, Spinella M. N-Alkylation of N-arylsulfonyl- α -amino acid methyl esters by trialkyloxonium tetrafluoroborates. *Tetrahedron*. **2011**;67:9708-14.
- [153] Rengasamy R, Curtis-Long MJ, Seo WD, Jeong SH, Jeong I-Y, Park KH. New Building Block for Polyhydroxylated Piperidine: Total Synthesis of 1,6-Dideoxynojirimycin. *The Journal of Organic Chemistry*. **2008**;73:2898-901.
- [154] Williams RM, Im MN. Asymmetric synthesis of monosubstituted and α,α -disubstituted α -amino acids via diastereoselective glycine enolate alkylations. *Journal of the American Chemical Society*. **1991**;113:9276-86.
- [155] Hupp CD, Tepe JJ. 1-Ethyl-3-(3-dimethylaminopropyl)carbodiimide Hydrochloride-Mediated Oxazole Rearrangement: Gaining Access to a Unique Marine Alkaloid Scaffold. *The Journal of Organic Chemistry*. **2009**;74:3406-13.
- [156] Malkov AV, Stončius S, MacDougall KN, Mariani A, McGeoch GD, Kočovský P. Formamides derived from N-methyl amino acids serve as new chiral organocatalysts in

the enantioselective reduction of aromatic ketimines with trichlorosilane. *Tetrahedron*. **2006**;62:264-84.

[157] Dzygiel P, Reeve TB, Piarulli U, Krupicka M, Tvaroska I, Gennari C. Resolution of Racemic N-Benzyl α -Amino Acids by Liquid-Liquid Extraction: A Practical Method Using a Lipophilic Chiral Cobalt(III) Salen Complex and Mechanistic Studies. *European Journal of Organic Chemistry*. **2008**;2008:1253-64.

[158] Williams RM, Baldwin JE. Synthesis of Optically Active Alpha-Amino Acids: *Elsevier Science*; **2013**.

[159] Theodoridis G. Nitrogen Protecting Groups: Recent Developments and New Applications. *Tetrahedron*. **2000**;56:2339-58.

[160] Robertson J. Protecting group chemistry: *New York : Oxford University Press*, 2000.; **2000**.

[161] Moriyama K, Izumisawa Y, Togo H. Brønsted Acid-assisted Intramolecular Aminohydroxylation of N-Alkenylsulfonamides under Heavy Metal-free Conditions. *The Journal of Organic Chemistry*. **2012**;77:9846-51.

[162] Nyasse B, Grehn L, Ragnarsson U. Mild, efficient cleavage of arenesulfonamides by magnesium reduction. *Chemical Communications*. **1997**:1017-8.

[163] Sharma GVM, Janardhan Reddy J, Sree Lakshmi P, Radha Krishna P. Rapid and facile Lewis acid catalysed Boc protection of amines. *Tetrahedron Letters*. **2004**;45:6963-5.

[164] Wuts PGM, Greene TW. Protection for the Amino Group. Greene's Protective Groups in Organic Synthesis: *John Wiley & Sons, Inc.*; **2006**. p. 696-926.

[165] Cheung ST, Benoiton NL. N-Methylamino acids in peptide synthesis. V. The synthesis of N-tert-butyloxycarbonyl, N-methylamino acids by N-methylation. *Canadian Journal of Chemistry*. **1977**;55:906-10.

[166] Malkov AV, Vranková K, Černý M, Kočovský P. On the Selective N-Methylation of BOC-Protected Amino Acids. *The Journal of Organic Chemistry*. **2009**;74:8425-7.

[167] Jakubec P, Berkeš D. Crystallisation-induced asymmetric transformation (CIAT) for the synthesis of dipeptides containing homophenylalanine. *Tetrahedron: Asymmetry*. **2010**;21:2807-15.

- [168] Stodulski M, Mlynarski J. Synthesis of N-alkyl-N-methyl amino acids. Scope and limitations of base-induced N-alkylation of Cbz-amino acids. *Tetrahedron: Asymmetry*. **2008**;19:970-5.
- [169] Bryant RG. The NMR time scale. *J Chem Educ*. **1983**;60:933.
- [170] Hurtado M, Guillermo Contreras J, Matamala A, Mo O, Yanez M. Conformational analysis, NMR properties and nitrogen inversion of N-substituted 1,3-oxazines. *New Journal of Chemistry*. **2008**;32:2209-17.
- [171] Dąbrowski J, Ejchart A, Kamieńska-Trela K. Some aspects of anisochronism of geminal methyl groups in quaternised α -dimethylamino esters (^1H and ^{13}C NMR). *Organic Magnetic Resonance*. **1973**;5:483-6.
- [172] Claydon C, Australian Institute of H, Welfare. 2010 National Drug Strategy Household Survey report / Australian Institute of Health and Welfare. **2011**.
- [173] Qi Y, Evans ID, McCluskey A. Australian Federal Police seizures of illicit crystalline methamphetamine ('ice') 1998–2002: Impurity analysis. *Forensic Science International*. **2006**;164:201-10.
- [174] Verkouteren JR, Staymates JL. Reliability of ion mobility spectrometry for qualitative analysis of complex, multicomponent illicit drug samples. *Forensic Science International*. **2011**;206:190-6.
- [175] Benson S, Lennard C, Maynard P, Roux C. Forensic applications of isotope ratio mass spectrometry—A review. *Forensic Science International*. **2006**;157:1-22.
- [176] Makino Y. Simple HPLC method for detection of trace ephedrine and pseudoephedrine in high-purity methamphetamine. *Biomedical Chromatography*. **2012**;26:327-30.
- [177] Li H.X, Ding M.Y, Lv K, Yu J.Y. Simultaneous separation and determination of ephedrine alkaloids and tetramethyl-pyrazine in ephedra sinica STAPF by HPLC. *Journal of Liquid Chromatography & Related Technologies*. **2002**;25:313-20.
- [178] O'Leary AE, Hall SE, Vircks KE, Mulligan CC. Monitoring the clandestine synthesis of methamphetamine in real-time with ambient sampling, portable mass spectrometry. *Analytical Methods*. **2015**;7:7156-63.
- [179] Pravadali-Cekic S, Kocic D, Stevenson P, Shalliker A. Outlining a Multidimensional Approach for the Analysis of Coffee using HPLC. *Journal of Chromatography & Separation Techniques*. **2015**;2015.

- [180] Vonk RJ, Gargano AFG, Davydova E, Dekker HL, Eeltink S, de Koning LJ, et al. Comprehensive Two-Dimensional Liquid Chromatography with Stationary-Phase-Assisted Modulation Coupled to High-Resolution Mass Spectrometry Applied to Proteome Analysis of *Saccharomyces cerevisiae*. *Analytical Chemistry*. **2015**;87:5387-94.
- [181] Regalado EL, Schariter JA, Welch CJ. Investigation of two-dimensional high performance liquid chromatography approaches for reversed phase resolution of warfarin and hydroxywarfarin isomers. *Journal of Chromatography A*. **2014**;1363:200-6.
- [182] Song SM, Marriott P, Kotsos A, Drummer OH, Wynne P. Comprehensive two-dimensional gas chromatography with time-of-flight mass spectrometry (GC × GC-TOFMS) for drug screening and confirmation. *Forensic Science International*. **2004**;143:87-101.
- [183] Lowe RH, Karschner EL, Schwilke EW, Barnes AJ, Huestis MA. Simultaneous quantification of Δ^9 -tetrahydrocannabinol, 11-hydroxy- Δ^9 -tetrahydrocannabinol, and 11-nor- Δ^9 -tetrahydrocannabinol-9-carboxylic acid in human plasma using two-dimensional gas chromatography, cryofocusing, and electron impact-mass spectrometry. *Journal of Chromatography A*. **2007**;1163:318-27.
- [184] Agapiou A, Zorba E, Mikić K, McGregor L, Spiliopoulou C, Statheropoulos M. Analysis of volatile organic compounds released from the decay of surrogate human models simulating victims of collapsed buildings by thermal desorption–comprehensive two-dimensional gas chromatography–time of flight mass spectrometry. *Analytica Chimica Acta*. **2015**;883:99-108.
- [185] Sampat A, Lopatka M, Sjerps M, Vivo-Truyols G, Schoenmakers P, van Asten A. The forensic potential of comprehensive two-dimensional gas chromatography. *TrAC Trends in Analytical Chemistry*.
- [186] Ping Zou S-yW, Zhi-qiang Zhang, Xiu-hong Wu. Analysis of ephedrine alkaloids in Chinese medicine by 2D HPLC. *Fenxi Ceshi Xuebao* **2007**;26:120-4.
- [187] Guiochon G. The limits of the separation power of unidimensional column liquid chromatography. *Journal of Chromatography A*. **2006**;1126:6-49.
- [188] Shalliker RA, Guiochon G. Solvent viscosity mismatch between the solute plug and the mobile phase: Considerations in the applications of two-dimensional HPLC. *Analyst*. **2010**;135:222-9.
- [189] Stevenson PG, Mnatsakanyan M, Francis AR, Shalliker RA. A discussion on the process of defining 2-D separation selectivity. *Journal of Separation Science*. **2010**;33:1405-13.

- [190] Gilar M, Olivova P, Daly AE, Gebler JC. Orthogonality of Separation in Two-Dimensional Liquid Chromatography. *Analytical Chemistry*. **2005**;77:6426-34.
- [191] Neue UD, O’Gara JE, Méndez A. Selectivity in reversed-phase separations: Influence of the stationary phase. *Journal of Chromatography A*. **2006**;1127:161-74.
- [192] Bassanese DN, Holland BJ, Conlan XA, Francis PS, Barnett NW, Stevenson PG. Protocols for finding the most orthogonal dimensions for two-dimensional high performance liquid chromatography. *Talanta*. **2015**;134:402-8.
- [193] Murahashi T, Tsuruga F, Sasaki S. An automatic method for the determination of carcinogenic 1-nitropyrene in extracts from automobile exhaust particulate matter. *Analyst*. **2003**;128:1346-51.
- [194] Gilar M, Fridrich J, Schure MR, Jaworski A. Comparison of Orthogonality Estimation Methods for the Two-Dimensional Separations of Peptides. *Analytical Chemistry*. **2012**;84:8722-32.
- [195] Li X, Stoll DR, Carr PW. Equation for Peak Capacity Estimation in Two-Dimensional Liquid Chromatography. *Analytical Chemistry*. **2009**;81:845-50.
- [196] A. Shalliker GG. How to improve your implementation of two-dimensional preparative HPLC : solvent viscosity considerations. *BioProcess International*. **2008**;6:52-60.
- [197] Giddings JC. Two-dimensional separations: concept and promise. *Analytical Chemistry*. **1984**;56:1258A-70A.
- [198] Krisko RM, McLaughlin K, Koenigbauer MJ, Lunte CE. Application of a column selection system and DryLab software for high-performance liquid chromatography method development. *Journal of Chromatography A*. **2006**;1122:186-93.
- [199] Dolan JW, Snyder LR, Quarry MA. Computer simulation as a means of developing an optimized reversed-phase gradient-elution separation. *Chromatographia*. **1987**;24:261-76.
- [200] Dugo P, Cacciola F, Kumm T, Dugo G, Mondello L. Comprehensive multidimensional liquid chromatography: Theory and applications. *Journal of Chromatography A*. **2008**;1184:353-68.
- [201] Barbarin N, Henion JD, Wu Y. Comparison between liquid chromatography–UV detection and liquid chromatography–mass spectrometry for the characterization of

impurities and/or degradants present in trimethoprim tablets. *Journal of Chromatography A*. **2002**;970:141-54.

[202] Stevenson PG, Mnatsakanyan M, Guiochon G, Shalliker RA. Peak picking and the assessment of separation performance in two-dimensional high performance liquid chromatography. *Analyst*. **2010**;135:1541-50.

[203] Shrivastava A, Gupta V. Methods for the determination of limit of detection and limit of quantitation of the analytical methods**2011**.

[204] Sultan DM. Simultaneous HPLC determination and validation of amphetamine, methamphetamine, caffeine, paracetamol and theophylline in illicit seized tablets. *International Journal of Pharmacy and Pharmaceutical Sciences*. **2014**;6:294-8.

[205] Deng D, Deng H, Zhang L, Su Y. Determination of Ephedrine and Pseudoephedrine by Field-Amplified Sample Injection Capillary Electrophoresis. *Journal of Chromatographic Science*. **2014**;52:357-62.

[206] Patel Bhoomi B. SBB, Gohil Kirtan N., Patel Piyush M. Development and Validation of Spectrophotometric Method For Simultaneous Estimation of Rosuvastatin Calcium and Aspirin In Bulk and Pharmaceutical Dosage Form. *International Journal of Research in Pharmacy and Science*. **2012**;2:115-22.

[207] Murphy RE, Schure MR, Foley JP. Effect of Sampling Rate on Resolution in Comprehensive Two-Dimensional Liquid Chromatography. *Analytical Chemistry*. **1998**;70:1585-94.

[208] Watson NE, Davis JM, Synovec RE. Observations on “Orthogonality” in Comprehensive Two-Dimensional Separations. *Analytical Chemistry*. **2007**;79:7924-7.

[209] Lee MJ, Chung I-M, Kim H, Jung MY. High resolution LC–ESI-TOF-mass spectrometry method for fast separation, identification, and quantification of 12 isoflavones in soybeans and soybean products. *Food Chemistry*. **2015**;176:254-62.

[210] Singh S, Handa T, Narayanam M, Sahu A, Junwal M, Shah RP. A critical review on the use of modern sophisticated hyphenated tools in the characterization of impurities and degradation products. *J Pharm Biomed Anal*. **2012**;69:148-73.

[211] Smith CA, Want EJ, O'Maille G, Abagyan R, Siuzdak G. XCMS: processing mass spectrometry data for metabolite profiling using nonlinear peak alignment, matching, and identification. *Analytical chemistry*. **2006**;78:779-87.

- [212] Sturm M, Bertsch A, Gropl C, Hildebrandt A, Hussong R, Lange E, et al. OpenMS - An open-source software framework for mass spectrometry. *BMC Bioinformatics*. **2008**;9:163.
- [213] Kessner D, Chambers M, Burke R, Agus D, Mallick P. ProteoWizard: open source software for rapid proteomics tools development. *Bioinformatics*. **2008**;24:2534-6.
- [214] Prince JT, Marcotte EM. mspire: mass spectrometry proteomics in Ruby. *Bioinformatics*. **2008**;24:2796-7.
- [215] Horlacher O, Nikitin F, Aloci D, Mariethoz J, Müller M, Lisacek F. MzJava: An open source library for mass spectrometry data processing. *Journal of proteomics*. **2015**;129:63-70.
- [216] Katajamaa M, Miettinen J, Orešič M. MZmine: toolbox for processing and visualization of mass spectrometry based molecular profile data. *Bioinformatics*. **2006**;22:634-6.
- [217] Goloborodko AA, Levitsky LI, Ivanov MV, Gorshkov MV. Pyteomics—a Python framework for exploratory data analysis and rapid software prototyping in proteomics. *Journal of The American Society for Mass Spectrometry*. **2013**;24:301-4.
- [218] Aiche S, Sachsenberg T, Kenar E, Walzer M, Wiswedel B, Kristl T, et al. Workflows for automated downstream data analysis and visualization in large-scale computational mass spectrometry. *Proteomics*. **2015**;15:1443-7.
- [219] Tautenhahn R, Patti GJ, Rinehart D, Siuzdak G. XCMS Online: a web-based platform to process untargeted metabolomic data. *Analytical chemistry*. **2012**;84:5035-9.
- [220] Yetukuri L, Ekroos K, Vidal-Puig A, Orešič M. Informatics and computational strategies for the study of lipids. *Molecular BioSystems*. **2008**;4:121-7.
- [221] Kohlbacher O, Reinert K, Gröpl C, Lange E, Pfeifer N, Schulz-Trieglaff O, et al. TOPP—the OpenMS proteomics pipeline. *Bioinformatics*. **2007**;23:e191-e7.
- [222] Jolliffe I. Principal component analysis: *Wiley Online Library*; **2002**.
- [223] Bro R, Smilde AK. Principal component analysis. *Analytical Methods*. **2014**;6:2812-31.
- [224] Hotelling H. Analysis of a complex of statistical variables into principal components. *Journal of educational psychology*. **1933**;24:417.

- [225] Bicchi CP, Binello AE, Pellegrino GM, Vanni AC. Characterization of green and roasted coffees through the chlorogenic acid fraction by HPLC-UV and principal component analysis. *Journal of Agricultural and Food Chemistry*. **1995**;43:1549-55.
- [226] Shima N, Miyawaki I, Bando K, Horie H, Zaitso K, Katagi M, et al. Influences of methamphetamine-induced acute intoxication on urinary and plasma metabolic profiles in the rat. *Toxicology*. **2011**;287:29-37.
- [227] Chen CY, Stemberger RS, Klaue B, Blum JD, Pickhardt PC, Folt CL. Accumulation of heavy metals in food web components across a gradient of lakes. *Limnology and Oceanography*. **2000**;45:1525-36.
- [228] Qu D, Li W, Zhang Y, Sun B, Zhong Y, Liu J, et al. Support vector machines combined with wavelet-based feature extraction for identification of drugs hidden in anthropomorphic phantom. *Measurement*. **2013**;46:284-93.
- [229] Bunker CE, Hamilton NB, Sun YP. Quantitative application of principal component analysis and self-modeling spectral resolution to product analysis of tetraphenylethylene photochemical reactions. *Analytical Chemistry*. **1993**;65:3460-5.
- [230] Ghosh D, Chattopadhyay P. Application of principal component analysis (PCA) as a sensory assessment tool for fermented food products. *Journal of food science and technology*. **2012**;49:328-34.
- [231] Quayle K. Elemental and Molecular and Profiling of Illicit Tobacco: University of Central Lancashire; **2014**.
- [232] Guimet F, Ferré J, Boqué R, Rius FX. Application of unfold principal component analysis and parallel factor analysis to the exploratory analysis of olive oils by means of excitation–emission matrix fluorescence spectroscopy. *Analytica Chimica Acta*. **2004**;515:75-85.
- [233] Theodoridis G, Gika HG, Wilson ID. LC-MS-based methodology for global metabolite profiling in metabonomics/metabolomics. *TrAC Trends in Analytical Chemistry*. **2008**;27:251-60.
- [234] Burns NK, Andrighetto LM, Conlan XA, Purcell SD, Barnett NW, Denning J, et al. Blind column selection protocol for two-dimensional high performance liquid chromatography. *Talanta*. **2016**;154:85-91.
- [235] Phenomenex I. The Ultimate Guide to HPLC/UHPLC Reversed Phase Selectivity. **2013**. p. 32.

- [236] Mirali M, Ambrose SJ, Wood SA, Vandenberg A, Purves RW. Development of a fast extraction method and optimization of liquid chromatography–mass spectrometry for the analysis of phenolic compounds in lentil seed coats. *Journal of Chromatography B*. **2014**;969:149-61.
- [237] Lemasson E, Bertin S, Hennig P, Boiteux H, Lesellier E, West C. Development of an achiral supercritical fluid chromatography method with ultraviolet absorbance and mass spectrometric detection for impurity profiling of drug candidates. Part I: Optimization of mobile phase composition. *Journal of Chromatography A*. **2015**;1408:217-26.
- [238] Olšovská J, Kameník Z, Čejka P, Jurková M, Mikyška A. Ultra-high-performance liquid chromatography profiling method for chemical screening of proanthocyanidins in Czech hops. *Talanta*. **2013**;116:919-26.
- [239] Kimata K, Iwaguchi K, Onishi S, Jinno K, Eksteen R, Hosoya K, et al. Chromatographic Characterization of Silica C18 Packing Materials. Correlation between a Preparation Method and Retention Behavior of Stationary Phase. *Journal of Chromatographic Science*. **1989**;27:721-8.
- [240] Gatti R. Development and Validation of a Liquid Chromatographic Method Useful for the Determination of Amino Acids in New and Commercial Alimentary Supplements. *Chromatographia*. **2015**;78:1095-9.
- [241] Gurke R, Rossmann J, Schubert S, Sandmann T, Rößler M, Oertel R, et al. Development of a SPE-HPLC–MS/MS method for the determination of most prescribed pharmaceuticals and related metabolites in urban sewage samples. *Journal of Chromatography B*. **2015**;990:23-30.
- [242] Michalak J, Gujska E, Kuncewicz A. RP-HPLC-DAD studies on acrylamide in cereal-based baby foods. *Journal of food composition and analysis*. **2013**;32:68-73.
- [243] Long W. Fast Screening Methods for Steroids by HPLC with Agilent Poroshell 120 Columns. *Optimization*. **2012**.
- [244] Xiong X.t, Tan J.h, Li H.y, Zhao T.t, Zhao Q.w, Jia F. Rapid Determination of 8 Prohibited Drugs in Hair Growth Cosmetics by HPLC/DAD. *Journal of Instrumental Analysis*. **2013**;4:012.
- [245] Patel KB, Thula KC, Maheshwari DG. Stability Indicating HPLC Method for Simultaneous Estimation of Ciprofloxacin and Phenylephrine in Pharmaceutical Dosage form. *Pharmacophore*. **2014**;5.

- [246] Dioumaeva I, Choi S.B, Yong B, Jones D, Arora R. Understanding Orthogonality in Reversed-Phase Liquid Chromatography for Easier Column Selection and Method Development. *Application Note, Agilent Technologies*, <http://www.chem.agilent.com/Library/applications/SI-02425.pdf>.
- [247] Rehder DS, Dillon TM, Pipes GD, Bondarenko PV. Reversed-phase liquid chromatography/mass spectrometry analysis of reduced monoclonal antibodies in pharmaceuticals. *Journal of Chromatography A*. **2006**;1102:164-75.
- [248] Jiang D, Peterson DG. Identification of bitter compounds in whole wheat bread. *Food chemistry*. **2013**;141:1345-53.
- [249] Liu M, Chen EX, Ji R, Semin D. Stability-indicating hydrophilic interaction liquid chromatography method for highly polar and basic compounds. *Journal of chromatography A*. **2008**;1188:255-63.
- [250] Gritti F, Guiochon G. Adsorption mechanism in reversed-phase liquid chromatography: Effect of the surface coverage of a monomeric C18-silica stationary phase. *Journal of Chromatography A*. **2006**;1115:142-63.
- [251] Gray M, Dennis GR, Wormell P, Andrew Shalliker R, Slonecker P. Two dimensional reversed-phase–reversed-phase separations: Isomeric separations incorporating C18 and carbon clad zirconia stationary phases. *Journal of Chromatography A*. **2002**;975:285-97.
- [252] Verweij AM. Impurities in illicit drug preparations: amphetamine and methamphetamine. *Forensic Sci Rev*. **1989**;1:1-11.
- [253] Cantrell T, John B, Johnson L, Allen A. A study of impurities found in methamphetamine synthesized from ephedrine. *Forensic Science International*. **1988**;39:39-53.
- [254] Windahl K, McTigue M, Pearson J, Pratt S, Rowe J, Sear E. Investigation of the impurities found in methamphetamine synthesised from pseudoephedrine by reduction with hydriodic acid and red phosphorus. *Forensic science international*. **1995**;76:97-114.
- [255] Courant F, Pinel G, Bichon E, Monteau F, Antignac J-P, Le Bizec B. Development of a metabolomic approach based on liquid chromatography-high resolution mass spectrometry to screen for clenbuterol abuse in calves. *Analyst*. **2009**;134:1637-46.